Fall 2013

Coupled geomechanical reservoir simulation

Amin Amirlatifi

Department: Geosciences and Geological and Petroleum Engineering

COUPLED GEOMECHANICAL RESERVOIR SIMULATION

by

AMIN AMIRLATIFI

A DISSERTATION

Presented to the Faculty of the Graduate School of the

MISSOURI UNIVERSITY OF SCIENCE AND TECHNOLOGY

In Partial Fulfillment of the Requirements for the Degree

DOCTOR OF PHILOSOPHY

in

PETROLEUM ENGINEERING

2013

Approved by
Andreas Eckert, Advisor
Runar Nygaard, Co-advisor
Baojun Bai
Shari Dunn-Norman
Keita Yoshioka

PUBLICATION DISSERTATION OPTION

This dissertation is organized into two sections, three journal and one conference articles. Section one gives an outline of the dissertation and introduces the problem, research objectives, and research plan. The first article "An Explicit Partial Coupling Approach for Simulating CO_2 Sequestration," from page 17 to 54, has been submitted to the International Journal of Green House Gas Control and is under review. The second article "Role of Geometrical Influences of CO_2 Sequestration in Anticlines," from page 55 to 80 has been published in proceeding of the 46th American Rock Mechanics Association (ARMA) US Rock Mechanics / Geomechanics Symposium held in Chicago, IL, USA, 24-27 June 2012. The third paper "Fluid Flow Boundary Conditions: The Need for Pressure Transient Analysis for CO_2 Sequestration Studies," from page 81 to 107 has been submitted to the International Journal of Green House Gas Control and is under review. The forth paper "Geomechanical Risk Assessment for CO_2 Sequestration in a Candidate Storage Site in Missouri," from page 108 to 140 will be submitted to the International Journal of Green House Gas Control. Section two summarizes the major conclusions and includes recommendations for future work.

ABSTRACT

Founded by Department Of Energy, the Plains CO_2 Reduction (PCOR) Partnership is investigating the Williston Basin as a candidate for sequestering CO_2 emissions from power plants. The State of Missouri, a member of PCOR, lies at the outermost point on the proposed transportation route and consequently faces the highest CO_2 compression and transportation costs. In order to minimize the cost of CO_2 sequestration, it is desirable to find a storage site within the state. The Lamotte sandstone is identified as a suitable sequestration aquifer formation in Missouri with acceptable permeability, porosity, extension, rock strength and water salinity. Using the finite element analysis package ABAQUS for the geomechanical analysis and the fluid flow simulator Eclipse for pore pressure determination, this work looks at pore pressure – stress coupling which has significant implications for failure mechanism, fault reactivation and caprock integrity. The present work also suggests the use of Pressure Transient Analysis (PTA) to quantify the lateral fluid flow boundary type and differentiating between open, closed and infinite systems. The present work also suggests a new boundary condition, Semi-Open, which is a transitional lateral boundary condition between Fully Open and Closed boundary conditions. Results of the present work provide a coupling module that can be used to conduct coupled geomechanical analysis for CO_2 sequestration projects, facilitate the building of 3D mechanical earth models and provide insight into the role of boundary conditions with respect to CO_2 storage capacity. The coupling procedure is utilized to evaluate CO_2 storage potential and assess the geomechanical risks for CO_2 sequestration in a candidate storage site in the North-Eastern part of the state of Missouri for sustainable CO_2 sequestration.

ACKNOWLEDGMENTS

I would not have made it to and through my PhD without the countless blessings from the almighty God. He is the one that deserves all the praise. I would like to thank my advisor, Dr. Andreas Eckert for his constant inspiration, encouragement, advice, help and support throughout my studies at the Missouri University of Science and Technology (MST). This research would not have been possible without his mentorship and provision.

My humble appreciation also goes to my co-advisor, Dr. Runar Nygaard, for his far-reaching knowledge and continuous support. His level of professionalism has been a persistent motivation for me. I would like to acknowledge the financial support I received from both my advisors and the Department of Energy, National Energy Technology Laboratory (grant # DE-FE0001132).

I would also like to thank my committee members, Dr. Baojun Bai, Dr. Shari Dunn-Norman, and Dr. Keita Yoshioka, for honoring me by being on my committee and for their invaluable suggestions. I would specially thank Dr. Baojun Bai for his financial support and continuous mentorship.

My special thanks to my family for their unwavering support and prayers throughout my life. My sincere and heartfelt gratitude go out to my mother, my father, my brother and my sister. I wish to express special appreciation to my wife, Somayeh Bakhtiari for sacrifices she made so that I could accomplish one of my biggest dreams in life. I love you sweetheart and thanks for your love and support. My love and devotion extends to our beloved daughter Lily, who brings joy and meaning to our life. I cannot imagine how we lived before you enchanted our life!

TABLE OF CONTENTS

LIST OF ILLUSTRATIONS

PAPER 2.

PAPER 3.

PAPER 4.

LIST OF TABLES

PAPER 4.

NOMENCLATURE

Symbol	Description
H_α	Enthalpy Of Phase A
q_l	Flow Rate Of Phase L
U_α	Specific Internal Energy Of Phase A
B	Fracture Aperture
C	Empirical Constant For Shale, 0.27
C_f	Compressibility Of The Fluid
C_r	Compressibility Of The Rock
C_s	Specific Heat Capacity
D	Diffusivity(M^2/S)
E_D	Drained Young's Modulus
E_S	Saturated Rock Young's Modulus
F	Force Vector (N)
I	Identity Matrix
K	Absolute Permeability (M^2)
k_0	Initial Permeability
K_D	Drained Bulk Modulus
k_f	Hydraulic Conductivity (M/S)
k_f	Fracture Permeability (M^2)
k_m	Matrix Permeability (M^2)
k_{rl}	Relative Permeability To Phase L
K_S	Saturated Bulk Modulus
K_T	Thermal Conductivity
k_z	Vertical Permeability (M^2)
L_f	Fracture Length
L_v	Length Of The Element In The Direction Of Maximum Principal Stress.
N_p	Number Of Phases
q_H	Enthalpy Source
q_L	Heat Loss

T	Temperature
T	Time
U	Displacement Vector (M)
V	Darcy Velocity Vector
Greek symbols	
σ	Total Stress Tensor
σ'	Effective Stress Tensor
σ'_n	Effective Normal Stress
v_D	Drained Poisson's Ratio
v_S	Saturated Rock Poisson's Ratio
∇Φ	Flow Potential (Psia)
A	Biot's Coefficient
B	Angle Of Internal Friction
Γ	Boundary
ϕ	Porosity
Θ	Failure Angle
M	Viscosity (Cp)
P	Density (Kg/M^3)
Ω	Domain
λ	Lamé Parameter
λ_u	Drained Lamé Parameter
ε	Strain Tensor
Operators	
∇	Gradient
$()^T$	Matrix Transpose
Δa	Virtual Variation Of The Quantity a

1. INTRODUCTION

1.1. DISSERTATION OUTLINE

Section one gives an overview of the problem statement and research objectives. A general introduction to the study area including an overview of coupled geomechanical reservoir simulation and the need for CO_2 sequestration is given. Available data sets used in this study are also mentioned.

The two journal submissions under peer review, one conference paper and the manuscript discuss the three main objectives of my research as follows. Paper one (Amirlatifi et al., "An Explicit Partial Coupling Approach for Simulating CO_2 Sequestration," in review) discusses the first objective of this study, which is assessing existing coupling methods and developing a new module to perform coupled 3D reservoir and multi scale geomechanical simulations using existing commercial simulators to simulate leakage and reservoir stability. The results reported in this paper suggest a strong dependence of modeling accuracy on coupling of pore pressure variation with geomechanical effects. Paper 2 (Amirlatifi et al. 2012, "Role of Geometrical Influences of CO_2 Sequestration in Anticlines") and paper 3 (Amirlatifi and Eckert, "Fluid Flow Boundary Conditions: The Need for Pressure Transient Analysis for CO_2 Sequestration Studies," in review) discuss objective 2, which is the impact of fluid flow boundary conditions and geometry on the CO_2 storage capacity of aquifers. The results suggest that fluid flow boundary conditions, combined with realistic reservoir geometry play a significant role in safe sequestration limits. These results also suggest that the use of pressure transient analysis as a quantifier of fluid flow boundary conditions has practical

viability. Paper 4 (Amirlatifi et al., "Geomechanical Risk Assessment for CO_2 Sequestration in a Candidate Storage Site in Missouri" to be submitted for peer review) discusses objective 3, which is creating realistic 3D mechanical earth models for possible CO_2 storage sites in the state of Missouri and locating a candidate aquifer for in state CO_2 sequestration, in order to avoid the cost involved in compression and transportation of CO_2 emissions from coal fired plants in the state of Missouri to Williston basin for storage. The results suggest that the Lamotte pinchout in Lincoln fold which is located in North-Eastern Missouri is a promising candidate for sustainable CO_2 sequestration.

Section two presents the dissertation's major conclusions, which represent the outcomes and contribution of this research. The section also offers recommendations for future work based upon the questions that have been raised in this dissertation.

1.2. PROBLEM STATEMENT

Many processes in oil and gas industry require coupling of geomechanics and reservoir simulation to study the effects of pore pressure variation on the stability of the medium; these processes include, but are not limited to, CO_2 sequestration, Steam injection, Water flooding, or Steam Assisted Gravity Drainage. Increased pore pressure due to the injection of CO_2 may result in generation of new fractures or reactivation of existing faults or fractures, providing preferred fluid flow pathways along which dissolved CO_2 may escape into the atmosphere or freshwater zones above and resulting in environmental hazards (Streit and Hillis, 2004). In order to assess and mitigate these geomechanical risks, a thorough simulation coupling fluid flow through porous media and

geomechanics of a realistic representation of the reservoir as well as the overburden is required (Lucier et al., 2006; Rutqvist et al., 2008, 2006).

Conventional reservoir simulation software packages have minimal support to consider geomechanical effects resulting from the change in the pore pressure, and are limited to the compressibility and permeability change (constant or as a function of pressure), which in turn may lead to wrong conclusions on the stability and storage of the medium. On the contrary, problems arise when commercial finite element analysis packages are utilized to simulate fluid flow in porous medium. As an example, ABAQUS, which is one of the major finite element analysis packages used for geomechanical analyses, can only model single component and single phase fluid flow with limited control over the fluid, which is generally taken to be water. Modeling reservoir deformation under different states of stress caused by increased pore pressure resulting from fluid injection requires precise coupled modeling of fluid flow through porous medium and geomechanical analysis of the medium at different pore pressure distributions. The former can be achieved through finite difference fluid flow simulators that can handle multi fluid, multi-phase systems with different fluid saturation distributions and the latter through finite element analysis packages that include geomechanics analysis built into them, but only handle single phase, single fluid systems.

The present coupled reservoir simulation study utilizes a shared earth model for simulation of fluid flow through porous media using the commercial fluid flow simulator ECLIPSE and the optimized finite element discretization using the commercial finite element solver ABAQUS for the geomechanical analysis of rock deformation that is caused by the pore pressure difference associated to CO_2 sequestration. This study aims to

determine the maximum sustainable pore pressure difference that does not yield significant surface uplift and does not result in fracturing of the caprock which opens a leakage pathway for CO_2 to escape into the overburden. It also aims to provide a seamless way of performing partial coupling to study long term effects of CO_2 sequestration at a suitable sequestration site in the state of Missouri. Based on geologic information and rock property measurements conducted on the Lamotte sandstone at Missouri University of Science and Technology (Akpan, 2012; Miller, 2012) a 3D mechanical earth model (MEM) of a pinchout structure in the northeast of Missouri is constructed. The construction of the MEM utilizes the advanced capabilities of the developed coupling module to account for the geometrical complexity of this structure.

1.3. EXISTING METHODOLOGIES AND KNOWLEDGE GAPS

During CO_2 sequestration different physical processes that involve multiphase and multi-component fluid flow in a geologic system take place. In order to study the mechanical deformations during CO_2 sequestration, numerical modeling of fluid flow through porous medium coupled with a geomechanical analysis of the medium at different pore pressure distributions (Rutqvist et al., 2002; Settari and Mourits, 1998; Settari and Walters, 1999; Thomas et al., 2003; Vidal-Gilbert et al., 2009) is required. This coupling can be achieved either by a fully or partially coupled numerical simulation.

In the fully coupled simulation approach, the fluid flow through pores and elasticity calculations are carried out simultaneously. (Lewis and Sukirman, 1993; Tortike and S.M., 1987; Xikui and Zienkiewicz, 1992) have presented formulations for the fully coupled approach, and (Gutierrez and Lewis, 1998) have presented a fully coupled reservoir

simulator. However, the complexity of a fully coupled physical system results in very high computational costs and thus the applicability of the fully coupled approach is limited (Inoue and Fontoura, 2009).

In order to mitigate this disadvantage a variety of partially coupled modeling approaches have been developed (Helmig et al., 1998; Longuemare et al., 2002; Rutqvist et al., 2002; Settari and Mourits, 1998, e.g. 1994; Tsang, 1999). Partial coupling approaches are based on an external coupling between separate numerical simulations. In general, a conventional reservoir simulator based on the finite difference (FD) method is used to process the fluid flow problem and a finite element (FE) model is used to solve the stress equilibrium equations, respectively. This method benefits from the latest developments in each field, has lower computational costs and hence the best simulator available can be employed. In general, partial coupling can be divided into two families: explicit and iterative coupling. Figure 1.1 shows the general algorithm for explicit (one way) and iterative (two way) partial couplings. In the explicit coupling approach (Figure 1.1-a) a reservoir simulator carries out fluid flow calculations at each time-step, however stress-displacement calculations are only carried out on selected time-steps, the choice of which depends on the variation in the accessible pore space due to the change in pore pressure, i.e. if the variation in pore space between time-steps is not significant, then geomechanical calculations may be ignored. Once the change in pore space is considerable, the stress-displacement analysis is carried out (Minkoff et al., 2003, 1999; Settari and Walters, 1999). This approach can significantly reduce the computation cost of the coupled analysis through reduced number of stress-displacement simulation runs, but may result in unstable solutions and loss of accuracy due to the coupled nature of the processes (Dean et al., 2006).

In the iterative coupling approach (Figure 1.1-b) the two simulators are coupled at each time-step.

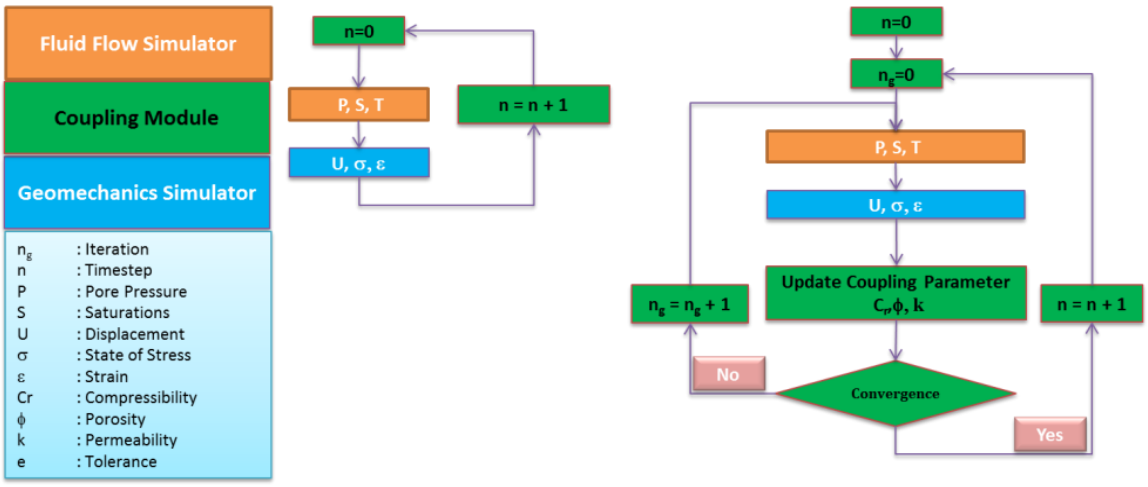

Figure 1.1. Partial coupling techniques: (a) One way coupling, (b) Two way partial coupling (Inoue and Fontoura, 2009)

An important attribute of partial coupling approaches is the capability of mapping different domain discretizations, i.e. connecting and interchanging data parameters of the FD grid to the FE mesh and vice versa. If the model geometry can be discretized using cuboid hexahedral finite elements, the FE mesh can be directly translated into a FD pillar discretization and the nodal coordinates for both simulations are identical (Cappa and Rutqvist, 2011), thus facilitating parameter exchange. However, if the model geometry is complex and the FE mesh uses tetrahedral elements, the data exchange requires a mapping approach capable of interpolating between the different spatial coordinates of the FD pillar discretization and the tetrahedral FE mesh (Bostrom, 2009).

The majority of CO_2 sequestration simulations, though, is simplified to horizontally layered basin model geometries and utilizes a shared numerical discretization for the fluid flow and geomechanical simulations (i.e. based on FD pillar grids; Figures 1.2 and 1.3; Rutqvist et al., 2002, 2008; Zhou et al., 2008; Cappa and Rutqvist, 2011). This setup prevents the consideration of more realistic, complex geologic structures and requires a simplification of any acute angles in the geometry. Acute angles, though, are a source of geometric stress concentrations and thus regions of failure at these stress concentrators are being neglected. Thus a flexible meshing algorithm capable of utilizing the optimized meshing style of each simulator is required for more realistic coupled simulations.

The current practice for CO_2 sequestration studies distinguishes between two types of lateral fluid flow boundary conditions, namely open and closed aquifer systems. Open systems, which are assumed to be interchangeable with infinite systems represent aquifer systems in large scale sedimentary basins where the system boundary is characterized by a constant pressure and often assumed to be hydrostatic (Baklid et al., 1996; Ehlig-Economides and Economides, 2010; Izgec et al., 2006; Kumar et al., 2005; Nghiem et al., 2004; Pruess et al., 2001; Sengul, 2006) enabling that the displaced brine can escape the formation. Pressure changes for such scenarios are limited to the immediate vicinity of the injection well (Amirlatifi et al., 2011; Ehlig-Economides and Economides, 2010) and the risk for geomechanical failure of the reservoir and cap rock is often negligible. Closed systems represent a compartmentalized geologic storage formation bound on all sides by low permeability formations similar to what is often observed in hydrocarbon reservoirs.

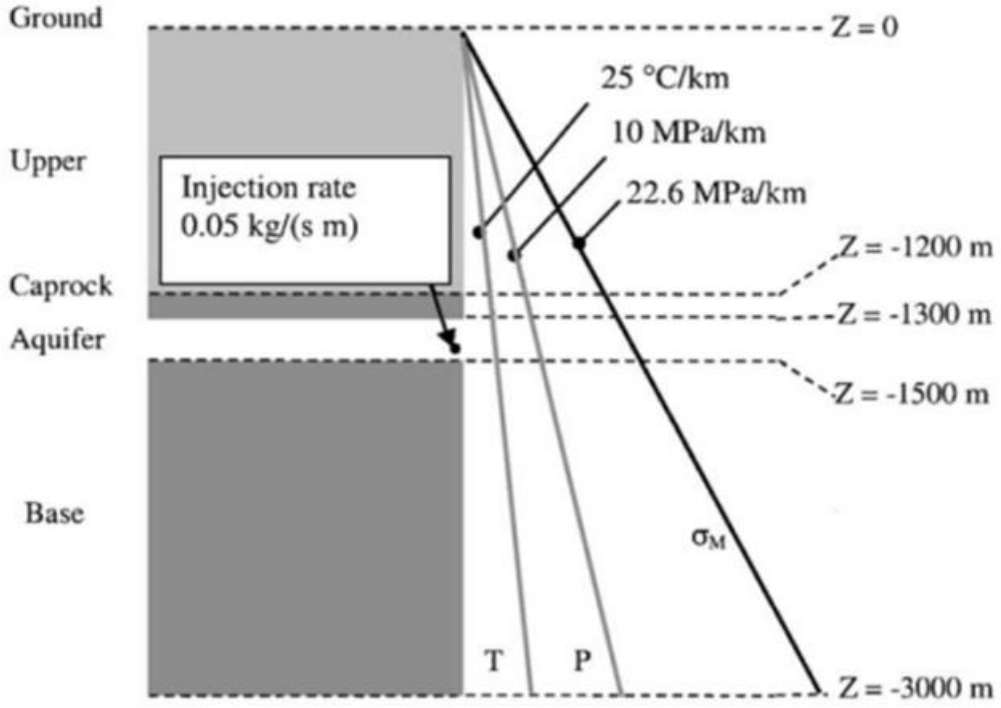

Figure 1.2. Example of horizontally layered basin used for coupled geomechanical analysis (Zhou et al., 2008)

Injection of fluids into closed systems results in significant pressure build-ups (Amirlatifi et al., 2012; Ehlig-Economides and Economides, 2010; Zhou and Birkholzer, 2007) mitigating the storage potential and the risk for geomechanical failure is high (Comerlati, 2006; Lucier et al., 2006; Rutqvist et al., 2008, 2007; Tran et al., 2010, 2009; Zoback et al., 2006).

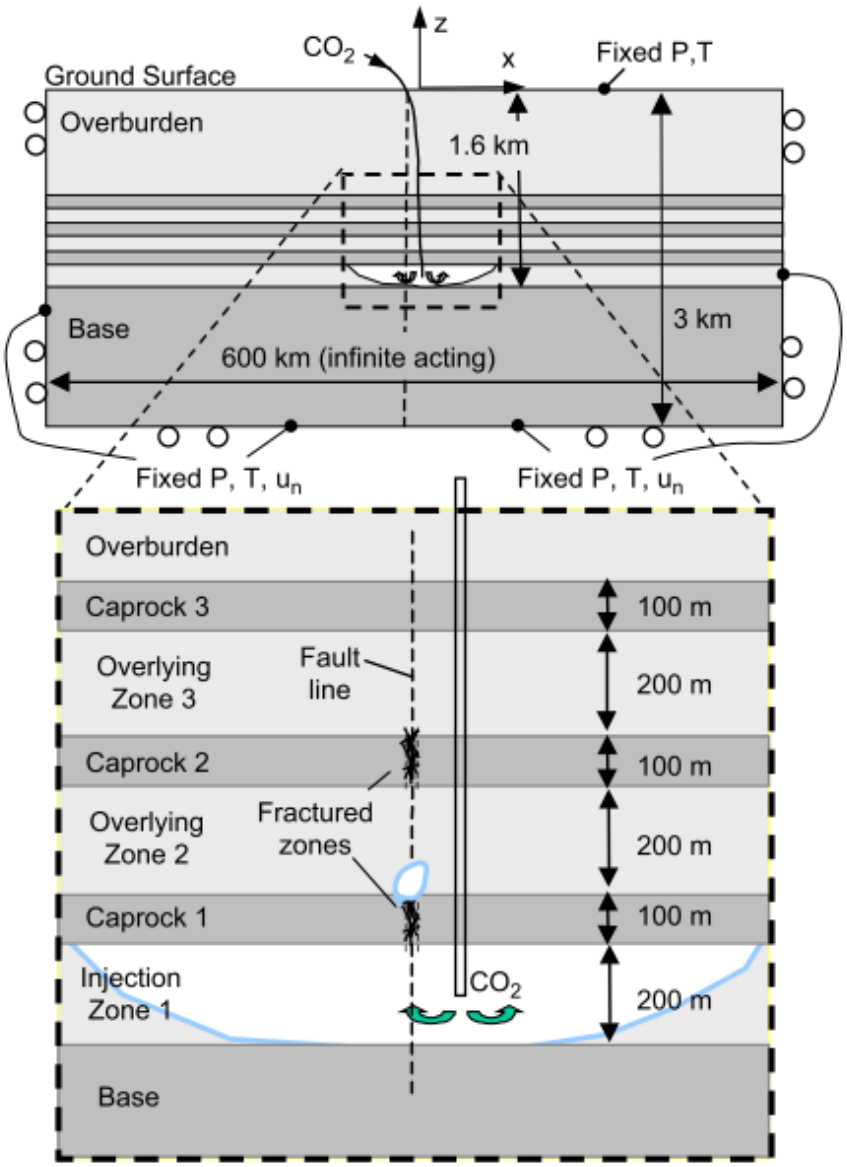

Figure 1.3. Another example of horizontally layered basins used for coupled geomechanical analysis (Rutqvist et al., 2008)

Application of knowledge from hydrology and petroleum engineering in this analogous field suggests that other intermediary fluid flow boundary conditions should be considered and open boundary condition should not be taken the same as an infinite aquifer.

1.4. APPROACH FOR ADDRESSING THE KNOWLEDGE GAPS

This study will present an iterative partial coupling implementation, the "Coupled Geomechanical Reservoir Simulator" (CGRS) that uses Schlumberger ECLIPSE™ (trademark of Schlumberger) for the fluid flow simulation and ABAQUS™ (trademark of Dassault Systèmes) for the geomechanical analysis. Both ECLIPSE™ and ABAQUS™ represent two of the most advanced and most widely used (both in academia and the hydrocarbon industry) software packages of their respective genre and as of now (to the authors' knowledge) a coupling module between the two codes has not been published. CGRS is addressing the limitations of structured FD pillar grids in modeling of complex geometries without the need of local grid refinement. This is achieved by either mapping a complex tetrahedral based FE mesh to a simplified FD pillar grid, or by utilizing FE pre-processors to generate a high quality cuboid hexahedral mesh which can be directly translated into a FD pillar grid sharing the identical nodal points. This capability of CGRS represents a significant improvement of model generation for FD simulations. In addition CGRS identifies pore pressure variation related failure, updates hydraulic permeabilities in the failed regions and is able to calculate the associated fracture outflow.

In order to quantify the fluid flow boundary conditions and remove the uncertainty of lateral flow boundary conditions, this work applies concept of a short draw down test followed by a prolonged build up test and analysis of pressure derivative curve, results of which clearly shows the difference between an open boundary, versus a closed or an infinite aquifer. An intermediate boundary condition, Semi-Open boundary, that covers an spectrum of partial pressure equivalence at the boundary is also presented that uses the concept of flu factor (Kumar, 1977a, 1977b).

1.5. AVAILABLE DATA

The Lamotte sandstone is identified as a suitable sequestration aquifer formation in the state with acceptable permeability, porosity, extension, strength and water salinity (Akpan, 2012; Govindarajan, 2012; Kumar, 2012; Miller, 2012). The Lamotte Sandstone is the first formation of the Cambrian period throughout most of Missouri that overlays the Precambrian granite. The Lamotte sandstone is capped by the Bonneterre Dolomite and higher up the shale rich Davis formation which due to its low permeability, can serve as a barrier for upward migration of fluids (Figure 1.4).

Period	Lithology	Formation Name	Group	Rock Type	Maximum Thickness (m)
Lower Ordovician		Jefferson City	Ozark	Cherty / Drusy Dolomite	3050
		Roubidoux			
		Gasconade			
Upper Cambrian		Eminence			
		Potosi			
		Derby Doerun	St Francois Confining Unit	Shaly Dolomite	394
		Davis		Dolomite Shale	510
		Bonne Terre	St Francois	Dolomite/Limestone	1030
		Lamotte		Sandstone and Conglomerate	720
Precambrian Rocks			Basement Confining Unit	Granitic, Basic and Felsitic	>720

Figure 1.4. Stratigraphy of the Lamotte sandstone and the overlying formations

An initial candidate aquifer was located in Greene County, MO, near the Springfield power plant (Nygaard et al., 2012) but the water quality assessment using (Brookshire, 1997) did not comply with the minimum admissible solid content level for CO_2 sequestration and the site was abandoned.

Assuming that the rock properties of Lamotte and Derby-Doerun formations in North-Eastern part of the state are comparable to the outcrops and the formations in the South-Eastern part of the state, the present work will use log, core and rock mechanic analysis conducted at Missouri University of Science and Technology (Akpan, 2012; Govindarajan, 2012; Kumar, 2012; Miller, 2012) to set up the rock physics models.

Figures 1.5 and 1.6 show acoustic logs and core samples used for property determination by Akpan (2012) for this study.

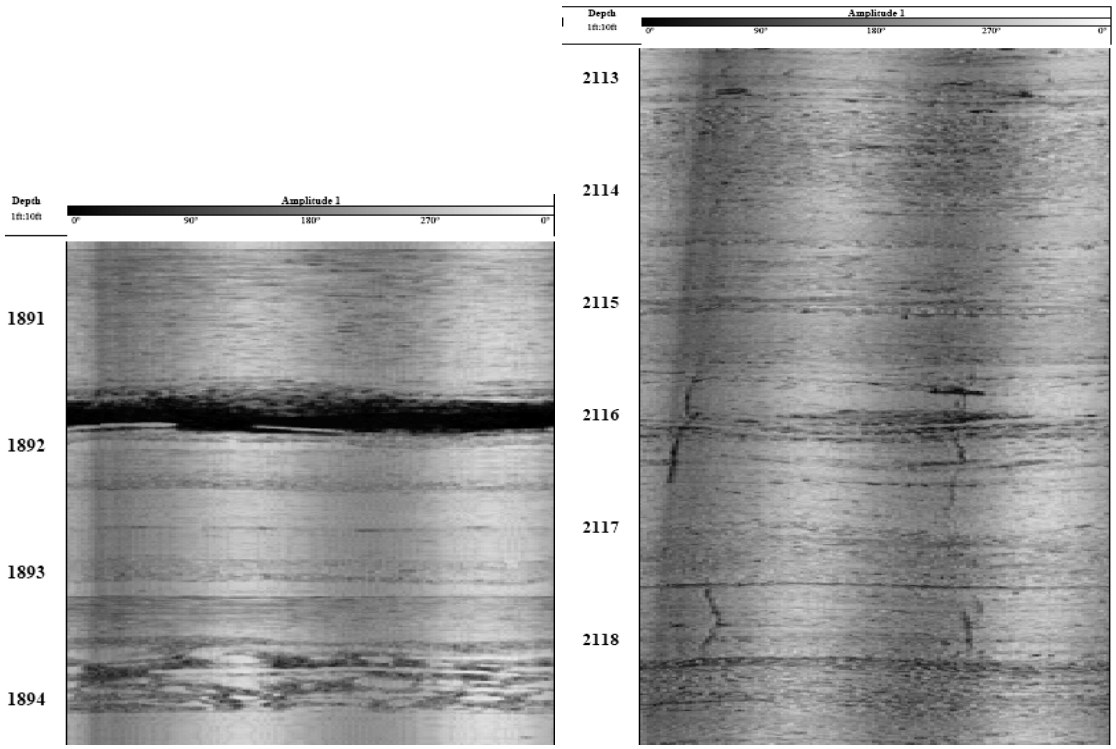

Figure 1.5. Bonneterre (left) and Lamotte (right) acoustic image (Akpan, 2012)

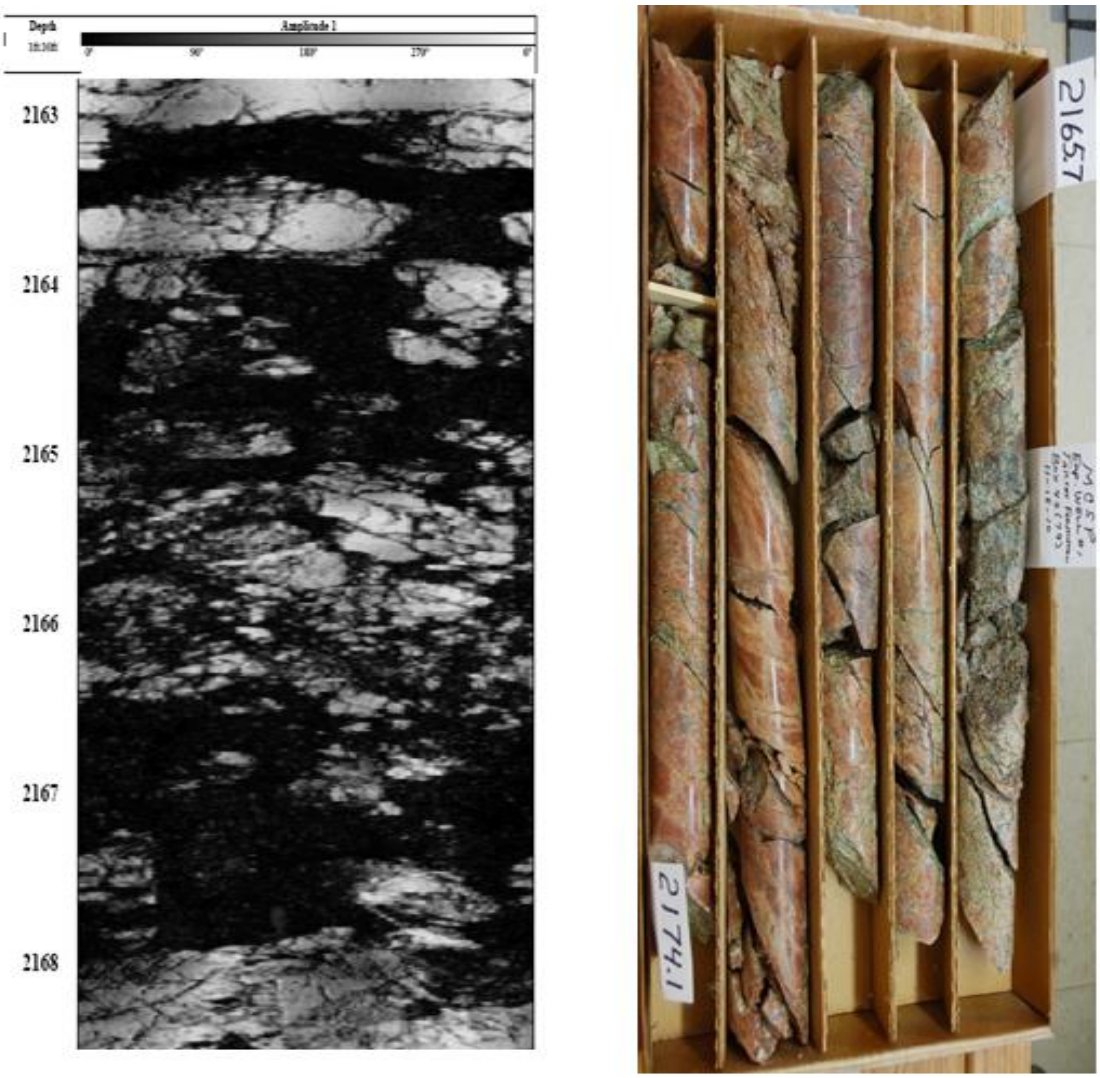

Figure 1.6. Precambrian formation borehole images (Akpan, 2012)

Figures 1.7 and 1.8 show assembly and testing of an outcrop sample undergoing Brazilian test for determination of mechanical properties of the rock conducted by Govindarajan (2012).

The analysis is also based on structural and salinity level maps for the state of Missouri published by USGS and Missouri Department of Natural Resources.

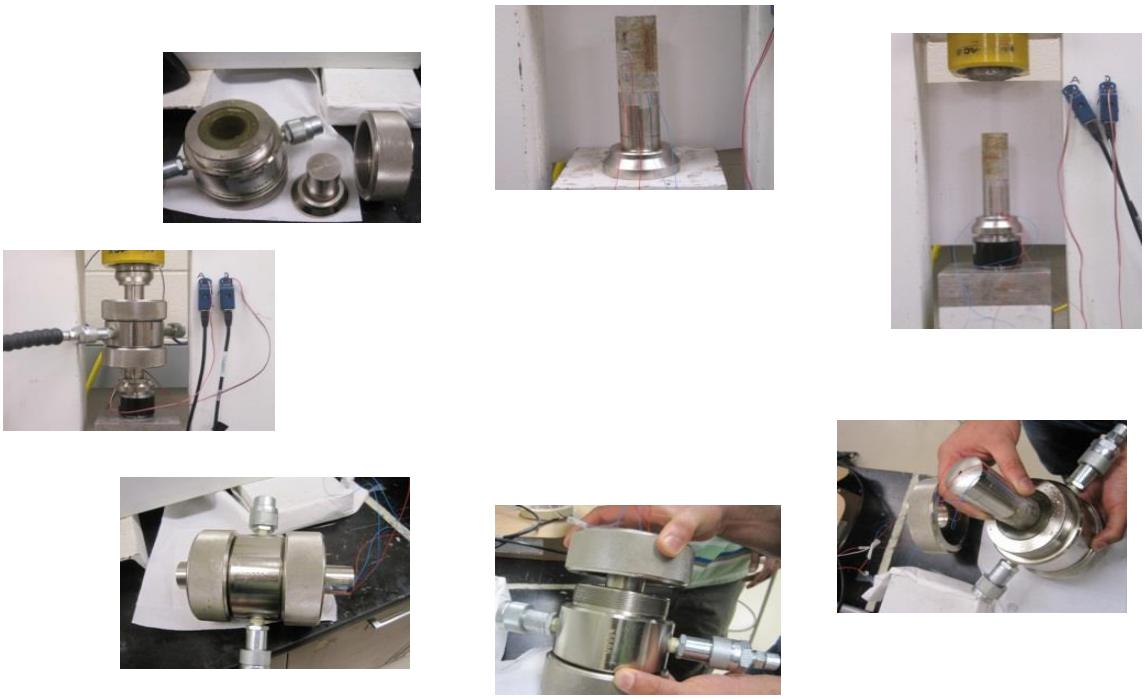

Figure 1.7. Images showing the mounting of the outcrop samples used for triaxial testing (Govindarajan, 2012).

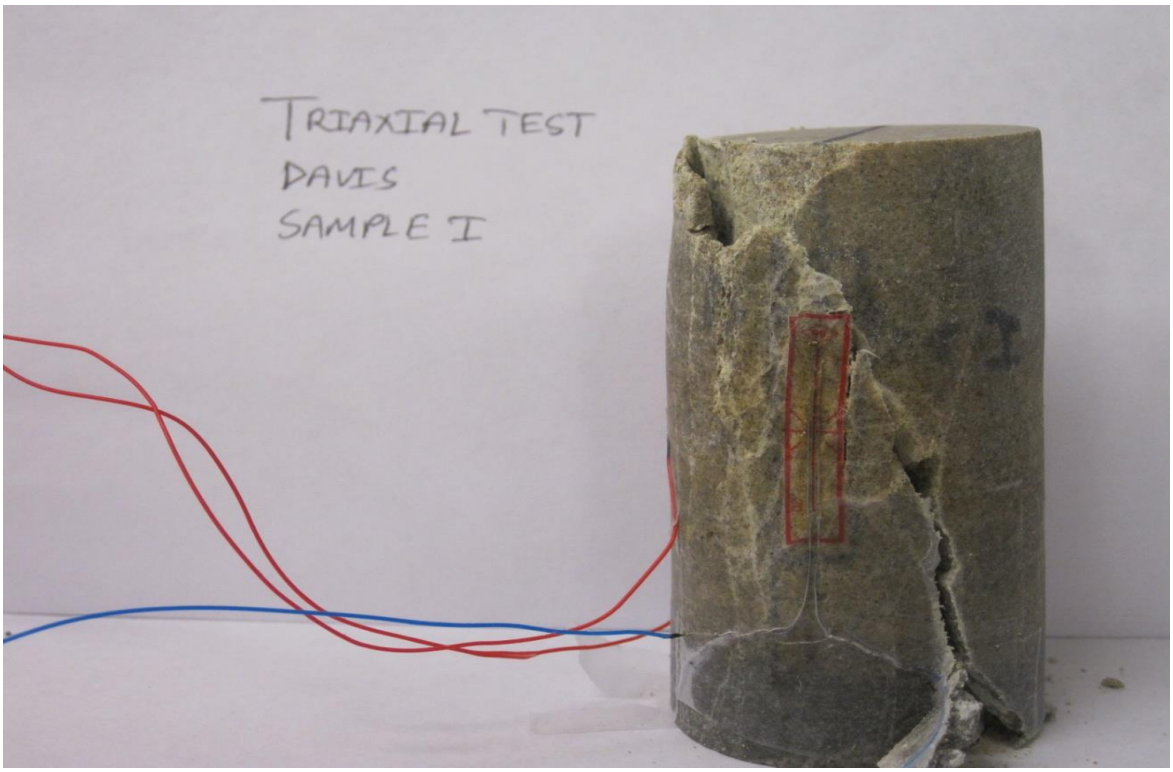

Figure 1.8. Davis rock sample after triaxial testing (Govindarajan, 2012).

1.6.RESEARCH OBJECTIVES

This research addresses the following three objectives:

1. Developing methods to perform coupled 3D reservoir and multi scale geomechanical simulations,
2. Quantifying fluid flow boundary conditions, and
3. Assessing CO_2 sequestration feasibility in Missouri.

The objectives are described in more details below:

1.5.1. Objective 1 - Developing Methods to Perform Coupled Reservoir and Geomechanical Simulations. The first objective comprises the analysis of existing methods and filling the knowledge gap by developing methods to perform coupled 3D reservoir and multi-scale geomechanical simulations using existing commercial simulators to simulate leakage and reservoir stability.

1.5.2. Objective 2 - Quantifying Fluid Flow Boundary Conditions. In order to attain the second objective a set of analytical relationships together with different realizations of fluid flow boundary conditions are presented. Boundary conditions that are examined include open, closed (Ehlig-Economides and Economides, 2010; Zhou et al., 2008), infinite and semi-open. This study is limited to a horizontally layered basin model with variable boundary conditions. Results of this study will abolish the guess from fluid flow boundary condition and help in quantifying it through pressure transient analysis, differentiating between the commonly mistaken open and infinite boundary conditions and most importantly, the notion of semi-open lateral fluid flow boundary which acts as an intermediary between open and closed boundary conditions.

1.5.3. Objective 3 – Assessing CO_2 Sequestration Feasibility in Missouri. A suitable pinchout formation in the North-Eastern part of the state is identified in the Lincoln fold, where the Lamotte sandstone has a favorable thickness, depth and extent for shallow CO_2 sequestration, Figure 1.9. This formation is located in the proximity of several coal fired power plants, Figure 1.10, which makes it a favorable candidate spot for long term CO_2 sequestration in the state. In order to achieve objective 3, coupled geomechanical reservoir simulation is conducted on the shared earth model representation of this candidate

formation and safe injection limits of the formation, together with geomechanical risks are identified.

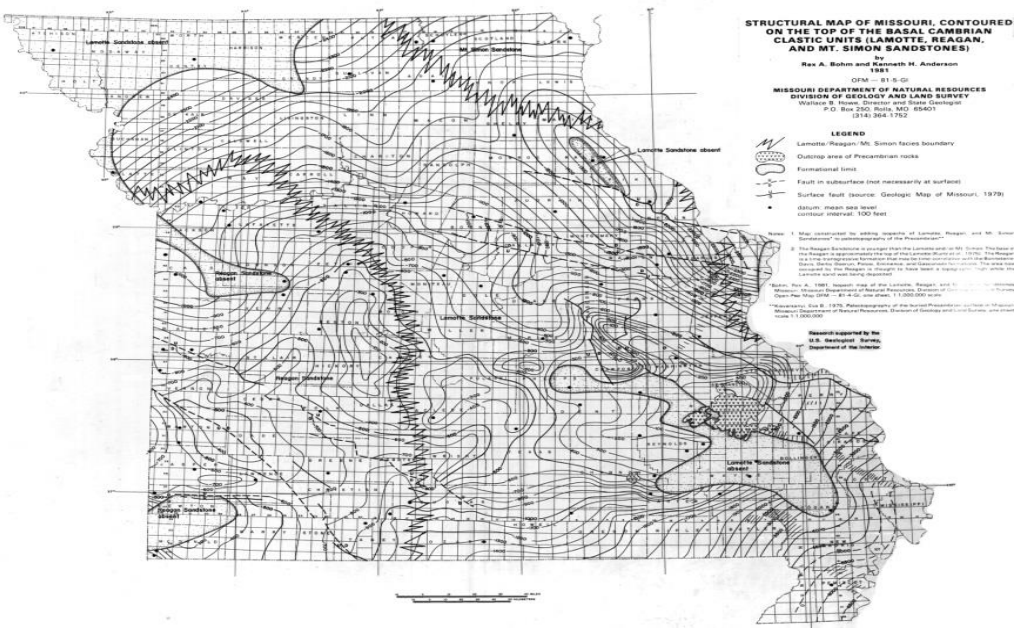

Figure 1.9. Structural map of Missouri contoured on the top of the Basal Cambrian Clastic units (Lamotte, Reagan and Mount Simon sandstones) (Bohm and Anderson, 1981)

Figure 1.10. Missouri Coal Fired Power Plants ("Missouri and Coal - Sourcewatch," 2013)

PAPER

1. AN EXPLICIT PARTIAL COUPLING APPROACH FOR SIMULATING CO_2 SEQUESTRATION

(Submitted for review to the International Journal of Greenhouse Gas Control)

Amirlatifi[1], Amin, Eckert, Andreas, Nygaard, Runar, and Bai, Baojun.

Geological Sciences & Engineering, Missouri University of Science and Technology, 129 McNutt Hall 1400 N. Bishop, Rolla, MO 65409, USA

Abstract

This paper presents the methodology for coupled geomechanical fluid flow simulations to study effects of pore pressure and temperature variation on permeability, porosity and rock stability during fluid injection/production processes. A coupling module is developed that employs coupled fluid flow analysis using Schlumberger Eclipse® as the fluid flow simulator and ABAQUS® as the geomechanical analysis package. The coupling module employs a 2-way explicit partial coupling scheme and is capable of interpolating model parameters between different domain discretizations of the finite difference model and the finite element model. This capability ensures a high degree of flexibility to handle complex geometries. Furthermore, the formation of new fractures or reactivation of existing faults or fracture sets is simulated by a variation in structural permeability and the associated fracture outflow can be calculated. Application of this coupling module on the study of long term CO_2 sequestration in three realizations using different discretization schemes of a theoretical pinchout formation is demonstrated and the results are compared with a scenario that does not employ geomechanics. The results of this study show the

[1] Corresponding author. Tel.: +1-573-341-6059; fax: +1- 573-341-6953. E-mail address: aar38@mst.edu

significance and necessity of coupled geomechanical and fluid flow simulations for reliable modeling of such processes.

Highlights:

1. We present an overview of coupled geomechanical reservoir simulation.
2. We present a new fully automated two way coupling module that couples Eclipse and ABAQUS.
3. Coupled analysis is required for CO_2 sequestration studies.

Keywords: geomechanics, reservoir simulation, coupling, CO_2 sequestration, plastic deformation

1. Introduction

Geologic sequestration of CO_2 into depleted hydrocarbon fields, deep saline aquifers, or coal seems has been identified as a viable procedure to reduce the CO_2 content in the atmosphere and as a measure to counteract global warming (Ipcc, 2005). It is clear that the long term feasibility and sustainability of CO_2 sequestration projects depends on minimizing the associated risks, a variety of which are related to the fluid injection associated pore pressure increase in the rock formation. Not only does fluid injection change the formation pore pressure, but also the magnitude of the minimum horizontal stress, σ_h, varies, e.g. Engelder and Fischer (1994), a phenomena termed "pore pressure – stress coupling" (Hillis, 2001; Tingay et al., 2003). This coupling has significant implications for failure mechanism (Cappa and Rutqvist, 2011; Hillis, 2003; Philip et al., 2005; Rutqvist et al., 2008; Settari and Mourits, 1998; Thomas et al., 2003) fault reactivation (Cappa and Rutqvist, 2011; Streit and Hillis, 2004) and caprock integrity

(Cappa and Rutqvist, 2011; Rutqvist et al., 2008, 2007; Zhou and Birkholzer, 2007; Zhou et al., 2008).

CO_2 sequestration represents physical processes that involve multiphase and multi-component fluid flow in a geologic system. The study of mechanical deformations under such conditions is achieved by numerical modeling of fluid flow through porous medium coupled with a geomechanical analysis of the medium at different pore pressure distributions (Rutqvist et al., 2002; Settari and Mourits, 1998; Settari and Walters, 1999; Thomas et al., 2003; Vidal-Gilbert et al., 2009). The coupling of the different physical processes can be achieved either by a fully or partially coupled numerical simulation.

In the fully coupled simulation approach, the fluid flow through pores and elasticity calculations are carried out simultaneously. (Lewis and Sukirman, 1993; Tortike and S.M., 1987; Xikui and Zienkiewicz, 1992) have presented formulations for the fully coupled approach, and Gutierrez and Lewis (1998) have presented a fully coupled reservoir simulator. However, the complexity of a fully coupled physical system results in very high computational costs and thus the applicability of the fully coupled approach is limited (Inoue and Fontoura, 2009).

In order to mitigate this disadvantage a variety of partially coupled modeling approaches have been developed (Helmig et al., 1998; Longuemare et al., 2002; Rutqvist et al., 2002; Settari and Mourits, 1998, e.g. 1994; Tsang, 1999). Partial coupling approaches are based on an external coupling between separate numerical simulations. In general, a conventional reservoir simulator based on the finite difference (FD) method is used to process the fluid flow problem and a finite element (FE) model is used to solve the stress equilibrium equations, respectively. This method benefits from the latest developments in

each field, has lower computational costs and hence the best simulator available can be employed. In general, partial coupling can be divided into two families: explicit and iterative coupling. Fig. 1 shows the general algorithm for explicit (one way) and iterative (two way) partial couplings. In the explicit coupling approach (Fig. 1-a) a reservoir simulator carries out fluid flow calculations at each time-step; however, stress-displacement calculations are only carried out on selected time-steps, the choice of which depends on the variation in the accessible pore space due to the change in pore pressure, i.e. if the variation in pore space between time-steps is not significant, then geomechanical calculations may be ignored. Once the change in pore space is considerable, the stress-displacement analysis is carried out (Minkoff et al., 2003, 1999; Settari and Walters, 1999). This approach can significantly reduce the computation cost of the coupled analysis through reduced number of stress-displacement simulation runs, but may result in unstable solutions and loss of accuracy due to the coupled nature of the processes (Dean et al., 2006). In the iterative coupling approach (Fig. 1-b) the two simulators are coupled at each time-step.

An important attribute of partial coupling approaches is the capability of mapping different domain discretizations, i.e. connecting and interchanging data parameters of the FD grid to the FE mesh and vice versa.

If the model geometry can be discretized using cuboid hexahedral finite elements, the FE mesh can be directly translated into a FD pillar discretization and the nodal coordinates for both simulations are identical (Capasso and Mantica, 2006; Cappa and Rutqvist, 2011; Dean et al., 2006), thus facilitating parameter exchange. However, if the model geometry is complex and the FE mesh uses tetrahedral elements, the data exchange

requires a mapping approach capable of interpolating between the different spatial coordinates of the FD pillar discretization and the tetrahedral FE mesh (Bostrom, 2009; Verdon et al., 2011).

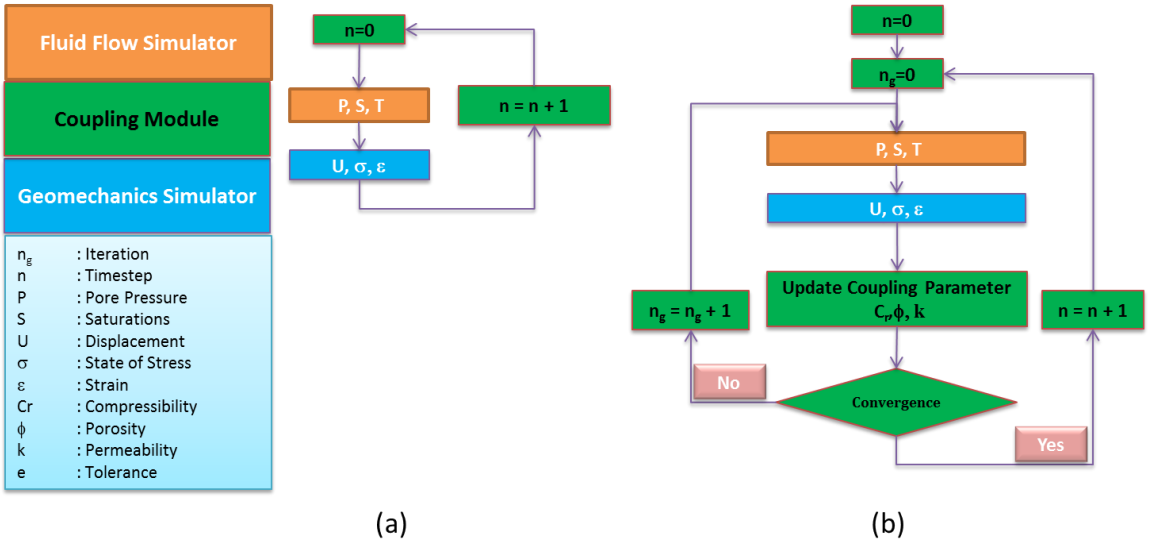

Fig. 1 - Partial coupling techniques:
(a) One way coupling – Fluid flow simulations are carried out at each time-step, but stress-displacement calculations are only carried out when there is a significant change in the pore pressure.
(b) Two way partial coupling – Fluid flow and stress-displacement calculation are carried out at each time-step and results of one simulator are used to update the input parameters of the other simulator (Inoue and Fontoura, 2009).

In this paper, an iterative partial coupling implementation, the "Coupled Geomechanical Reservoir Simulator" (CGRS), is presented that uses Schlumberger ECLIPSE™ (trademark of Schlumberger) for the fluid flow simulation and ABAQUS™ (trademark of Dassault Systèmes) for the geomechanical analysis. CGRS is addressing the limitations of structured FD pillar grids in modeling of complex geometries without the need of local grid refinement. This is achieved by either mapping a complex tetrahedral

based FE mesh to a simplified FD pillar grid, or by utilizing FE pre-processors to generate a high quality cuboid hexahedral mesh which can be directly translated into a FD pillar grid sharing the identical nodal points. This capability of CGRS represents a significant improvement of model generation for FD simulations. In addition, CGRS identifies pore pressure variation related failure, updates hydraulic permeabilities in the failed regions and is able to calculate the associated fracture outflow.

1.1 . Theoretical Background

1.1.1 Fluid flow equations. Fluid flow simulation is based on the conservation of mass and energy for the oil, gas and water in the system with the assumption that the overall composition of the phases stays the same throughout the simulation, or the compositions change with the change in pressure, temperature and exposure to injected material. The former is referred to as black oil simulation while the latter is termed compositional simulation. The two approaches share the same basis which is briefly outlined.

The conservation of mass for a control volume is expressed as (Chen et al., 2006):

$$-\nabla.(\rho_l v_l) + q_l = \frac{\partial(\phi \rho_l S_l)}{\partial t} \qquad l = Oil, Gas, Water \tag{1}$$

The overall fluid saturation in the medium will equal unity at all times:

$$\sum_{l} \mathrm{S_i} = 1 \tag{2}$$

Conservation of momentum for the multi-component system is expressed by Darcy's law (Darcy, 1856):

$$v_l = -\frac{k_l}{\mu_l}(\nabla p_l - \rho_l g \nabla z) \tag{3}$$

The combined mass and momentum balance equation is then given by (Chen et al., 2006):

$$\nabla\left[\frac{\rho_l k_l}{\mu_l}(\nabla p_l - \rho_l g \nabla z)\right] + q_l = \frac{\partial}{\partial t}(\phi \rho_l S_l) \tag{4}$$

This can be written in terms of the piezometric head or flow potential as:

$$\nabla\left[\left(\frac{\rho_l}{\mu_l}k_l\right)\nabla\Phi_l\right] + q_l = \frac{\partial}{\partial t}(\phi \rho_l S_l) \tag{5}$$

Where Φ_l is:

$$\Phi_l = \mathrm{p}_l - \rho_l \mathrm{g}\mathrm{z} \tag{6}$$

The conservation of energy in a non-isothermal system is given by (Chen et al., 2006):

$$\frac{\partial}{\partial t}\left(\phi \sum_{\alpha=1}^{N_p} \rho_\alpha S_\alpha U_\alpha + (1-\phi)\rho_s c_s T\right) + \nabla . \sum_{\alpha=1}^{N_p} \rho_\alpha u_\alpha H_\alpha - \nabla . (K_T \nabla T) = q_H - q_L \tag{7}$$

Depending on the numerical simulator that is used, the continuous model domain in a FD model is discretized into a structured (pillar grid) or an unstructured grid and the governing equations are solved in different schemes, including Implicit Pressure Explicit Saturation, IMPES, (Aziz and Settari, 1979; Sheldon et al., 1959; Stone and Garder Jr., 1961) and Adaptive Implicit Method, AIM, (Thomas and Thurnau, 1983). A further and more extensive review of the FD method is beyond the scope of this paper and can be found in many standard text books (Aziz and Settari, 1979; Chen et al., 2006; Peaceman, 1977).

1.1.2 FE equations. ABAQUS™ is a standard finite element (FE) software package which supports a wide range of structural, geomechanical, thermal, diffusion, and coupled analyses. Providing both linear and nonlinear response options, solutions for a large variety of engineering and scientific problems can be obtained. In an ABAQUS™ stress-displacement analysis a solution to a boundary value problem is found when both force and moment equilibrium is maintained at all times over any arbitrary volume of the model domain. This is achieved by solving the equation of motion (representing the conservation of linear momentum):

$$\nabla\cdot\sigma + \mathrm{F} = \rho\frac{\partial^2 u}{\partial t^2} \tag{8}$$

Conservation of angular momentum is guaranteed by the use of the Cauchy stress tensor. If accelerations are negligible, a common assumption for rock mechanical purposes, the stress equilibrium equations result:

$$\nabla\cdot\sigma + \mathrm{F} = 0 \tag{9}$$

In order to solve this equation the constitutive relationship between stress and strain in a porous, liquid filled system needs to be defined (Jaeger et al., 2007) .

$$\varepsilon = \frac{1}{2G}\sigma - \frac{\upsilon}{2G(1+\nu)}\,trace(\sigma)I \tag{10}$$

The strain-displacement relationship is given by the infinitesimal strain tensor:

$$\varepsilon = \frac{1}{2}[\nabla \mathrm{u} + (\nabla u)^{\mathrm{T}}] \tag{11}$$

Further constitutive equations including plasticity laws can be included. ABAQUS finds a solution of such boundary value problems by transforming Eq. (11) into a weaker statement which results in the principle/statement of virtual work ("ABAQUS 6.12 User Documentation," 2012; Zienkiewicz et al., 2005):

$$\int_{\Gamma} \delta u^T T d\Gamma + \int_{\Omega} \delta u^T F \,\mathrm{d}\Omega = \int_{\Omega} \delta\varepsilon^T \sigma \,\mathrm{d}\Omega \tag{12}$$

The continuous model domain in a FE model is discretized into an arbitrary number of finite elements and by introducing approximation functions for each finite element, $\boldsymbol{u} \approx \sum_a \boldsymbol{N}_a \tilde{\boldsymbol{u}}_a^e$, Eq. (12) can be written in the general FE equation $\boldsymbol{K}\,\boldsymbol{u} + \boldsymbol{F} = 0$, and be solved. A further and more extensive review of the FE method is beyond the scope of this paper and can be found in many standard text books, e.g. Zienkiewicz et al. (2005).

In a nonlinear 'effective stress'-displacement analysis (such as CO_2 injection related effective stress changes) a solution cannot be calculated by solving a single system of linear equations. In ABAQUS™ the solution of the nonlinear equilibrium equations is found by specifying the loading as a function of time and Newton's algorithm is used to obtain the solution during a series of time increments. Several iterations to obtain equilibrium may be needed within each increment ("ABAQUS 6.12 User Documentation," 2012).

1.2. Coupling approach

The present work uses an iterative explicit partial coupling, i.e. a two way coupling, of ABAQUS™ for finite element geomechanical stress/displacement analysis and Eclipse™ for finite difference fluid flow simulations. A coupling module is developed in Java™ that performs coupling at user specified time intervals and checks for several different coupling parameters. The coupled simulation requires the FD and FE codes to be solved sequentially and coupling parameters are transferred to each simulator at each time interval. Coupling is performed based on the change in hydraulic properties as a function of strain. The two simulators are coupled through volumetric change of the porous medium

by the change in pore pressure, Pp, from the FD which results in strains, ε, in the FE model. The new strains yield changes in the permeability, k, and porosity, ϕ. The explicit partial coupling means that the permeability and porosity values are updated at the end of each FE run and the new values are used for the next FD run.

1.3. Mapping approach and data transfer

The majority of coupled analyses utilize the same discretization for FD (extended to overburden and sides) and FE simulations. Such a shared mesh is limited by the resolution of pillar gridding for the FD approach in complex geometries (Rutqvist et al., 2002; Vidal-Gilbert et al., 2009). This means that location of stress concentrations in the reservoir and overburden, for example, need to be discretized using local grid refinements and/or a fine resolution FE mesh which can result in a considerable increase in the computation cost of the coupled analysis.

An alternative technique is to use the native discretization scheme of each simulator. The general advantage of a FE mesh over FD pillar grids is the use of tetrahedral elements at locations of stress concentrations, like faults, fractures or pinchouts. Thus, a FE mesh can discretize complex geometries more realistically.

In order for the coupling module to transfer and exchange parameters between the different simulators, it needs to reconstruct the two meshes and determine the spatial position of each nodal point with respect to the other mesh. Once new parameters are calculated in one simulator, the module will assign them to the corresponding nodes in the other mesh and the updated input data for this simulator is generated. This data transfer depends on the discretizations being used for the FD and the FE model, respectively.

Coupled Geomechanical Reservoir Simulator (CGRS) is able to transfer the coupling parameters for three different discretization scenarios. This is accomplished by a complete mapping of the two geometries before execution of a coupled analysis which results in the generation of a mapping file between the two geometries. The mapping file is used in the subsequent coupled simulation runs to check if the containments (Fig. 2) are still valid with the updated nodal coordinates of the finite elements due to the resulting displacements. If a finite element is no longer in the vicinity of the previously determined FD grid block, then the neighboring FD grid blocks are examined for its containment. If none of the neighboring grid blocks contain that element either, the whole FD grid is examined to find the new container for the element.

The mapping is performed in three categories:

a) FD and FE model use the same cuboid hexahedral mesh

   The nodal coordinates of each finite element in the mesh are checked against the corner points of each FD grid block. A match in coordinates means that the same mesh resolutions are used and that the coupling parameters can be exchanged without interpolation/averaging.

b) FD and FE model use cuboid hexahedral meshes of different resolution

   Assuming that the FD grid is the coarser of the two discretizations one or more finite elements will be located either exactly at the boundaries of the FD grid block, or be inside the boundaries of it. Thus, the coupling module needs to be able to determine the FD grid block that surrounds each element from the finite element mesh. This type of mapping can be done in several ways. Bostrom (2009) has demonstrated mapping through determination of the nearest

neighbor. We have employed a technique to determine the container grid block which enables us to overcome the limitations of current FD simulators in terms of discretization and precise handling of discontinuities. In this novel approach we find the centroid of the element and calculate the number of times that a ray drawn from the centroid to the origin will cut through the sides of each FD grid block (Fig. 2). This way we can determine the container grid block for different resolutions and also for different element types, such as tetrahedral elements.

A point in space, centroid in this case, is inside a cube if the number of times a ray drawn from that point cuts through the sides of the cube is an odd number. For example, points P1 and P2 (Fig. 2), are outside the cube because the rays drawn P1 does not cut through the cube and the ray drawn from P2 cuts through two sides of the cube, an even number. On the other hand, point P3 is inside the cube, because the ray drawn from this point cuts through one side of the cube, an odd number, and this cube is assigned as the container of point P3.

c) FD mesh is pillar based vs. tetrahedral FE mesh

The same approach as for a different mesh resolution (part b of this section) is employed for determination of the grid block that contains finite elements. Coordinates of the tetrahedral element's centroid is determined using the following equation:

$$\left(\frac{(x_1 + x_2 + x_3 + x_4)}{4}, \frac{(y_1 + xy_2 + y_3 + y_4)}{4}, \quad \frac{(z_1 + z_2 + z_3 + z_4)}{4}\right) \qquad (13)$$

and a ray is drawn from this point to the origin.

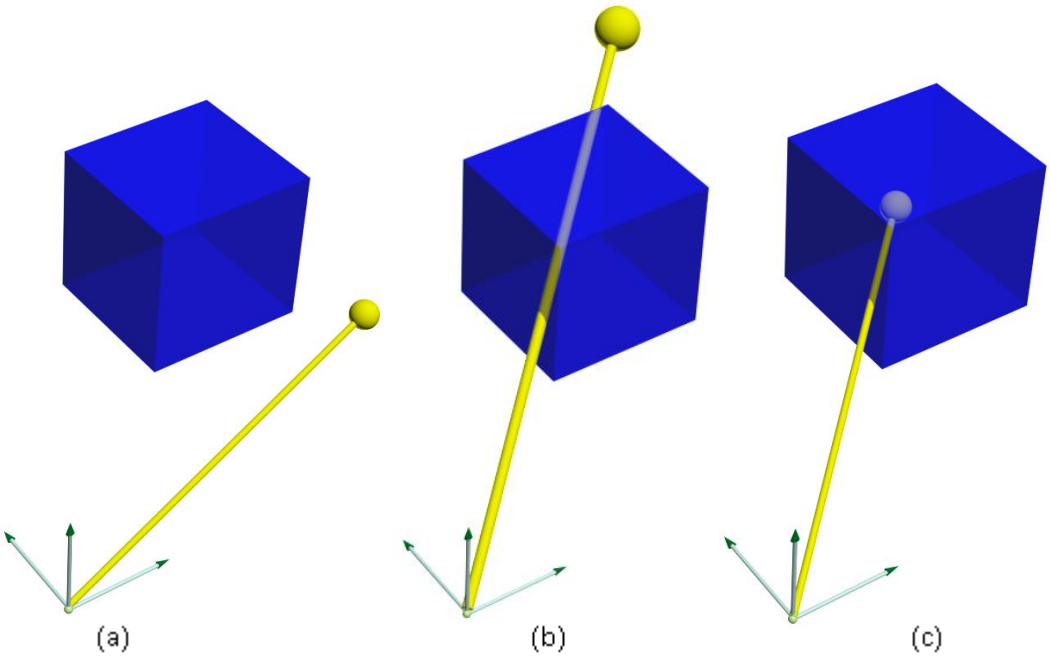

Fig. 2 - Relative position of points with respect to a grid block.
A ray is drawn from the point to the origin and number of times that the ray cuts through faces of a grid block are counted. No intersection with the grid block or an even number of intersections indicates that the point is outside the grid block (P1 and P2) while an odd number indicates that the point is inside the grid block (P3).

In general FD models are generated within 3D Mechanical Earth Modeling software packages (e.g. Petrel™ or GOCAD™) which utilize 3D seismic information, well logging data, maps, etc. to generate 3D surfaces which are then transformed into a FD grid. In order to generate a unified and realistic FE model, a file convertor is developed that transforms the FD pillar grid into the equivalent FE mesh, which can later be optimized in a FE preprocessor.

1.4. Coupling module

The coupling module of CGRS is the main driver of the coupled analysis and runs the simulators in sequential order and passes the coupling parameters between the two

simulators at specified time intervals. ABAQUS™ and Eclipse™ are coupled by the change of effective stresses due to a change in pore pressure, and by varying hydraulic rock properties which change due to the effective stresses. In addition to the standard two-way partial coupling approach (Fig. 1-b), the coupling module presented in this study has the ability to check for formation/reactivation of fractures (F condition) and excessive uplift at the surface (U condition) (Fig. 3).

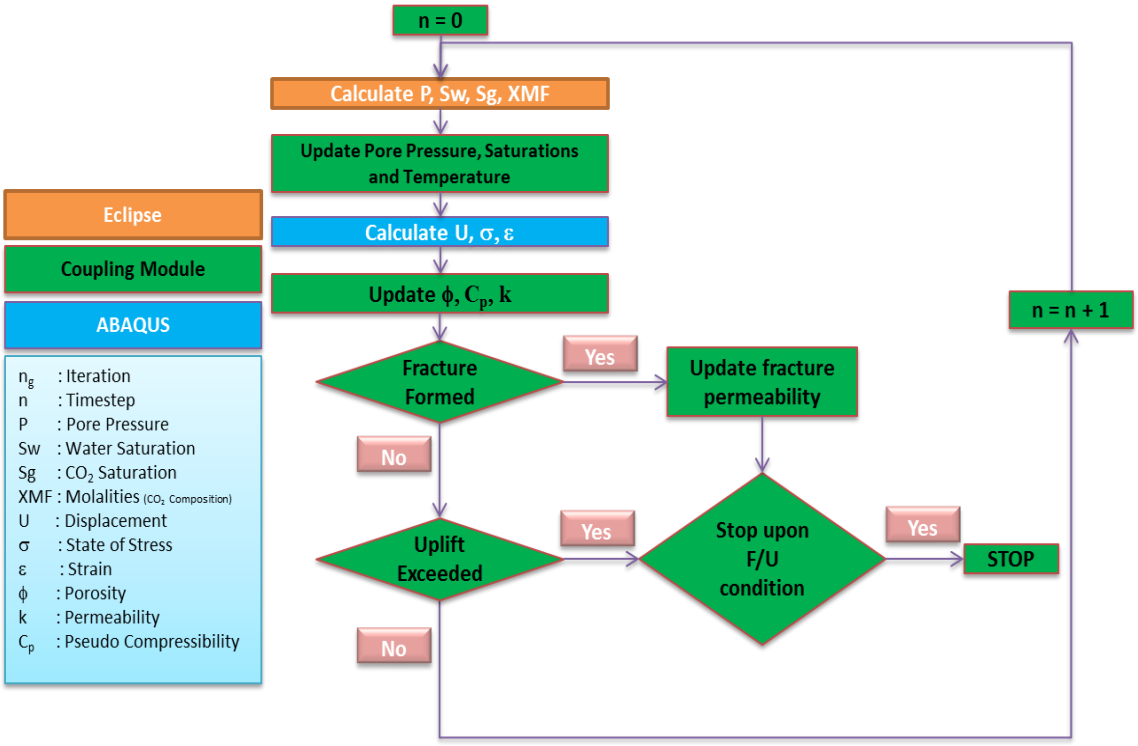

Fig. 3 – Schematic of the coupling algorithm – In addition to the standard iterative partial coupling algorithm, this study detects formation of fractures and surface uplift (F/U conditions) and updates the models such that increased permeabilities due to fracturing are accounted for.

In order to simulate realistic stress magnitudes the coupled process requires a stress initialization procedure for the finite element model (also termed pre-stressing) wherein

the modeled effective stresses (we assume hydrostatic pore pressure conditions) as a result of gravitational compaction reach a state of equilibrium. A common procedure to simulate realistic in situ stresses involves the following steps (Buchmann and Connolly, 2007; Eckert and Connolly, 2007; Hergert and Heidbach, 2011):

1) gravitational pre-stressing;

2) application of horizontal strain in order to simulate any tectonic contribution.

Once the respective initial state of stress is established the coupled routine outlined in Fig. 4 is followed.

Iterations start by determining pore pressure, fluid saturation and temperature distribution in the model assuming that rock intrinsic properties remain constant (Fig. 4). Pore pressures and temperatures calculated by the fluid flow simulator are transferred into the geomechanics simulator by rewriting the corresponding input data files of the geomechanics simulator. The geomechanics simulator then calculates nodal displacements and the state of stress and strain under the new pore pressure and temperature distribution, along with the possibility of rock failure and the extent of such failures. The new resulting strain of the system is then used to update the porosity and permeability and the corresponding input data files of the fluid flow simulator. In the advent of rock failure or reactivation of existing fractures, i.e. if plastic strain values within an element reach threshold values of 1% for extensional stresses and 5% for compressional stresses (Collins et al., 2004), the orientation and location of failure are investigated to identify caprock penetrating fractures. Since the fluid flow simulation is conducted utilizing the conventional single porosity assumption, the presence of the fracture is emulated by the placement of a virtual well that yields the same fluid through pass as the fracture. On top

of the lower computation cost compared to a fractured reservoir simulation, this technique can predict the volume of fluid that passes through the fracture.

In order to calculate the new pseudo compressibility and porosities as a function of pressure and volumetric strain (Inoue and Fontoura, 2009), the change in pore pressure and the elemental volumetric strain values are averaged over the grid block. The pseudo compressibility of rock, C_{Pseudo} is given by:

$$C_{Pseudo} = \frac{(\varepsilon_V^{n+1} - \varepsilon_V^{n})}{\phi_0 (P_p^{n+1} - P_p^{n})} \tag{14}$$

where ε_V^n is the volumetric strain at pore pressure P_p^n and ε_V^{n+1} is the new volumetric strain under the new pore pressure, P_p^{n+1} and change in porosity is given by:

$$\phi^{n+1} = \phi^{n} + \alpha(\varepsilon_V^{n+1} - \varepsilon_V^{n}) + \frac{1}{Q}(P_p^{n+1} - P_p^{n}) \tag{15}$$

where ϕ^n is the existing porosity, at pore pressure P_p^n and volumetric strain ε_V^n and ϕ^{n+1} is the new porosity resulting from the new pore pressure, P_p^{n+1} and the new volumetric strain ε_V^{n+1}.

Q is defined as:

$$Q = \frac{1}{C_f \phi^n + C_r(\alpha - \phi^n)} \tag{16}$$

and α, is defined as:

$$\alpha = 1 - \frac{K_D}{K_S} \tag{17}$$

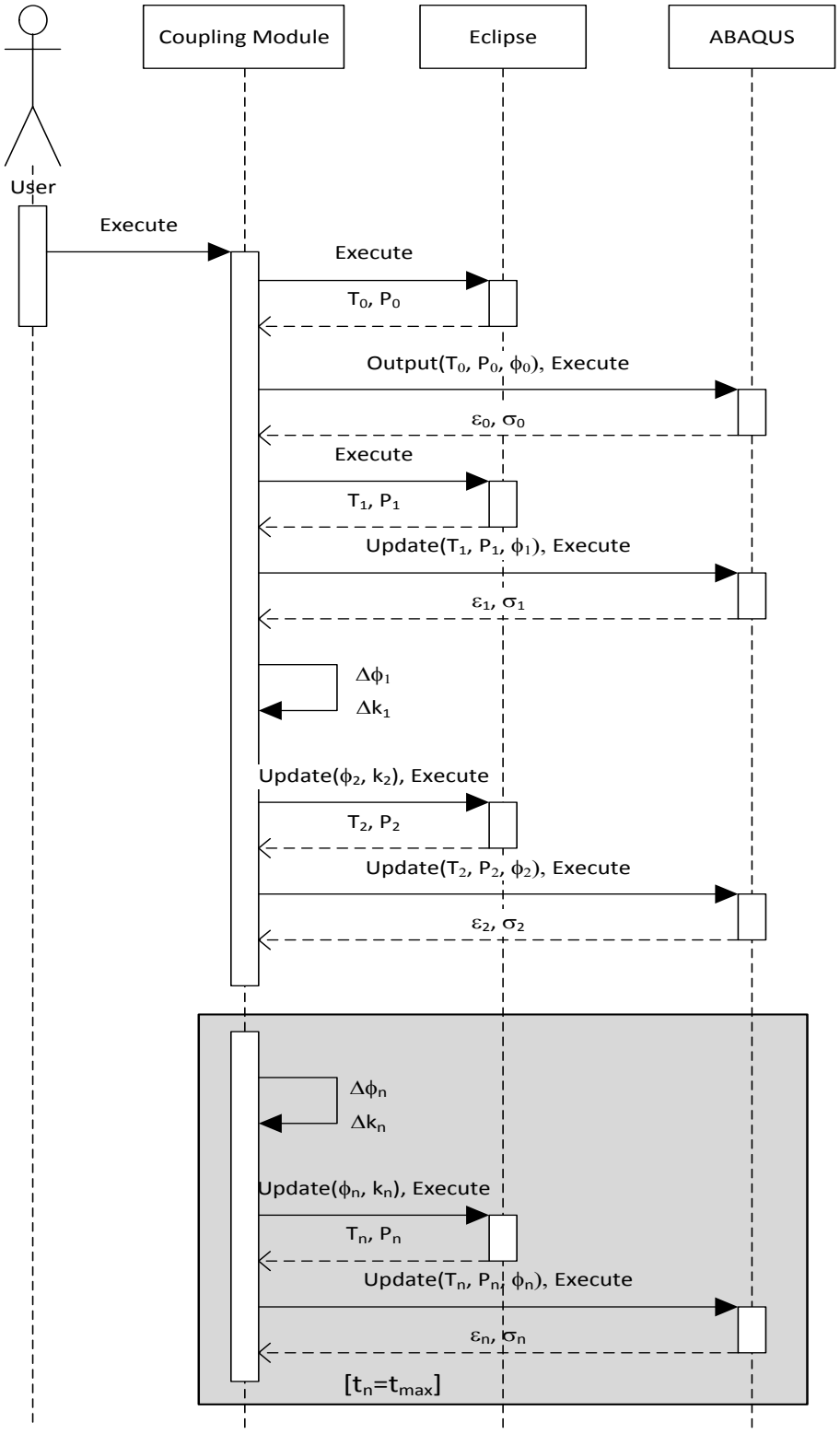

Fig. 4 - Sequence diagram of the coupling module.

Assuming homogenous isotropic linear elastic material K_S and K_D are defined as:

$$K_S = \frac{E_S}{3(1-2v_S)} \tag{18}$$

$$K_D = \frac{E_D}{3(1-2v_D)} \tag{19}$$

Permeability change is correlated to the change in porosity (Rutqvist et al., 2002) by the modified permeability-porosity relationship originally presented by (Davies and Davies, 1999):

$$k = k_0 e^{c*(\frac{\phi}{\phi_0}-1)} \tag{20}$$

where k_0 is the permeability at zero normal stress and c is an experimentally determined exponent.

1.5. Rock failure

Should an element undergo plastic strain as determined by the Mohr-Coulomb (Coulomb, 1776) or Drucker-Prager (Drucker and Prager, 1952) failure criteria that results in fracture initiation or reactivation, the coupling module will calculate the fracture permeability from the parallel plates law (Snow, 1968):

$$k_f = \frac{b^2}{12} \tag{21}$$

In subsequent runs, the fracture permeability is replaced by the equivalent fracture permeability. A modified version of fracture permeability variation with effective stress (Gutierrez et al., 2000), is used to calculate the permeability under the new state of stress.

$$k_f = k_{f0} \exp(-C.\sigma'_m) \tag{22}$$

where C = 0.27 is an empirical constant for shales and σ'_m is the effective mean stress acting on the element that contains the fracture. We assume that the effective mean stress acting

on the element represents a close approximation to the effective normal stress acting on the fracture and that the error introduced by this simplification is negligible.

Tensile failure in the rock will form perpendicular to the direction of minimum principal stress, while assuming the angle of internal friction of the rock specimen is ϕ, fractures due to shear failure will form at an angle β from the direction of maximum principal stress, as shown in Fig. 5, where β is:

$$\beta = \pm\frac{1}{2}(\phi - \frac{\pi}{2}) \tag{23}$$

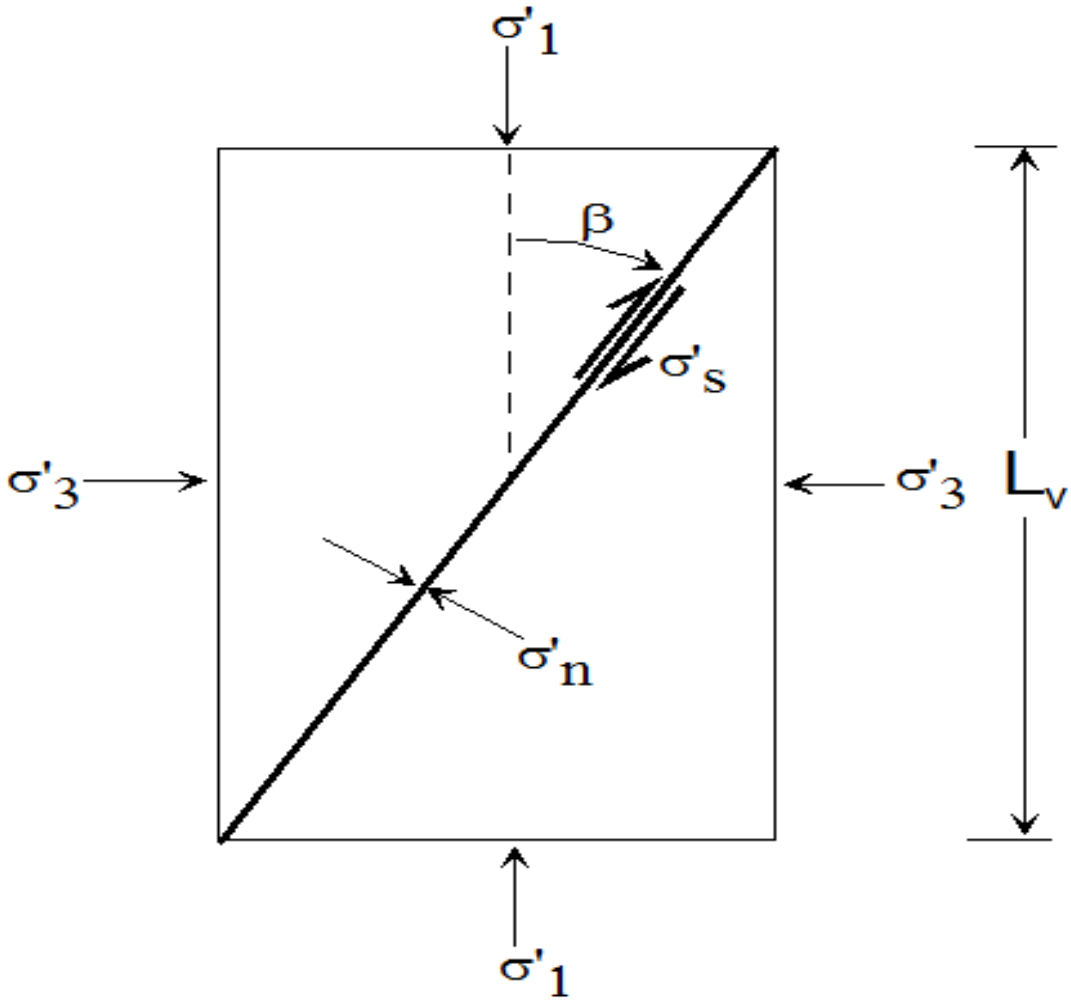

Fig. 5 – Representation of failure plane in a rock sample under stress.

The resulting length of the initiated or reactivated fracture is assumed to be given by:

$$L_f = \frac{L_v}{\cos(\beta)} \tag{24}$$

where L_v is the length of the element in the direction of maximum principal stress.

If a fracture is long enough to entirely penetrate the caprock, such that the reservoir layer is connected to the overburden, the amount of fluid flow through the fracture is calculated by placing a virtual well in the fluid flow simulation input files at the location of the fracture. This virtual well produces the same amount of fluid flow (i.e. equivalent permeability) as the fracture. This approach not only enables us to determine the likelihood of fluid seepage to the overburden, but also makes it possible to model the fractured reservoir as a single porosity conventional reservoir, knowing that the reservoir is locally fractured and cannot be modeled as a completely fractured reservoir.

2. Results and Discussion

2.1. Validation of CGRS

The necessity for coupled simulations is a consequence of the principle of pore pressure - stress coupling (Altmann et al., 2010; Bachu, 2008; Hillis, 2003, 2001; Settari and Mourits, 1994; Tingay et al., 2003; Tortike and S.M., 1987). Dean et al. (2006) have shown the necessity to include coupled simulations when geomechanical considerations are important. Their results suggest that fully coupled simulations represent the most reliable simulation technique. Employing a fully coupled approach, Altmann et al. (2010) have shown that the finite element solver ABAQUS^{TM} is capable to match the analytic solution (Rudnicki, 1986) of a single point fluid source for the case of water injection.

ABAQUS^{TM} is not capable of handling multi-phase, multi component fluid systems such as CO_2 sequestration and hence the approach is limited to water injection. However, if time step increments and convergence tolerances are chosen correctly, partial coupling approaches, including iterative partial coupling, are capable of reproducing the results of fully coupled simulations (Dean et al., 2006).

To check the validity of CGRS simulation results a simple homogenous horizontal basin model (Tables 1and 2) is subjected to CO_2 injection for a period of 5 years. The results of the coupled simulations are checked against the analytical solution by Rudnicki (1986) and are presented in Fig. 6.

Table 1 - Overall simulation properties for the horizontal basin model

CO_2 injection rate (Kg/Sec)	40
CO_2 injection period (Years)	5
Overall model dimensions, *length*width*height*,(m)	10,000 x 5,000 x 3,000
Reference depth of the injection (m)	1700

Table 2 - Properties for the simulation of CO_2 sequestration in the horizontal basin model

ρ_m (Kg/m^3)	G (GPa)	ν []	ϕ []	λ (GPa)	λ_u (GPa)	c (m^2/s)	α []	k_f ($10^{-6}m/s$)
2210	6.5	0.25	0.2	26	27	0.082	0.7	1.61

The comparison between the coupled simulation results and the analytical model show that the coupling results are in good agreement with the analytical solution which in turn ensures validity of the results for other cases.

2.2. Application of CGRS to CO_2 Sequestration

As CO_2 injection related pore pressure changes induce geomechanical risks such as the generation or reactivation of fractures and the associated seismicity or surface uplift, an accurate geometrical representation of the injection system is required to account for all possible factors resulting in stress changes or stress concentrations. A large variety of CO_2 sequestration studies are based on simplified geometries reflecting horizontally layered sedimentary basins (Dean et al., 2006; Gutierrez and Lewis, 1998; Mainguy et al., 2001; Minkoff et al., 2003; Rutqvist et al., 2008, 2002; Tran et al., 2009). Thus, potentially unstable areas of the reservoir - cap rock system, which would be able to sustain a much lower pore pressure increase due to the injection, cannot be identified. However, a variety of different 3D Finite Element Analysis studies (Buchmann and Connolly, 2007; Eckert and Connolly, 2007; Goodman and Connolly, 2007) have shown that geometry on multiple scales plays an important role on the in situ state of stress. This is also consistent with conclusions from Rutqvist et al. (2007) who state that an analysis of mechanical stress changes is necessary to completely assess the potential for failure under the existing conditions.

In order to demonstrate the capability of CGRS to include more complex geometric features, and to show the necessity of coupled simulation we consider a CO_2 injection scenario (Table 3) into a multi-layer 3D representation of a generic pinch-out structure (Fig. 7). For the convenience of the discussion, either an extensional ($\sigma_v' = \int_0^H (\rho_{rock} - \rho_{fluid}).\, g\, dz, \quad \sigma_H' = 0.8\sigma_v', \quad \sigma_h' = \frac{\nu}{1-\nu}\sigma_v'$) or a compressional ($\sigma_H' = 1.5\sigma_v',\ \sigma_h' = 1.25\sigma_v'$) stress regime is considered for the various points. The FE

model is pre-stressed based on the initial state of stress for the two settings. Table 4 presents the material properties of the pinch out settings.

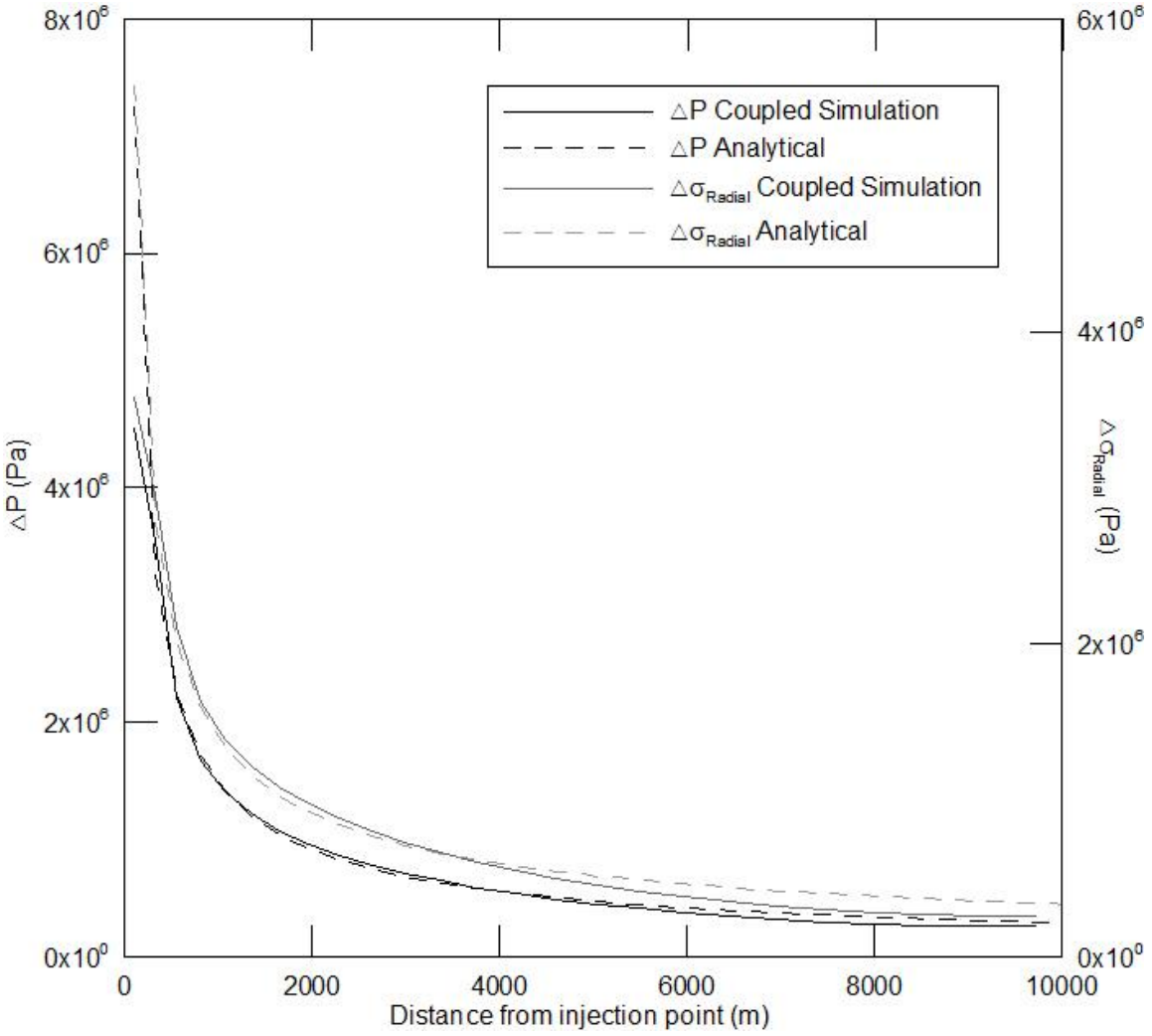

Fig. 6 - Comparison between pore pressure and radial stress differences calculated using the analytical solution (Rudnicki, 1986) and the coupled simulations from CGRS after five years of CO_2 injection. The results of the coupled simulation are in good agreement with the analytical solution for the far-field. The results slightly deviate near the wellbore because the domain discretization in the simple verification model is not fine enough and thus cannot resolve the rapid changes in pore pressure. In addition, the analytical solution is derived for a single phase single fluid system (i.e. water injection scenario). The coupled simulation considers a multi-phase CO_2 sequestration study and the higher compressibility of CO_2 near the wellbore regions results in less pronounced differences.

Table 3 - Overall simulation properties for the pinchout model.

CO_2 injection rate (kTons/Year)	207
CO_2 injection period(Years)	60
Overall model dimensions, *length*width*height,*(m)	10,000 x 1,000 x 3,000

Fig. 7 – Schematic representation of the pinch out model.

To verify the effect of meshing and resolution on the accuracy of simulations, and to verify the validity of the mapping algorithm, three different meshing approaches are considered for this study. The mesh style used (and required) for the fluid flow simulation is pillar grids. The geomechanical simulator input mesh is divided into three categories:

1. Same discretization as the fluid flow pillar grid (Fig. 8 - a).
2. Finer pillar grid discretization than the fluid flow simulator (Fig. 8 - b).
3. Tetrahedral mesh (Fig. 8 - c).

For an extensional stress regime, Fig. 9 shows the increase in pore pressure due to the CO_2 injection over the course of 60 years with and without inclusion of geomechanics in the calculations for the three different mesh settings. As illustrated in this figure, the three models that use coupled reservoir simulation show the same pressure trend while the model without incorporation of geomechanics has a higher pore pressure prediction. In addition, Fig. 10 visualizes an enlargement of the region at the tip of the pinch out and

shows that the coupling module is populating the different meshes with the corresponding pore pressure values from the reservoir simulation.

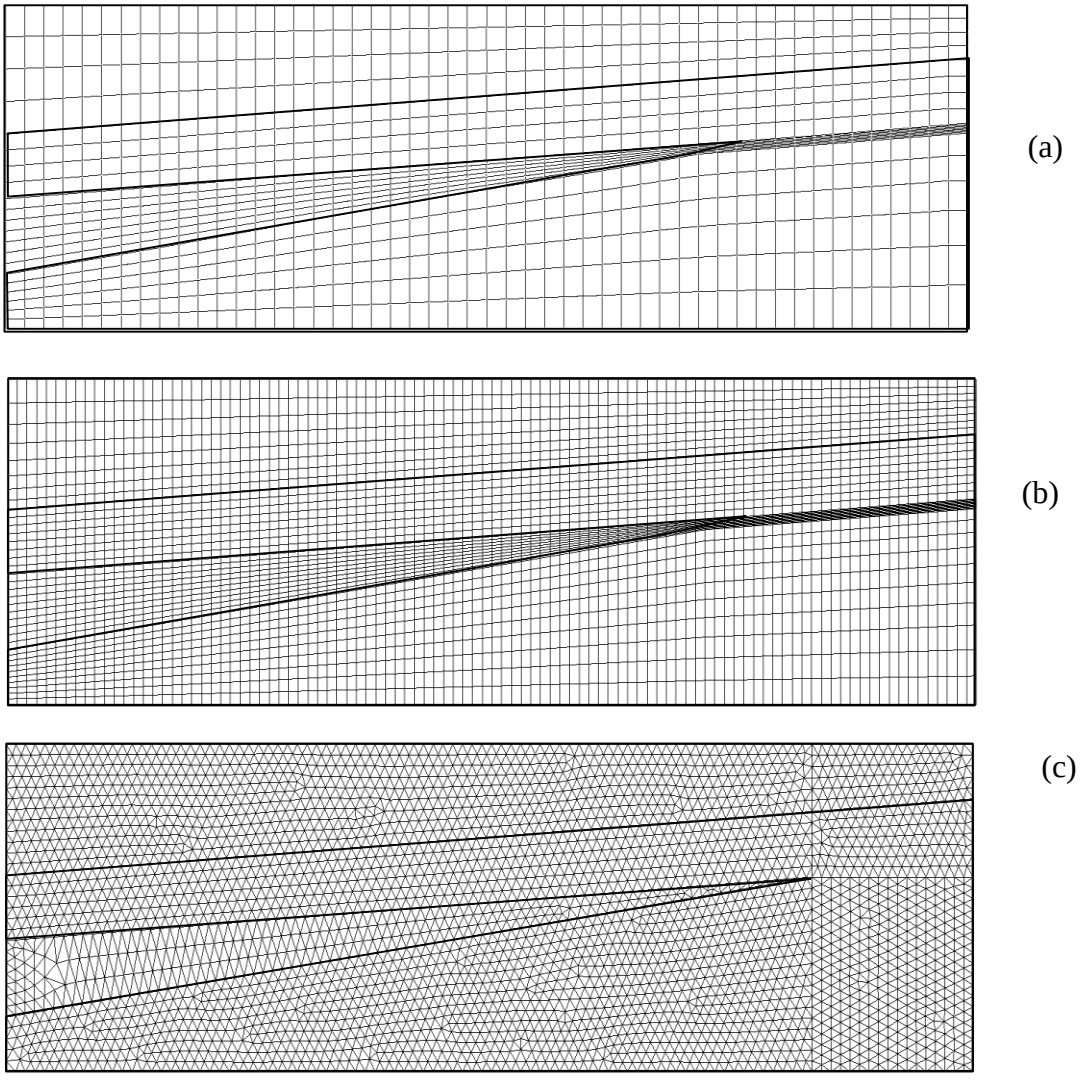

Fig. 8 - Different discretizations of the pinchout geometry.
(a) A coarse cuboid pillar grid that has the necessary resolution for fluid flow simulation. Tip of the pinchout is flattened.
(b) Fine resolution cuboid grid with twice the resolution of (a). Tip of the pinchout is flattened.
(c) Tetrahedral mesh. The model is meshed in tetrahedral elements that overcome the flattening of the tip of the pinchout.

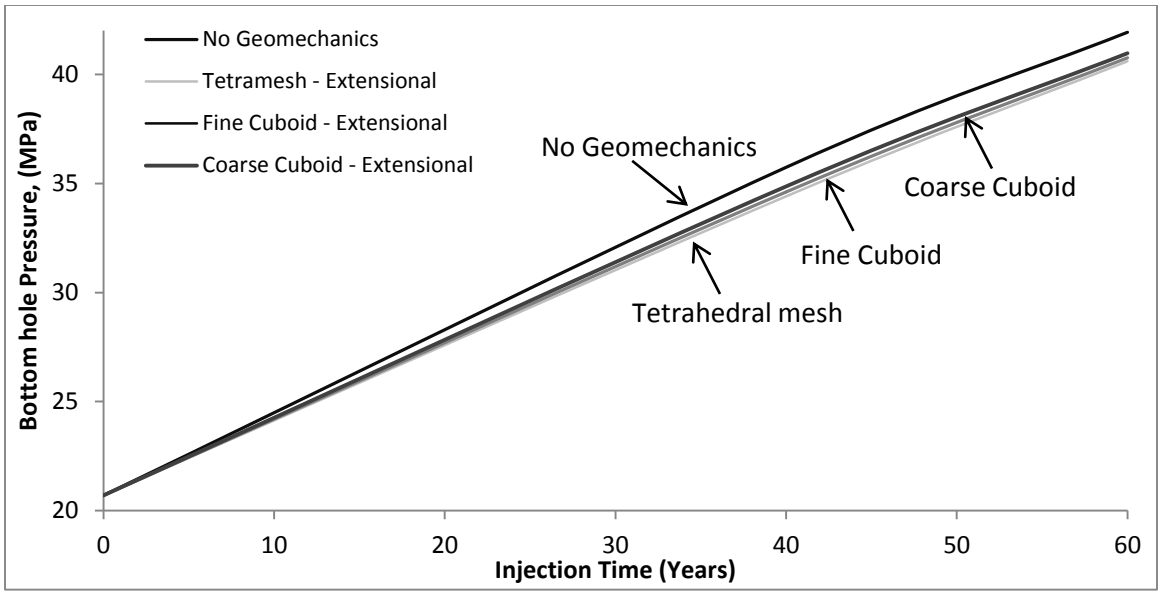

Fig. 9 - Pressure at the point of injection as a function of time in the extensional regime for different mesh styles with and without geomechanics. Different mesh styles in the coupled simulation show similar pore pressure trend, but this trend is not observed in fluid flow simulation without geomechanics, which emphasis on the contribution of geomechanics in the model.

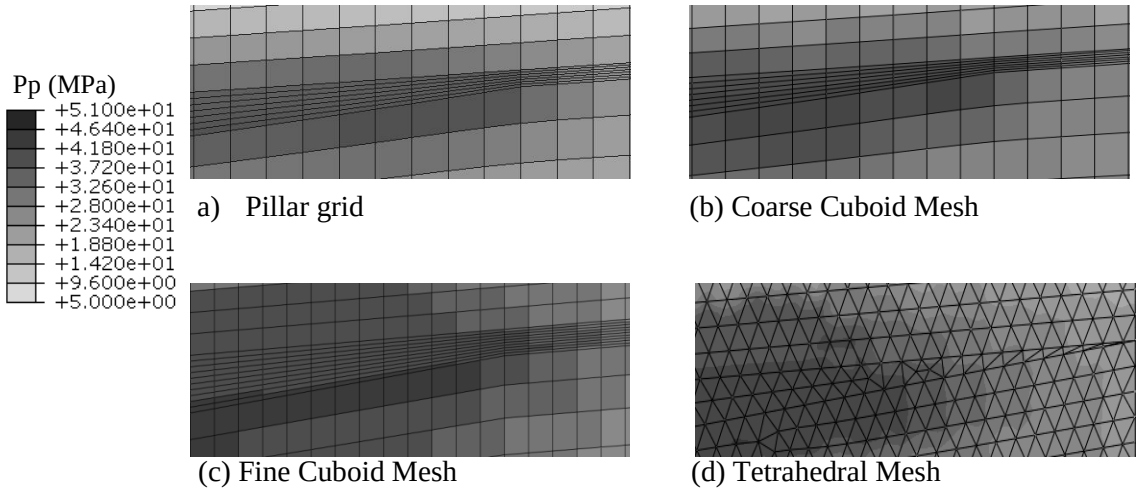

Fig. 10 – Comparison of pore pressure distribution at the tip of the pinchout in different meshes. Pore pressure values from the reservoir simulation grid (a) are reproduced in the coarse (b), fine (c) and tetrahedral (d) meshes which signify the correct functioning of the coupling module in general and the validity of the mapping algorithm in particular.

In order to demonstrate the change of the simulation results with respect to failure, the compressional stress regime is considered. The increase in pore pressure (Fig. 11-a) results in an increase in differential stress (Fig. 11-b) at different parts of the reservoir and the cap rock. Considering Mohr Coulomb failure (Table 4) the increase in differential stress results in the generation of shear fractures, and CGRS applies an effective fracture permeability to the failed elements (Fig. 11-c). As Fig. 11-c shows, shear fractures are initiated in the cap rock and these fractures are designated by a significant increase in permeability ($k_{m+f}=6*10^{-16}\ m^2$ vs. $k_m= 9*10^{-20}\ m^2$).

Table 4 - Properties for the simulation of CO_2 sequestration in the pinchout model.

Property	Overburden	Top Shale	Reservoir	Basement
Saturated rock density, ρ_m (Kg/m^3)	2210	2130	2210	2130
Young's modulus, E (GPa)	15	15	20	15
Poisson's ratio, ν (dimensionless)	0.25	0.25	0.25	0.25
Zero stress porosity, ϕ, %	0.01	0.01	20	0.01
Zero stress permeability, k (10^{-16}m^2)	0.098	0.0009	986.9	0.0009
Height, h (m)	1200	600	700	500
Cohesion, C_0(MPa)	5	5	5	5
Tensile Strength, T_0(MPa)	2.5	2.5	2.5	2.5
Angle of internal friction, $\boldsymbol{\phi}$	30	30	30	30

The coupling between stress and permeability also results in an increased permeability as a consequence. This change in permeability is not reflected in the model that does not account for the geomechanics.

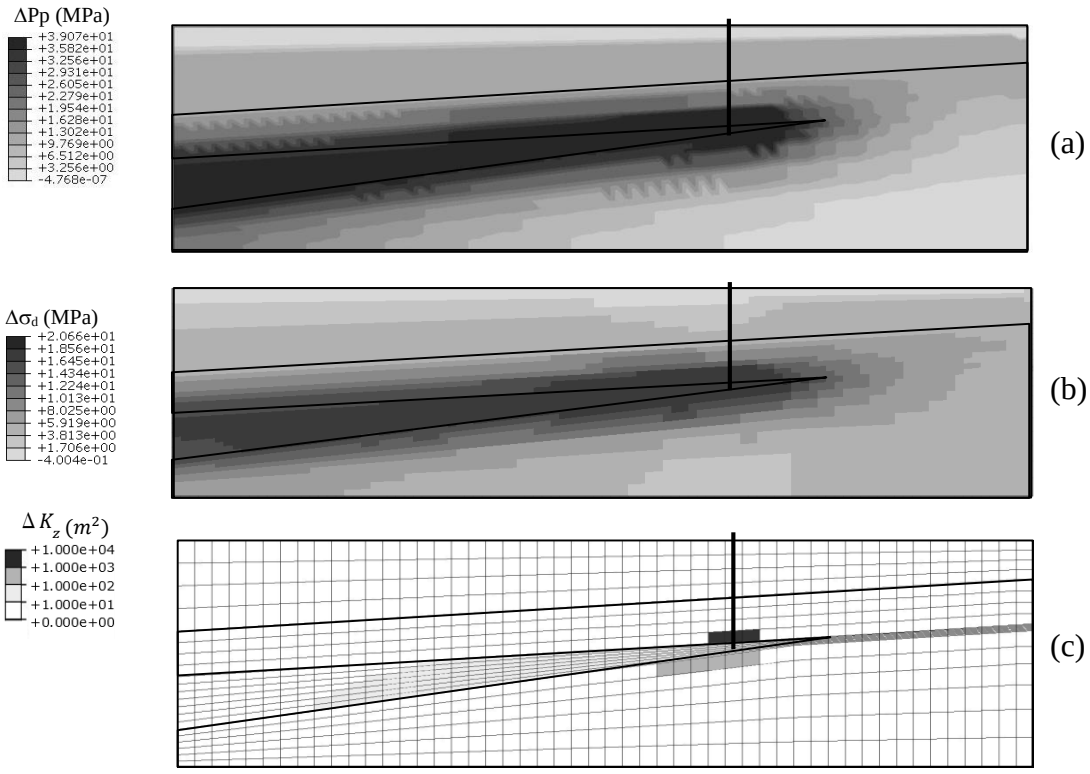

Fig. 11 - Evolution of pore pressure and differential stress over the injection period. (a) Difference in pore pressure after 60 years of injection and initial pore pressure distribution. The reservoir layer undergoes a 39MPa increase in pore pressure over the course of injection while the differential pore pressure in the neighboring shale blocks is in the range of 10 to 20 MPa.
(b) Difference in differential stress over the 60 years of injection. The increase in differential stress in the vicinity of the injection well denotes the likelihood of fracturing.
c) Change in permeability (ΔK_z) due to stress related permeability changes and due to the formation of shear fractures.

In order to calculate the equivalent fracture outflow CGRS places a virtual well at the locations of these fractures and the amount of CO_2 escaping from the reservoir can be determined. This feature becomes important if these fractures were to completely penetrate the caprock and thus connecting the reservoir to the overburden aquifer. In this study, placement of the virtual well in the failed caprock grid blocks results in an outflow of brine and CO_2 from the reservoir. The cumulative fluid outflow from the reservoir layer over the

course of 60 years of injection is 1070.8 m^3. If the virtual wells are not placed at the location of fractures the spreading of the CO_2 plume beyond the reservoir can be monitored (Fig. 12).

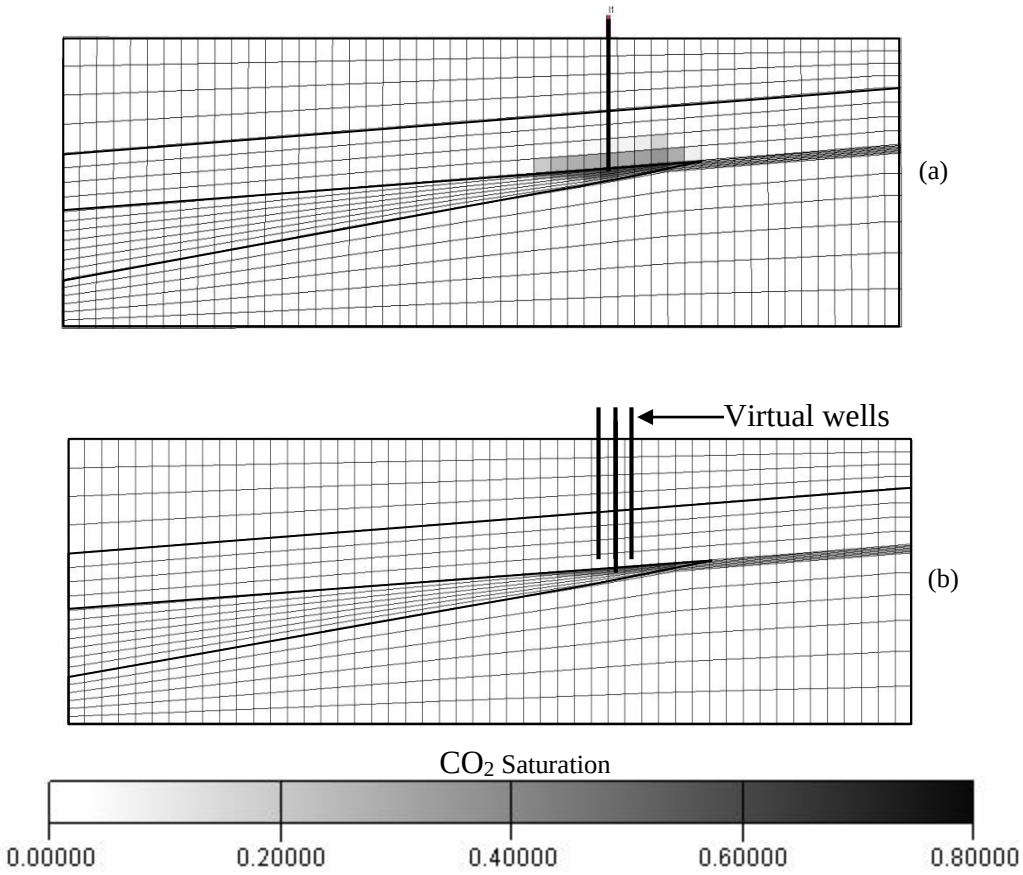

Fig. 12 - Lateral spreading of CO_2 plume in the models after 60 years of injection.
(a) Coupled simulation results show the formation of shear fractures in the reservoir layer and lower parts of the caprock which results in upwards migration of CO_2 as well as the lateral spreading.
(b) Coupled fluid flow simulation with virtual wells placed in elements that undergo shear failure in the caprock. CO_2 spreading in the reservoir layer is not affected by virtual wells, but CO_2 plume does not form in the caprock because CO_2 that goes into caprock is removed by virtual wells.

3. Concluding Remarks

Coupled fluid flow and geomechanical simulation is necessary for proper modeling of hydromechanical processes such as CO_2 sequestration projects. As CO_2 is injected into complex geologic structures, adequate meshing techniques that meet the requirements of fluid flow and geomechanics analysis simulators need to be employed so that realistic modeling of existing geologic features, such as pinchout structures or fracture sets, can be achieved. We have developed a fully automated 2-way coupled geomechanical reservoir simulator (CGRS) that addresses the limitations of structured FD pillar grids when complex geometries are modeled without the need of local grid refinement. It is capable to utilize the natural and optimal meshing algorithm for each simulator. This includes the use of tetrahedral elements for complex geologic geometries and quadratic elements for homogenous geometries for precise finite element modeling and cubic grid blocks for finite difference modeling. CGRS is capable of mapping different grid geometries for populating finite difference and finite element models with corresponding data. Results of this coupling module were validated by an analytical model.

The change in porosity and permeability due to the change in pore pressure and the state of stress is reflected in the analysis by updating of corresponding parameters. The coupling module treats permeability as a non-linear function of stresses and is capable of detecting plastic deformation. Once fractures are initiated or reactivated, CGRS updates hydraulic permeabilities in the failed regions and, by placing a virtual well at the location of the failed elements, is able to calculate the associated fracture outflow. For CO_2 sequestration studies this feature proves significant as it provides the amount of CO_2 flowing into the overburden aquifer system once failure completely penetrates the caprock.

The use of fluid flow simulation, geomechanical analysis and fracture modeling represents a well understood procedure in the hydrocarbon industry, and many different software suites are coupled using a variety of approaches. However, many of these coupling modules are proprietary “in-house” applications and are not available for public access. CGRS is an open source code and with modifications in input/output sections, CGRS can be used to couple different fluid flow simulators with different geomechanical analysis packages.

Acknowledgements

The authors gratefully acknowledge financial support from US Department of Energy’s National Energy Technology Laboratory under grant # DE-FE0001132. Disclaimer: "This paper was prepared as an account of work sponsored by an agency of the United States Government. Neither the United States Government nor any agency thereof, nor any of their employees, makes any warranty, express or implied, or assumes any legal liability or responsibility for the accuracy, completeness, or usefulness of any information, apparatus, product, or process disclosed, or represents that its use would not infringe privately owned rights. Reference herein to any specific commercial product, process, or service by trade name, trademark, manufacturer, or otherwise does not necessarily constitute or imply its endorsement, recommendation, or favoring by the United States Government or any agency thereof. The views and opinions of authors expressed herein do not necessarily state or reflect those of the United States Government or any agency thereof."

References

Altmann, J.B. et al., 2010. Poroelastic contribution to the reservoir stress path. International Journal of Rock Mechanics and Mining Sciences, 47(7), pp.1104–1113. Available at: http://linkinghub.elsevier.com/retrieve/pii/S136516091000136X [Accessed February 1, 2013].

Anon, 2012. ABAQUS 6.12 User Documentation.

Aziz, K. & Settari, A., 1979. Petroleum Reservoir Simulation, London: Applied Science Publishers Limited.

Bachu, S., 2008. Comparison between Methodologies Recommended for Estimation of CO_2 Storage Capacity in Geological Media. the CSLF Task Force on CO_2 Storage Capacity Estimation and the US DOE Capacity and Fairways Subgroup of the Regional Carbon Sequestration Partnerships Program, (February). Available at: http://www.cslforum.net/publications/documents/PhaseIIIReportStorageCapacityEstimationTaskForce0408.pdf [Accessed November 21, 2012].

Bostrom, B., 2009. Development of a Geomechanical Reservoir Modeling Workflow and Simulations. In Proceedings of SPE Annual Technical Conference and Exhibition. New Orleans, Louisiana: Society of Petroleum Engineers. Available at: http://www.onepetro.org/mslib/servlet/onepetropreview?id=SPE-124307-MS&soc=SPE [Accessed November 21, 2012].

Cappa, F. & Rutqvist, J., 2011. Modeling of coupled deformation and permeability evolution during fault reactivation induced by deep underground injection of CO_2. International Journal of Greenhouse Gas Control, 5(2), pp.336–346. Available at: http://linkinghub.elsevier.com/retrieve/pii/S1750583610001337 [Accessed November 5, 2012].

Chen, Z., Huan, G. & Ma, Y., 2006. Computational methods for multiphase flows in porous media, Dallas, Texas: Society for Industrial and Applied Mathematics. Available at: http://books.google.com/books?hl=en&lr=&id=H1LAX96UauIC&oi=fnd&pg=PR15&dq=Computational+Methods+for+Multiphase+Flows+in+Porous+Media&ots=OhLHZ5d2_J&sig=l1nKXNafWTkIveiTYAAFNXox1AI [Accessed November 27, 2012].

Collins, G.S., Melosh, H.J. & Ivanov, B. a., 2004. Modeling damage and deformation in impact simulations. Meteoritic & Planetary Science, 39(2), pp.217–231. Available at: http://doi.wiley.com/10.1111/j.1945-5100.2004.tb00337.x.

Coulomb, C.A., 1776. Essai sur une application des regles des maximis et minimis a quelquels problemesde statique relatifs. a la architecture. Mem. Acad. Roy. Div. Sav., 7, pp.343–387.

Darcy, H., 1856. Les fontaines publiques de la ville de Dijon, 1856. Dalmont, Paris. Available at: http://scholar.google.com/scholar?hl=en&btnG=Search&q=intitle:Les+Fontaines+Publiques+de+la+Ville+de+Dijon#1 [Accessed November 27, 2012].

Davies, J. & Davies, D., 1999. Stress-Dependent Permeability: Characterization and Modeling. Proceedings of SPE Annual Technical Conference and Exhibition. Available at: http://www.spe.org/elibrary/servlet/spepreview?id=00056813.

Dean, R. et al., 2006. A Comparison of Techniques for Coupling Porous Flow and Geomechanics. SPE Journal, 11(1), pp.132–140. Available at: http://www.spe.org/ejournals/jsp/journalapp.jsp?pageType=Preview&jid=ESJ&mid=SPE-79709-PA&pdfChronicleId=09014762800db157 [Accessed November 21, 2012].

Drucker, D.C. & Prager, W., 1952. Soil mechanics and plastic analysis or limit design. Quarterly of applied mathematics, 10(2), pp.157–165. Available at: http://www.citeulike.org/group/13900/article/8650519 [Accessed December 14, 2012].

Engelder, T. & Fischer, M.P., 1994. Influence of poroelastic behavior on the magnitude of minimum horizontal stress, Sh, in over pressured parts of sedimentary basins. Geology, 22, pp.949–952.

Gutierrez, M. & Lewis, R.W., 1998. The Role of Geomechanics in Reservoir Simulation. In Proceedings of SPE/ISRM Rock Mechanics in Petroleum Engineering. Trondheim, Norway: Society of Petroleum Engineers. Available at: http://www.onepetro.org/mslib/servlet/onepetropreview?id=00047392&soc=SPE [Accessed November 21, 2012].

Gutierrez, M., Øino, L. & Nygård, R., 2000. Stress-dependent permeability of a de-mineralized fracture in shale. Marine and Petroleum Geology, 17(8), pp.895–907. Available at: http://www.sciencedirect.com/science/article/pii/S0264817200000271 [Accessed November 21, 2012].

Helmig, R. et al., 1998. Architecture of the Modular Program System MUFTE-UG for Simulating Multiphase Flow and Transport Processes in Heterogeneous Porous Media. Mathematische Geologie, 2, pp.123–131.

Hillis, R.R., 2001. Coupled changes in pore pressure and stress in oil fields and sedimentary basins. Petroleum Geoscience, 7(4), pp.419–425. Available at: http://pg.lyellcollection.org/cgi/doi/10.1144/petgeo.7.4.419 [Accessed November 22, 2012].

Hillis, R.R., 2003. Pore pressure/stress coupling and its implications for rock failure. Geological Society, London, Special Publications, 216, pp.359–368. Available at: http://sp.lyellcollection.org/content/216/1/359.abstract?sid=b9b29274-7312-4c79-815f-12595560cc51.

Inoue, N. & Fontoura, S., 2009. Answers to Some Questions About the Coupling Between Fluid Flow and Rock Deformation in Oil Reservoirs. In Proceedings of SPE/EAGE Reservoir Characterization and Simulation Conference. Abu Dhabi, UAE: Society of Petroleum Engineers, pp. 1–13. Available at: http://www.onepetro.org/mslib/servlet/onepetropreview?id=SPE-125760-MS&soc=SPE [Accessed November 21, 2012].

Ipcc, 2005. IPCC special report on carbon dioxide capture and storage B. Metz et al., eds., Cambridge University Press. Available at: http://www.ipcc.ch/pdf/special-reports/srccs/srccs_wholereport.pdf.

Jaeger, J.C., Cook, N.G.W. & Zimmerman, R.W., 2007. Fundamentals of Rock Mechanics 4th Edition., John Wiley & Sons.

Lewis, R.W. & Sukirman, Y., 1993. Finite element modeling of three-phase flow in deforming saturated oil reservoirs. International Journal for Numerical and Analytical Methods in Geomechanics, 17(8), pp.577–598. Available at: http://doi.wiley.com/10.1002/nag.1610170804 [Accessed November 22, 2012].

Longuemare, P. et al., 2002. Geomechanics in Reservoir Simulation: Overview of Coupling Methods and Field Case Study. Oil & Gas Science and Technology, 57(5), pp.471–483. Available at: http://ogst.ifpenergiesnouvelles.fr/articles/ogst/abs/2002/05/longuemare_v57n5/longuemare_v57n5.html [Accessed November 24, 2012].

Minkoff, S.E. et al., 2003. Coupled fluid flow and geomechanical deformation modeling. Journal of Petroleum Science and Engineering, 38(1-2), pp.37–56. Available at: http://linkinghub.elsevier.com/retrieve/pii/S0920410503000214 [Accessed November 3, 2012].

Minkoff, S.E. et al., 1999. Staggered In Time Coupling of Reservoir Flow Simulation and Geomechanical Deformation: Step 1 — One-Way Coupling. In Proceedings of SPE Reservoir Simulation Symposium. Houston, Texas: Society of Petroleum Engineers, p. 2. Available at: http://www.onepetro.org/mslib/servlet/onepetropreview?id=00051920&soc=SPE [Accessed November 24, 2012].

Peaceman, D.W., 1977. Fundamentals of Numerical Reservoir Simulation, Amsterdam, The Netherlands: Elsevier Scientific Publishing Company.

Philip, Z. et al., 2005. Modeling Coupled Fracture-Matrix Fluid Flow in Geomechanically Simulated Fracture Networks. SPE Reservoir Evaluation & Engineering, 8(4), pp.300–309. Available at: http://www.onepetro.org/mslib/servlet/onepetropreview?id=SPE-77340-PA [Accessed November 6, 2012].

Rudnicki, J., 1986. Fluid mass sources and point forces in linear elastic diffusive solids. Mechanics of Materials, 5, pp.383–393. Available at:

http://www.sciencedirect.com/science/article/pii/0167663686900426 [Accessed February 4, 2013].

Rutqvist, J. et al., 2002. A modeling approach for analysis of coupled multiphase fluid flow, heat transfer, and deformation in fractured porous rock. International Journal of Rock Mechanics and Mining Sciences, 39(4), pp.429–442. Available at: http://linkinghub.elsevier.com/retrieve/pii/S1365160902000229.

Rutqvist, J. et al., 2007. Estimating maximum sustainable injection pressure during geological sequestration of CO_2 using coupled fluid flow and geomechanical fault-slip analysis. Energy Conversion and Management, 48(6), pp.1798–1807. Available at: http://linkinghub.elsevier.com/retrieve/pii/S0196890407000337 [Accessed November 13, 2012].

Rutqvist, J., Birkholzer, J.T. & Tsang, C.-F., 2008. Coupled reservoir–geomechanical analysis of the potential for tensile and shear failure associated with CO_2 injection in multilayered reservoir–caprock systems. International Journal of Rock Mechanics and Mining Sciences, 45(2), pp.132–143. Available at: http://linkinghub.elsevier.com/retrieve/pii/S1365160907000548 [Accessed November 16, 2012].

Settari, A. & Mourits, F.M., 1998. A Coupled Reservoir and Geomechanical Simulation System. SPE Journal, 3(3), pp.219–226. Available at: http://www.onepetro.org/mslib/servlet/onepetropreview?id=00050939&soc=SPE [Accessed November 21, 2012].

Settari, A. & Mourits, F.M., 1994. Coupling of geomechanics and reservoir simulation models. In H. J. Siriwardane & M. M. Zaman., eds. Computer methods and advances in geomechanics. (Edited by H. J. Siriwardane and M. M. Zaman.). Morgantown, W. Va, USA, pp. 2151–2158.

Settari, A. & Walters, D., 1999. Advances in Coupled Geomechanical and Reservoir Modeling With Applications to Reservoir Compaction. In Proceedings of SPE Reservoir Simulation Symposium. Houston, Texas: Society of Petroleum Engineers. Available at: http://www.onepetro.org/mslib/servlet/onepetropreview?id=00051927&soc=SPE [Accessed November 21, 2012].

Sheldon, J.W., Zondek, B. & Cardwell, W.T., 1959. One-dimensional, incompressible, non-capillary, two-phase fluid flow in a porous medium. Petroleum Transactions SPE AIME, 216, pp.290–296.

Snow, D.T., 1968. Rock fracture spacings, openings, and porosities. Journal of Soil Mechanics & Foundations Div, 94, pp.73–91. Available at: http://trid.trb.org/view.aspx?id=126926 [Accessed December 14, 2012].

Stone, H.L. & Garder Jr., A.O., 1961. Analysis of Gas-Cap or Dissolved-Gas Drive Reservoirs. Society of Petroleum Engineers Journal, 1(2), pp.92–104. Available at:

http://www.onepetro.org/mslib/servlet/onepetropreview?id=SPE-001518-G&soc=SPE [Accessed November 29, 2012].

Streit, J.E. & Hillis, R.R., 2004. Estimating fault stability and sustainable fluid pressures for underground storage of CO_2 in porous rock. Energy, 29(9-10), pp.1445–1456. Available at: http://linkinghub.elsevier.com/retrieve/pii/S0360544204001616 [Accessed November 22, 2012].

Thomas, G.W. & Thurnau, D.H., 1983. Reservoir Simulation Using an Adaptive Implicit Method. Society of Petroleum Engineers Journal, 23(5), pp.759–768. Available at: http://www.onepetro.org/mslib/servlet/onepetropreview?id=00010120&soc=SPE [Accessed November 29, 2012].

Thomas, L.K. et al., 2003. Coupled Geomechanics and Reservoir Simulation. SPE Journal, 8(4), pp.350–358. Available at: http://www.onepetro.org/mslib/servlet/onepetropreview?id=00087339&soc=SPE [Accessed November 21, 2012].

Tingay, M.R.P. et al., 2003. Pore pressure/stress coupling in Brunei Darussalam—implications for shale injection. In: Van Rensbergen, P., Hillis, R.R., Maltman, A.J. and Morley, C.K. (eds.) Subsurface Sediment Mobilization. Geological Society of London Special Publication, 216, pp.369–379. Available at: http://sp.lyellcollection.org/content/216/1/369.short [Accessed November 22, 2012].

Tortike, W.S. & S.M., F.A., 1987. A Framework for Multiphase Nonisothermal Fluid Flow in a Deforming Heavy Oil Reservoir. In Proceedings of SPE Symposium on Reservoir Simulation. San Antonio, Texas: Society of Petroleum Engineers. Available at: http://www.onepetro.org/mslib/servlet/onepetropreview?id=00016030&soc=SPE [Accessed November 21, 2012].

Tsang, C.-F., 1999. Linking Thermal, Hydrological, and Mechanical Processes in Fractured Rocks. Annual Review of Earth and Planetary Sciences, 27(1), pp.359–384. Available at: http://www.annualreviews.org/doi/abs/10.1146/annurev.earth.27.1.359 [Accessed November 27, 2012].

Vidal-Gilbert, S., Nauroy, J.-F. & Brosse, E., 2009. 3D geomechanical modelling for CO_2 geologic storage in the Dogger carbonates of the Paris Basin. International Journal of Greenhouse Gas Control, 3(3), pp.288–299. Available at: http://linkinghub.elsevier.com/retrieve/pii/S175058360800100X [Accessed November 5, 2012].

Xikui, L. & Zienkiewicz, O.C., 1992. Multiphase flow in deforming porous media and finite element solutions. Computers & Structures, 45(2), pp.211–227. Available at: http://www.sciencedirect.com/science/article/pii/004579499290405O [Accessed November 21, 2012].

Zhou, Q. et al., 2008. A method for quick assessment of CO_2 storage capacity in closed and semi-closed saline formations. International Journal of Greenhouse Gas Control, 2(4), pp.626–639. Available at: http://linkinghub.elsevier.com/retrieve/pii/S1750583608000091 [Accessed November 21, 2012].

Zhou, Q. & Birkholzer, J., 2007. Sensitivity study of CO_2 storage capacity in brine aquifers with closed boundaries: dependence on hydrogeologic properties. In Sixth Annual Conference on Carbon Capture and Sequestration - DOE/NETL. Pittsburgh, PA. Available at: http://www.netl.doe.gov/publications/proceedings/07/carbon-seq/data/papers/wed_131.pdf [Accessed November 22, 2012].

Zienkiewicz, O., Taylor, R. & Zhu, J., 2005. The finite element method: its basis and fundamentals 6th ed., Oxford: Elsevier Butterworth-Heinemann. Available at: http://books.google.com/books?hl=en&lr=&id=YocoaH8lnx8C&oi=fnd&pg=PP2&dq=The+Finite+Element+Method:+Its+Basis+and+Fundamentals&ots=i9Yu7sRVhN&sig=ZrcYURuKG1sXTZDs9-DFmaXECJY [Accessed November 25, 2012].

PAPER

2. ROLE OF GEOMETRICAL INFLUENCES OF CO_2 SEQUESTRATION IN ANTICLINES

Amirlatifi, A.

Missouri University of Science and Technology, Rolla, MO, USA

Eckert, A., Nygaard, R., Bai, B., Liu, X., Paradeis, M.

Missouri University of Science and Technology, Rolla, MO, USA

This paper was prepared for presentation at the 46th US Rock Mechanics / Geomechanics Symposium held in Chicago, IL, USA, 24-27 June 2012.

Abstract

Most of the parametric fluid flow simulation studies are conducted using simplified horizontally layered basins or two dimensional models. These simple structures usually do not represent the structure of preferred structural and stratigraphic trap systems for geologic CO_2 sequestration. This paper presents a thorough parametric modeling study of generic anticline structures and investigates the influence of layer thickness, wavelength and amplitudes at different depths and under different boundary conditions on the maximum

CO_2 storage amount. We present a new approach for generating more realistic three dimensional generic models using finite element analysis preprocessors and converting them into finite difference grids for fluid flow simulations under different geometrical and physical conditions. The results of this study show that CO_2 sequestration simulations should not be conducted under simplified conditions and that the combination of geometrical parameters and fluid flow boundary conditions have a significant influence on the amount of CO_2 that can be injected in anticline trap systems.

1. Introduction

Annual CO_2 emissions in the United States of approximately 2 billion metric tons from coal-fired power plants represent a major contributor to global warming [1]. Geologic CO_2 sequestration in deep saline aquifers, depleted oil and gas fields and unmineable coal seams has been identified as a possibility to mitigate high emissions of CO_2 into the atmosphere and the resulting greenhouse effects [1], provided that a thorough understanding of the storage site is conducted. Abundance and capacity of saline aquifers have made them very promising geologic storage sites that unlike depleted oil and gas fields, do not have the risks of casing failure due to old cement jobs and may not require a complete well work over [2]. This huge CO_2 storage potential can be further enhanced by the production of brine out of the aquifer to increase the amount of CO_2 that can be stored. A key aspect of safe CO_2 sequestration is a critical assessment of the risk of aquifer pressurization and potential CO_2 leakage by numerical analyses.

Often numerical CO_2 injection scenarios are based on the simplified assumption of a horizontally layered sedimentary basin [3, 4, 5, 6, 7, 8, 9, 10, 11, 12, 13]. While this scenario serves well to study the impact of different parameters (such as permeability,

injection rate, fluid flow boundary conditions and seal efficiency) on CO_2 flow and pressurization [3, 4, 5, 6, 11], for a geomechanical risk analysis a model geometry reflecting the actual geologic scenario, which exhibits a heterogeneous state of stress is required.

The geomechanical risks accompanying aquifer pressurization due to the CO_2 injection have been investigated by several authors [3, 4, 5, 6, 7, 8, 11, 12, 14, 15, 16] with one of the most important being the reactivation of existing faults or fracture sets which can result in induced seismicity [2, 12, 14, 15, 16] and potential leakage pathways. [11, 16] have shown that the pressure build-up in models representing horizontally layered sedimentary basins is strongly dependent, amongst others, on the fluid flow boundary conditions. A closed system, reflecting a compartmentalized reservoir, results in a much higher and faster pressure increase than open-flow boundary conditions. This influence of the fluid flow boundary conditions on the pressure build-up becomes increasingly relevant for geomechanical risk analyses of storage sites exhibiting a heterogeneous state of stress [17]. Possible geologic scenarios may represent an aquifer being trapped in a closed system bounded by faults or an anticline structure which may have existing fracture sets along the hinge. Anticline/Antiform structures as an example of folded sedimentary layers are among the most common structural traps for hydrocarbon reservoirs and thus become a prime target of the emerging challenge of safe geologic sequestration of CO_2 [1].

One reason for the utilization of simple geometries for generic fluid flow simulation studies is due to the lack of flexible pre-processors, which can generate finite difference grids of more complex geometries. Pre-processors for the finite element method have the ability to generate complex structures but do not yield discretization formats which can be

used in finite difference based reservoir simulations [19, 20]. In this paper we address this limitation by using a commercial finite element pre-processor (Altair® Hypermesh®) and use the Coupled Geomechanical Reservoir Simulator, CGRS, a coupling module for geomechanical reservoir simulation developed at Missouri University of Science and Technology [19, 20] to convert several synthetic reservoir geometries from the finite element file format to the reservoir simulation grid file format. We then study the effects of anticline geometry on CO_2 injection parameters. We use the commercial fluid flow simulation package Schlumberger® Eclipse® to investigate the effects of different amplitudes, wavelengths and height of generic anticline structures on the storability of CO_2 in these reservoirs at different depths and under different injection rates. The results of this study may finally serve as a guideline for possible injection sites and scenarios resembling the cases presented here. The methodology presented in this paper further enables coupling between the reservoir simulation and the geomechanical analysis whereby both simulations use the same discretization minimizing the use of interpolation algorithms.

2. Modeling Approach

2.1 Model Setup

Numerical modeling studies in the oil and gas industry assume a realistic reservoir geometry which is obtained by seismic data, well logs and surface mapping. The data collection may result in quite complex reservoir geometries. Although most state of the art commercial simulators are capable of handling unstructured grids that can accommodate these complex structural features, the computational cost of aforementioned simulators limits their applicability. This feature is not commonly employed and finite difference discretization is still the prominent practice. However, the limitation of finite difference

discretization algorithms [19, 20] for reservoir simulation studies requires up-scaling and simplification of the complex geometry. As a result, most of the pre-processors in the oil and gas industry are based on discretizing an existing geometry and it is very difficult, if not impossible, to use them for building parametric study models that incorporate anticlines, for example. This limitation has resulted in the implementation of simplified horizontal basin models in most of the literature, unless real field data are present.

As part of our efforts to couple the finite element (FE) analysis package Abaqus® with Eclipse® in the Coupled Geomechanical Reservoir Simulator, CGRS, we have created a file convertor and grid mapper in Java® that converts geometries created in the Abaqus 3D file format to the grid file format of Eclipse®. The FE pre-processor Altair® Hypermesh® is used to generate 3D anticline models of different amplitude, wavelengths and heights. Due to the requirements of finite difference grids, all grid blocks in the 3D FE model need to be hexahedral in columns sharing the same coordinates in horizontal directions albeit variable depth. Once the geometry is created in the FEA preprocessor, it is exported to the Abaqus® 3D file format and is transferred into the CGRS file convertor.

The initial step of the file conversion routine stores the nodal coordinates and the corresponding elements into the memory and organizes them into arrays of nodes and elements. In the next step, the nodes are sorted by their coordinates and the closest node to the origin is selected as the starting point of the finite difference grid. The nodes are then sorted by their X-coordinates for an initial constant y-coordinate. Once all nodes having the same Y-coordinates are identified, the next row in the Y direction is examined and so forth, until all elements and nodes in the first layer are determined and the process continues with the elements and nodes in the second and the following layers (z- coordinates). At

each step, the number of rows, columns and layers are determined as the maximum number of nodes in any row, column and layer. Once all nodes and elements in the finite element mesh are analyzed, the corresponding Eclipse® grid is generated. The coordinates of the nodes in the first layer are reported by the COORD keyword in the generated Eclipse® grid data file, followed by the vertical location of each node, reported under the ZCORN keyword. This efficient method enables us to generate highly flexible generic geometries for reservoir simulation studies with the ease of finite element analysis pre-processors.

2.2 Model Description

Sinusoidal curves with different amplitudes and wavelengths are used as the framework of the anticlines and synclines to be modeled. As it is shown in Fig. 1, the general layout of the anticline structures used throughout this modeling study comprises seven layers where all layers are assumed to be fully saturated with water.

The thickness of shale and sandstone layers together with the base layer stay the same, while the thickness of the overburden is increased or decreased during the study of the effect of depth (section 2.9). The pseudo 3D model employed here (Fig. 1) is part of a direct line CO_2 sequestration scheme with a lateral extension of 76 meters where the injection well is placed at the crest of the anticline and two brine production wells are placed at the sides to keep the hydrostatic pressure under open boundary conditions (section 2.8). No flow boundary condition along the longitudinal extension of the model results in the direct line sequestration configuration flow regime, with image wells acting as parallel well sets (Fig. 1).

Two sandstone layers are contained between three shale layers, which act as sealing caprock for each sandstone reservoir. Table 1 lists the intrinsic rock properties, thickness and the order of different layers used in this study. The "Sand Stone 2" layer is taken as the main aquifer in this study and the CO_2 is injected in this layer.

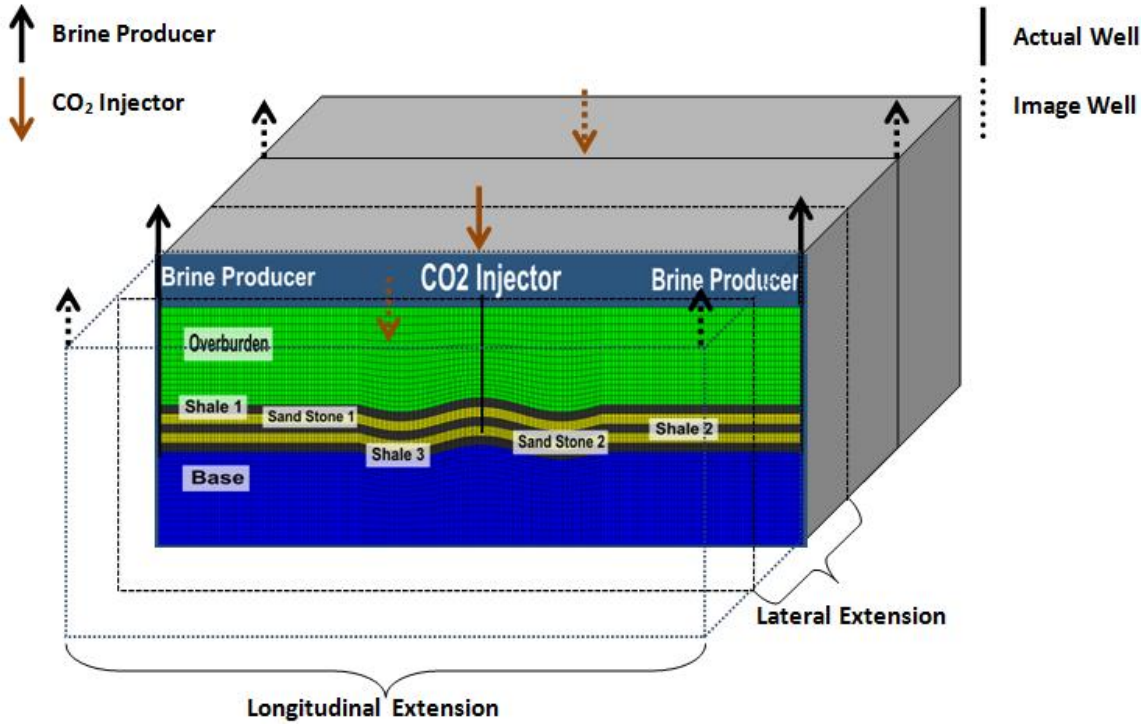

Fig. 1. General layout of the anticline structure used in this study

Table 1. Properties of layers used in the parametric study.

Layer Name	ρ (Kg/m^3)	E (GPa)	ν []	ϕ (%)	k ($10^{-16}m^2$)	h (m)
Overburden	2210	15	0.25	0.01	0.098	950
Shale 1	2130	15	0.25	0.01	0.0009	100
Sand Stone 1	2210	20	0.25	20	986.9	100
Shale 2	2130	15	0.25	0.01	0.0009	100
Sand Stone 2	2210	20	0.25	20	986.9	100
Shale 3	2130	15	0.25	0.01	0.0009	100
Base	2245	15	0.25	0.01	0.098	1050

Table 2 lists the range of geometrical and operational parameters that were used in this study. Wavelengths of 750, 1500 and 3000 meters and an infinite wavelength, resembling the horizontally layered basin are used (section 2.4). Reservoir thicknesses of 25, 50 and 100 meters are considered (section 2.5). In order to investigate effect of amplitude variation, anticlines with amplitudes of 50, 100 and 150 meters are modeled (section 2.6).

The simultaneous variation of wavelength, thickness and amplitude is examined as described in section 2.7 and Table 7. Effect of boundary condition is examined through modeling of the closed, Semi-Open and Open boundary conditions as described in section 2.8.

Depth of the model is varied between 500 to 3000 meters as described in section 2.9 which has resulted in different maximum allowable pore pressures. The lateral extent of the model is varied between 6, 23 and 103 Km as described in the discussion.

As a reference base case of this study we consider a reservoir at the depth of 1250 meters with an anticline of a wavelength of 1500 m, an amplitude of 150 m and a height of 100 meters. The injection well is located at the crest of the anticline and the boundaries are assumed to be closed.

In order to evaluate the validity of the simplified horizontally layered basin models, a simple horizontally layered basin model is created and is compared to the base model.

Simulations reflecting open boundary fluid flow conditions are carried out by placing water production wells at the boundaries that maintain hydrostatic pore pressure.

An initial CO_2 injection rate of 20.7 KTons/year (1798.71 lbs/MWhr) is based on the 50% reinjection of CO_2 emission rate of a common 495 MW capacity coal fired power

plant [18] with 75% efficiency over 100 years period and CO_2 density of 1.98 Kg/m3 and formation properties are based on the geology of common sedimentary rocks.

Table 2. Range of parameters used in the parametric study.

Values / Attribute	Units							
Wave Length	m	∞	3000	1500	750			
Reservoir Thickness	m	100	50	25				
Amplitude	m	150	100	50				
Boundary Type		Open	Semi-Open	Closed				
Model Size (Longitudinal Extension)	Km	6	23	103				
Depth	m	500	1000	1250	1500	2000	2500	3000
Maximum Allowable Pore Pressure	MPa	26.3	34.1	36.0	41.8	49.5	56.5	62.4
Well Location		Crest						
Injection Rate (STD)	KTons/Year	20.7						

2.3 Simulation Results

For the injection simulations we use a maximum allowable pore pressure before failure of intact rock is initiated as a threshold value before injection is stopped. These critical pore pressure values are determined by geomechanical finite element analysis for each geometry assuming a compressional stress regime, as described in [16, 17]. Based on these results the reservoir simulation analyses are conducted, thus a one way coupling procedure is followed here.

Simulations results are checked on a monthly basis until the pore pressure in any grid block of the reservoir layer or the surrounding shale layers reaches the maximum allowable pore pressure. The time to reach the maximum allowable pore pressure is identified as the Safe Injection Limit, SIL. The ratio of the reservoir volume of CO_2 at the SIL to the total pore volume, which is also equal to the average gas saturation, is considered as the degree of occupancy, an indication of how well the reservoir volume is utilized. Unless maximum allowable pore pressure is reached, the simulation is continued for 50 years.

The simulation results of the base anticline model of this study, Fig. 1 and Table 3, are taken as the basis for benchmarking the other simulation runs.

Fig. 2 shows the pressure distribution in the base model after the safe injection limit is passed. The black regions in the syncline show the parts of the syncline that will experience pressures exceeding the critical pressure limit.

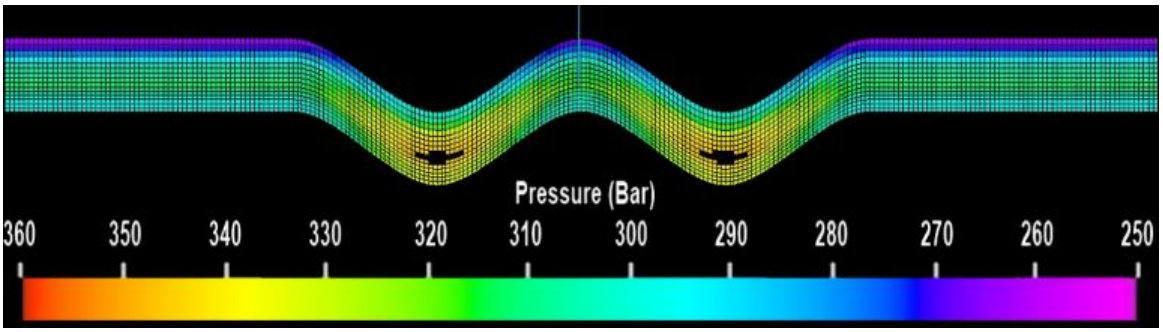

Fig. 2. Pressure distribution in base model after 7 years of injection, showing the failed regions

For the sake of comparison, we have not investigated the escape of injected fluid in this study and when the maximum allowable pore pressure is violated, the well is shut in and simulation is continued for the remainder of ten years, so that the average reservoir pressure at the end of the ten year interval can be determined.

Table 3. The base simulation case and its simulation results.

Attribute	Units	Value
Anticline Wavelength	m	1500
Anticline Amplitude	m	150
Anticline Height	m	100
Depth	m	1250
Reservoir Volume	m^3	9129120
Boundary	[]	Closed
CO_2 Injection Rate	KTons/Year	20.7
Critical Pore Pressure	MPa	36.0
Safe Injection Limit	Years	6.35
Maximum CO_2 Saturation at SIL	%	53
Average Pressure at SIL	MPa	32.45
Mass of Injected CO_2	KTons	117.583
Occupancy	%	1.62

2.4 Effect of Wavelength Variation

The effect of wavelength is investigated by varying the wavelength from one half of the base case to two times of the base case and the horizontally layered basin which has an infinite wavelength.

Results of this simulation show that the higher the wavelength of the anticline, the longer the SIL, the higher reservoir occupancy and finally the higher the CO_2 storage capacity of the reservoir becomes.

Table 4. Effect of wavelength on CO_2 storage capacity.

Wavelength (m)	SIL (Years)	Occupancy (%)	Average Pressure (MPa)	Mass of Injected CO_2 (KTons)
750	6.34	1.62	32.4	117.40
1500	6.35	1.62	32.5	117.58
3000	7.15	1.79	34.8	132.54
∞	7.80	1.93	35.1	144.59

2.5 Effect of Reservoir Layer Thickness Variation

The reservoir height directly controls CO_2 storage capacity through variation of accessible pore volume. Eq. (1) shows the pore volume for a simple case of a cubic reservoir of constant height, h, porosity,ϕ and area, A.

$$V=Ah\emptyset \quad (1)$$

An immediate conclusion from Eq. (1) is that the higher the reservoir thickness, the more pore space is available for CO_2 sequestration, assuming that we have a connected pore network. Table 5 shows the effect of variation in height on the CO_2 storage capacity of the base model.

Table 5. Effect of height on CO_2 storage capacity.

Height (m)	SIL (Years)	Occupancy (%)	Average Pressure (MPa)	Mass of Injected CO_2 (KTons)
25	1.65	1.62	31.8	30.56
50	3.29	1.62	32.5	60.95
100	6.35	1.62	32.4	117.58

The simulation results confirm that the increased volume of the reservoir results in increased safe injection limits and consequently an increase in injected gas volume is achieved, but the overall occupancy stays the same.

2.6 Effect of Amplitude Variation

Three different amplitude variations of the base case, presented in Table 3, are considered, ranging from 50 meters to 150 meters in the closed system. The simulation results of such variations are presented in Table 6.

Table 6. Effect of amplitude on CO_2 storage capacity.

Amplitude (m)	SIL (Years)	Occupancy (%)	Average Pressure (MPa)	Mass of Injected CO_2 (KTons)
50	7.32	1.83	34.2	135.56
100	6.82	1.72	33.3	126.39
150	6.35	1.62	32.4	117.58

As the results suggest, the lower amplitude anticline gives the highest CO_2 storage capacity of 135.56 kilo Tons. Assuming that the most favorable case is to increase the average reservoir pressure up to the maximum allowable pore pressure, an anticline with the low amplitude of 50 meters yields the best average reservoir pressure of 34.2 MPa.

2.7 Simultaneous Variation of Wavelength, Amplitude and Height

Simultaneous variation of wavelength, amplitude and reservoir height are studied through 15 simulations where the wavelength is varied between 750 meters and 1500 meters, the amplitude is varied between 50 meters, 100 meters and 150 meters and the height is varied between 25 meters, 50 meters and 100 meters. Results of these simulations are presented in Table 7.

The results show that the highest storage capacity is observed for the high wavelength of 1500 meters, the low amplitude of 50 meters and the thick reservoir of 100

meters thickness. As previously shown in Table 5 and confirmed in Table 7, height or net thickness of the reservoir has a direct effect on the CO_2 storage capacity.

Table 7. Simultaneous variation of wavelength, amplitude and height.

Wavelength (m)	Amplitude (m)	Height (m)	SIL (Years)	Occupancy (%)	Mass of Injected CO_2 (KTons)
750	50				
		25	1.81	1.75	32.54
		50	3.71	1.84	68.14
		100	7.23	1.82	134.66
	100				
		25	1.73	1.67	30.92
		50	3.46	1.73	63.46
		100	6.82	1.74	126.93
1500	50				
		25	1.9	1.82	33.98
		50	3.79	1.87	69.58
		100	7.32	1.83	136.10
	100				
		25	1.73	1.68	30.92
		50	3.57	1.76	64.90
		100	6.82	1.72	126.93
	150				
		25	1.65	1.6	30.56
		50	3.29	1.65	60.95
		100	6.35	1.62	117.58

2.8 Effect of Boundary Conditions

Three types of fluid flow boundary conditions can be thought for the aquifer systems, namely Open, Semi-Open and Closed boundaries [4, 11]. Many scholars have assumed fully open boundaries [5, 6, 9, 10, 13] where the pressure at the boundary remains hydrostatic. These studies show very promising results on the storage capacity and the safety of the project. We have considered 3 cases where storage under open boundary

condition is compared to the closed and semi-open boundaries. In order to simulate open boundary conditions per definition, two brine production wells are placed at the sides of the aquifer and the constraints are set such that the well flowing pressure, P_{wf}, remains at the hydrostatic pore pressure. The limit for the injection period is set equal to the CO_2 breakthrough time. In the semi-open model, the production rate of the brine producers is reduced by half and the pressure is allowed to increase at the boundaries until the safe sequestration pressure limit is reached, or until the CO_2 breaks through the production wells, which was the case here. Table 8 presents the simulation results of the base case under different boundary conditions.

Table 8. Effect of boundary conditions on CO_2 storage capacity of the base case.

Boundary Type	SIL (Years)	Occupancy (%)	Average Pressure (MPa)	Mass of Injected CO_2 (KTons)
Closed	6.35	1.62	32.4	117.58
Open	50	25.13	13.1	942.10
Semi- Open	80	25.96	20.4	1506.65

The results show the significant influence of the fluid flow boundary condition. Whilst a Closed system (resembling a compartmentalized reservoir) yields a SIL of only 6.35 years and an occupancy of only 1.62%, Open and Semi-Open systems yield much higher SIL (50-80 years) and much higher occupancies (25-26%). The Semi-Open system yields overall safer conditions and more CO_2 can be injected by allowing partial pressure increase in the reservoir, resulting in compression of CO_2 and contained spread of the plume. The contained spreading gives higher sweep efficiency and continuous flow of fluids in the system, which itself results in increased contact between the two fluids and

dissolution of CO_2 in the brine. While open systems benefit from the favorable pressure gradient that makes it possible for CO_2 to quickly spread in the system, mix with the brine as it spreads and dissolve in it, unconstrained spreading of the plume results in lower sweep efficiency than that of the Semi-Open system.

2.9 Effect of Depth

The depth of the reservoir determines the state of the stress, the resulting maximum allowable pore pressure as well as the CO_2 density and phase (Fig. 3), which in turn determines its compressibility and viscosity. The resulting effects on CO_2 storage capacity are studied through 7 simulations where the depth of the base case, as described in Table 3, is varied from 500 meters to 3000 meters. A compressional stress regime is assumed for the calculation of the maximum allowable pore pressure. Table 9 presents the simulation results for the base case at different depths.

The results show that CO_2 sequestration in deep formations results in longer safe CO_2 injection periods and consequently higher CO_2 storage capacity. The highest occupancy is observed in 2500 meters depth with a value of 2.13% and the deepest model at a depth of 3000 meters has the longest injection period of 9.78 years. Comparison between the increase in injection period and the increase in depth and the occupancy suggests that 2500 meters is the most favorable depth of all cases under closed boundary conditions.

3. Discussion

CO_2 sequestration based fluid flow simulations utilizing simplified horizontally layered basins show promising results regarding the amount of CO_2 that can be safely injected over long periods of time [11, 23]. The assumption of a horizontally layered basin,

however, neglects the requirement of a structural trap system to store the fluids. A prime example of such trap systems are anticline structures.

Table 9. Effect of depth variation on CO_2 storage limit.

Reservoir Depth (m)	Maximum Allowable Pore Pressure (MPa)	SIL (Years)	Occupancy (%)	Mass of Injected CO_2 (KTons)
500	26.3	5.266	1.57	97.45
1000	34.1	6.28	1.60	116.41
1250	36.0	6.35	1.62	117.58
1500	41.8	7.73	1.88	143.86
2000	49.5	8.877	2.04	165.52
2500	56.5	9.619	2.13	179.44
3000	62.4	9.78	2.10	182.53

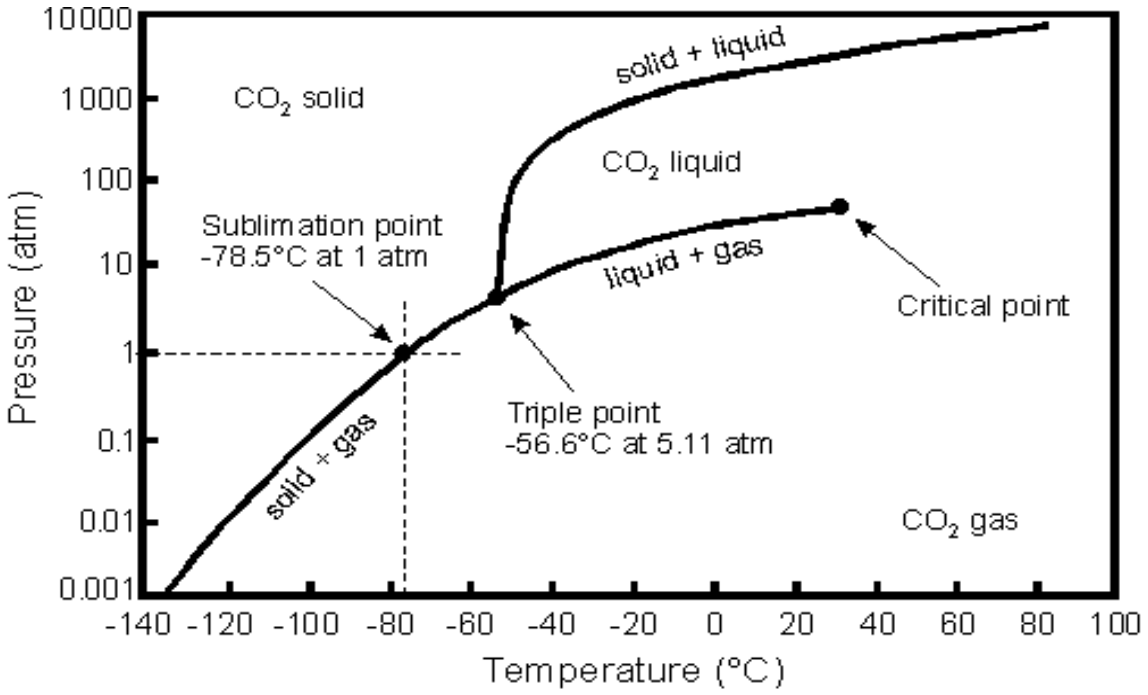

Fig. 3. Phase Diagram of CO_2 [22]

The results presented in this study show that once realistic structural geometries for CO_2 sequestration projects are considered, geometrical parameters such as anticline wavelength, anticline amplitude and respective aquifer depth influence the SIL, the occupancy and the total amount of injected CO_2 .The results presented in Tables 4, 6 and 7 suggest that the anticline wavelength and amplitude have direct influence on the CO_2 storage capacity. The larger the wavelength and the lower the amplitude, the longer it takes to get to the maximum allowable pore pressure in a closed system and thus the more CO_2 can be injected into the anticline. Comparison with the horizontally layered basin shows that the horizontally layered basins have more storage capacity than the actual capacity of an anticline structure. This suggests that the existence of anticline structures should not be ignored by simplifying the model with horizontally layered basins. Using simplified model geometries can result in the prediction of Safe Injection Limits that are longer than the actual tolerance of the medium.

When comparing the influence of the geometrical parameters on the CO_2 occupancy in closed systems, the results only show slight variations. However, once other fluid flow boundary conditions are considered the effects of the geometrical parameters become significantly more pronounced. Table 10 shows the effect of reservoir height and boundary condition variation on CO_2 storage capacity.

Although the occupancy of the two models in a closed system is the same, the thinner reservoir of 50 meter thickness shows a better sweep and occupancy of 28.95% under the open conditions, compared to the 25.13% of the 100 meter thick reservoir. While the difference in the volume of the two reservoirs controls the mass of injected CO_2 and

SIL, the difference in occupancy can show the influence of geometrical parameters that may be masked out otherwise by the influence of the fluid flow boundary conditions.

Table 10. Effect of reservoir height and boundary condition variation on CO_2 storage capacity

Height (m)	Boundary Type	SIL (Years)	Occupancy (%)	Average Pressure (MPa)	Mass of Injected CO_2 (KTons)
50	Closed	3.29	1.62	32.5	60.95
	Open	30.72	28.95	13.9	577.13
100	Closed	6.35	1.62	32.4	117.58
	Open	50	25.13	13.1	942.10

The simulation results confirm previous studies [4, 11] showing that the type of fluid flow boundary condition has a huge impact on the result parameters. CO_2 occupancy in closed systems is a function of total compressibility. When more pore space is available, assuming that the total compressibility stays the same, more CO_2 volume can be injected into the reservoir, but the overall occupancy of the reservoir stays the same regardless of the volume or the height, as shown in Table 5. Our results of maximum occupancy of 1.6%-2% compare well with results from [11] of 0.5% and [4] of ~1% for closed systems.

The effect of the lateral fluid flow boundary conditions on CO_2 storage capacity for the base anticline was presented in Table 8. These results suggest that the assumption of open boundary condition can significantly increase the CO_2 storage capacity but a semi-open boundary serves the purpose even better, as long as the pressure stays in the safe injection limit. The question, however, is whether the open boundary condition case can be observed in real life.

One way of achieving open boundary conditions is through the use of pore volume multipliers [24] which, in the authors' opinion, are only applicable to reservoir simulation studies, where exact knowledge about the size and water flux of the aquifer is not available. Under these circumstances one may use the pore volume multipliers on the aquifer grid blocks to achieve a history match. However, this is not the case in studies concerning CO_2 sequestration in saline formations where the aquifer is the most important part of the fluid system.

Another way of achieving open boundary conditions, as presented previously, is to drill brine production wells at the boundaries and control the pressure through these production wells. While drilling of these wells is possible, a question that needs to be addressed is where to dispose of the produced brine.

Another possibility is to have such large aquifers that the compressibility of the liquids in place doesn't result in the increased pore pressure. In order to investigate the typical size needed for such an aquifer, we have made two extensions of the base case where the boundaries are extended 10km and 50km on each side of the 3km wide anticline structure, resulting in reservoirs that are 23 and 103 km long respectively. As it is shown in Table 11, the large reservoir of 23 km width fails to replicate the results of the fully open boundary and the gigantic reservoir of 103km size is the minimum reservoir size capable of replicating such results. This conclusion leaves us with some fundamental questions that need to be answered before one can make the fully open boundaries assumption:

1. What is the likelihood of finding such gigantic reservoirs in the immediate vicinity of CO_2 producers?

2. Provided that such a reservoir is available, are there any faults/inhomogeneities or stress anomalies that influence the maximum allowable pore pressure?
3. What is the probability that no one else is injecting in the same aquifer of interest which would otherwise result in pressure interference in the premises of the well(s) that are planned for the CO_2 sequestration?

Table 11. Comparison of different model sizes and boundary conditions.

Reservoir Size (Km)	Reservoir Volume (10^6 m^3)	SIL (Years)	Boundary Type	Mass of Injected CO_2 (KTons)
6	9.13	6.35	Closed	117.58
6	9.13	50	Open	942.11
23	35.0	22.46	Closed	420.71
103	156.7	50	Closed	942.10

The presented results show that the lateral fluid flow boundary conditions have a significant influence on CO_2 sequestration parameters. Although huge aquifers such as Sleipner [25] exist throughout the world that have high potential for CO_2 sequestration, they may not be in the vicinity of the power plant(s) of interest or meet the salinity level requirements set forward by federal or state regulations; thus an important step in CO_2 sequestration feasibility study of a candidate aquifer should be determination of its size. This can be achieved by analogy between the existing and well established practices in petroleum engineering for well testing and estimation of the size/drainage radius of an oil well. Without knowing the exact size of the aquifer and matching boundary type, care should be taken before suggesting safe sequestration limits. In the authors' opinion, it is better to take the more conservative practice and assume semi-open or closed boundaries to stay within the safe sequestration limit, instead of assuming that the aquifer has fully

open boundaries and face the otherwise high risk of exceeding the maximum allowable pore pressure and causing the rock to fail. Note should be taken that the maximum allowable pore pressure used throughout this study is the pressure that will result in failure of intact rock, which is obviously greater than the critical pore pressure needed for reactivation of favorably oriented existing failed structures.

4. Conclusions

While the assumption of using horizontally layered basins for CO_2 sequestration studies may be valid for most cases, the need for an actual trap system requires a more realistic geometry for parametric studies and simulations. The geometry should be flexible enough to include faults or fractures and any unconformities that may exist. Our study shows that by using finite element analysis pre-processor geometries resembling structural trap systems can be generated and successfully converted into native fluid flow simulation formats. This novel approach enables us to study the influence of geometric parameters such as anticline wavelength, amplitude and thickness.

The results of our study show that higher wavelengths, lower amplitudes and relatively thick layers provide the best conditions for safe CO_2 sequestration. Further, the depth of the sequestration site also plays an important role. Our results conclude that for aquifer depths of 2500m and 3000m (for a closed system) the maximum occupancy and SIL can be obtained, respectively. If the economic costs of drilling to the deeper aquifers and compression of CO_2 for injection into such reservoirs can be justified, deep CO_2 sequestration results in higher storage capacity.

A major and not surprising conclusion is that the lateral fluid flow boundary condition of an aquifer system has the most significant influence on the CO_2 sequestration

parameters. The assumption of an open system requires gigantic aquifers (~100 km) that may be very difficult, if not impossible, to locate in the vicinity of many CO_2 producers. The open system assumption might also lead to over-simplified cases, unless brine production wells are included. A more realistic approach of semi-open fluid flow boundaries yields similar if not better results than the open system case. However, this approach seems only applicable if the total magnitude of the lateral flow boundary condition of an aquifer system can be determined e.g. by water drawdown tests similar to conventional pressure transient testing and production data analysis of the oil and gas wells. Our results show that for such a system, the anticline wavelength, amplitude and thickness have a pronounced influence on CO_2 sequestration parameters.

However, unless extensive field tests permit the application of semi-open or open aquifer, this study shows that the safest approach for a sustainable CO_2 sequestration project should be the assumption of closed fluid flow boundaries.

Acknowledgement

The authors gratefully acknowledge financial support from US Department of Energy's National Energy Technology Laboratory under grant # DE-FE0001132.

References

Metz, B., O. Davidson, Bosch. P, Dave. R and L. A. Meyer (eds.). IPCC, 2007: *Climate Change 2007: Mitigation of Climate Change*. Contribution of Working Group III to the Fourth Assessment Report of the Intergovernmental Panel on Climate Change. Cambridge University Press, Cambridge, United Kingdom and New York, NY, USA.

Loizzo, M., Lecampion, B., Bérard, T., Harichandran, A. and L. Jammes, 2009. Reusing O&G Depleted Reservoirs for CO_2 Storage: Pros and Cons. *Paper SPE 124317-MS presented at SPE Offshore Europe Oil & Gas Conference and Exhibition, Aberdeen, UK, 8-11 September 2009.*

Cappaa, F. and J. Rutqvist. 2011. Modeling of coupled deformation and permeability evolution during fault reactivation induced by deep underground injection of CO_2. *Int. J. of Greenhouse Gas Control. 5: 336-346.*

Ehlig-Economides, C. and M.J. Economides. 2010. Sequestering carbon dioxide in a closed underground volume. *J. Pet. Sci. & Tech.* 70: 123-130

Taberner. C., Cartwright, L. and T. Xu. 2009. Injection of supercritical CO_2 into deep saline carbonate formations, predictions from geochemical modeling. *Paper SPE 121272 presented at SPE EUROPEC/EAGE Annual Conference and Exhibition, Amsterdam, Netherlands, 8-11 June 2009.*

Inoue, N. 2009. Answers to some questions about the coupling between fluid flow and rock deformation in oil reservoirs. *Paper SPE 125760 presented at SPE/EAGE Reservoir Characterization and Simulation Conference, Abu Dhabi, UAE, 19-21 October 2009.*

Tran, D. Shrivastava, V. Nghiem, L. and B. Kohs. 2009. Geomechanical risk mitigation for CO_2 sequestration in saline aquifers. *Paper SPE 125167 presented in SPE Annual Technical Conference and Exhibition, New Orleans, USA, 4-7 October 2009.*

Settari, A. and F.M. Mourits, 1998. A coupled reservoir and geomechanical simulation system. *Paper SPE 50939. SPE J. 3 (3): 219-226.*

Thomas, L.K., Chin, L.Y., Pierson, R.G. and J.E. Sylte. 2003. Coupled Geomechanics and Reservoir Simulation. *SPE J. 8 (4): 350-358.*

Dean. R.H., Gai, X., Stone, C.M. and S.E. Minkoff. 2006. A Comparison of Techniques for Coupling Porous Flow and Geomechanics. *SPE J. 11 (1): 132-140.*

Zhou, Q., Birkholzer, J. T., Tsang, C.F. and J. Rutqvist. 2008. A method for quick assessment of CO_2 storage capacity in closed and semi-closed saline formations. *Int. J. of Greenhouse Gas Control 2: 626-639.*

Pettersen, O. 2006. A predictor for accelerated coupled rock mechanics and reservoir simulation. *In proceedings of 10th European Conference on the Mathematics of Oil Recovery, Amsterdam, Netherlands, 4-7 September 2006.*

Craupner, B. J., Li, D. and S. Bauer. 2011. The coupled simulator Eclipse-OopenGeoSys for the simulation of CO_2 storage in saline formations. *J. Energy Procedia 4: 3794-3800*

Schembre-McCabe, J. M. and R. Gurton. 2007. Mechanistic Studies of CO_2 Sequestration. *Paper IPTC11391 presented at The International Petroleum Technology Conference, Dubai, UAE, 4-6 December 2007.*

Van der Meer, L. G. H. and J. D. van Wees. 2006. Limitations to Storage Pressure in Finite Saline Aquifers and the Effects of CO_2 Solubility on Storage Pressure. *Paper SPE 103342 presented at the SPE Annual Technical Conference and Exhibition, San Antonio, Texas, 24-27 September.*

Rutqvist, J., Birkholzer, J., Cappa, F. and C.F. Tsang. 2007. Estimating maximum sustainable injection pressure during geological sequestration of CO_2 using coupled fluid flow and geomechanical fault-slip analysis. *J. of Energy Conversion and Management 48: 1798-1807.*

Paradeis, M., Eckert, A. and X. Liu. 2012. Influences of Anticline Reservoir Geometry on Critical Pore Pressures Associated with CO_2 Sequestration. *Paper ARMA 12-319, to be presented in 46th US Rock Mechanics Geomechanics Symposium, Chicago, USA, 24-27 June 2012.*

http://www.sourcewatch.org/index.php?title=Existing_U.S._Coal_Plants, accessed January 2012.

Amirlatifi, A., Eckert, A., Nygaard, R. and B. Bai. 2011. Prediction of caprock fractures during CO_2 sequestration by coupled modeling in complex geological fields. In *proceedings of tenth annual conference on carbon capture and sequestration, Pittsburgh, USA, 2-5 May 2011.*

Amirlatifi, A., Eckert, A., Nygaard, R. and B. Bai. 2011. Estimation of reservoir uplift, seismicity and failure likelihood during CO_2 injection through coupled reservoir simulation. *Paper CSUG/SPE 148946-PP presented in Canadian Unconventional Resources Conference, Calgary, Canada, 15–17 November 2011.*

Houseknecht, D.W. and F.G. Ethridge. 1978. Depositional history of the Lamotte sandstone of southeastern Missouri. *J. of Sedimentary Petrology 48 (2): 575-586.*

Bachu, S., Gunter, W.D. and E.H. Perkins. 1994. Aquifer disposal of CO_2: hydrodynamic and mineral trapping. Energy Conversion and Management, 35 (4): 269-279.

Birkholzer, J.T., Zhou, Q. and C.F. Tsang. 2009. Large-scale impact of CO_2 storage in deep saline aquifers: a sensitivity study on pressure response in stratified systems. *Int. J. of Greenhouse Gas Control 3: 181-194*

Samier, P. and S.D. Gennaro. 2007. Practical iterative coupling of geomechanics with reservoir simulation. *Paper SPE 106188, presented at SPE Reservoir Simulation Symposium, Houston, USA, 26-28 February 2007.*

Kongsjorden, H., Kårstad, O. and Tore A. Torp. 1998. Saline aquifer storage of carbon dioxide in the Sleipner project. *J. Waste Management 17 (5-6): 303-308*

PAPER

3. FLUID FLOW BOUNDARY CONDITIONS: THE NEED FOR PRESSURE TRANSIENT ANALYSIS FOR CO_2 SEQUESTRATION STUDIES

(Submitted to the International Journal of Green House Gas Control)

Amin Amirlatifi, Andreas Eckert

Geological Sciences & Engineering, Missouri University of Science and Technology, 129 McNutt Hall 1400 N. Bishop, Rolla, MO 65409, USA

Abstract

Current studies involving the simulation of fluid flow for CO_2 sequestration applications are based on assumptions regarding the lateral and vertical fluid flow boundary conditions for the storage medium. Common types of boundary conditions are limited to either open (steady state) or closed (semi-steady state) lateral boundaries, together with a complete or partial caprock seal. In this paper pressure transient analysis techniques are utilized to provide a quantitative analysis tool to assess a larger variety of fluid flow boundary conditions. A short drawdown followed by a prolonged buildup test is capable of identifying the type of fluid flow boundary condition, including closed, open, semi-open and infinite systems. The large difference in CO_2 storage capacity and the different levels of geomechanical risks associated to different fluid flow boundary conditions suggest that the presented methodology should be considered prior to fluid injection scenarios.

Highlights:

1. We present an overview of commonly used fluid flow boundary conditions for CO_2 sequestration studies.
2. Difference between commonly mistaken infinite and open systems is discussed.

3. Semi-open systems are presented as an intermediate boundary condition.
4. Pressure transient analysis is presented as a tool to quantify fluid flow boundary conditions.
5. A short drawdown followed by a prolonged build up can determine lateral boundary type.

Keywords: CO_2 sequestration, fluid flow boundary condition, semi-open, open, closed, infinite, flux, drawdown, buildup, well testing

1. Introduction

Geologic CO_2 sequestration has been identified as a promising strategy to reduce the CO_2 concentration in the atmosphere (Ipcc, 2005). The most viable sequestration targets include deep saline aquifers and mature hydrocarbon fields (Bachu and Adams, 2003; Holloway and Savage, 1993; Holloway, 2001; Klara et al., 2003). In order to predict the target formation's storage capacity, the spreading of the CO_2 plume and the geomechanical risks associated to the pore pressure increase, the fluid flow boundary conditions of the hydrologic system need to be known. The current practice distinguishes between open and closed aquifer systems. Open systems represent aquifer systems in large scale sedimentary basins where the system boundary is characterized by a constant pressure and often assumed to be hydrostatic (Baklid et al., 1996; Ehlig-Economides and Economides, 2010; Izgec et al., 2006; Kumar et al., 2005; Nghiem et al., 2004; Pruess et al., 2001; Sengul, 2006) enabling that the displaced brine can escape the formation. Pressure changes for such scenarios are limited to the immediate vicinity of the injection well (Amirlatifi et al., 2011; Ehlig-Economides and Economides, 2010) and the risk for

geomechanical failure of the reservoir and cap rock is often negligible. Closed systems represent a compartmentalized geologic storage formation bound on all sides by low permeability formations similar to what is often observed in hydrocarbon reservoirs. Injection of fluids into closed systems results in significant pressure build-ups (Amirlatifi et al., 2012; Ehlig-Economides and Economides, 2010; Zhou and Birkholzer, 2007) mitigating the storage potential and the risk for geomechanical failure is high (Comerlati, 2006; Lucier et al., 2006; Rutqvist et al., 2008, 2007; Tran et al., 2010, 2009; Zoback et al., 2006). This pressure build-up is strongly dependent on the radial extent of the reservoir, whereby large scale, i.e. infinite, reservoirs (~100km) effectively represents the case of the open system fluid flow boundary conditions (Zhou et al., 2008). For an assessment of formation storage capacity Zhou et al. (2008) also consider the case of a semi-permeable cap seal enabling some of the brine to migrate vertically whilst containing the CO_2 safely due to the capillary barriers. Their results show that the resulting pressure build-up is limited and the storage capacity is increased compared to a completely closed system. Amirlatifi et al. (2012) also showed that partially open or partially closed systems (laterally) has a significant impact on the safe sequestration limit and that the validation of fluid flow boundary conditions is of utmost importance in the design of CO_2 sequestration limits.

Within this context, in addition to infinite, open and closed systems, Kumar (1977a, 1977b) presented steady flow equations for reservoirs experiencing partial water drive or fluid injection under steady conditions. Kumar (1977a, 1977b) introduced a factor, f, into the fluid flow equations to account for the influx rate at the boundary, thus mimicking a semi-open or partially open boundary. In this paper we follow this concept and use pressure

transient analysis to determine location and type of fluid flow boundaries. Transient pressure analysis is a well-established technique employed in the oil and gas industries for determining the average characteristic parameters for the drainage area during the transient period and estimating the aquifer drive mechanisms once the pressure perturbation reaches the boundary. In this paper we show that the application of a draw down test followed by a prolonged buildup test to a candidate aquifer prior to CO_2 sequestration can give insight on the fluid flow boundaries.

1.1 Fluid flow boundary conditions and their relation to pressure transient analysis

Fluid flow in aquifers subjected to CO_2 sequestration is similar to the flow in oil and gas reservoirs subjected to fluid injection for pressure maintenance or improved recovery processes. Assuming that the storage medium is cylindrical with boundaries located at a radius of r_e from the injection location, the continuity equation can be written as:

$$\frac{1}{r}\frac{\partial(r\rho u_r)}{\partial r} = -\phi\frac{\partial \rho}{\partial t} \tag{1}$$

Darcy's law for radial flow can be expressed in terms of $p(r,t)$ (Stewart, 2011):

$$u_r(r,t) = -\frac{k}{\mu}\frac{\partial p(r,t)}{\partial r} \tag{2}$$

The radial flow equation can then be written as:

$$\frac{\partial p}{\partial t} = \alpha.\frac{1}{r}.\frac{\partial\left(r\frac{\partial p}{\partial r}\right)}{\partial r} \tag{3}$$

where $\alpha = \frac{k}{\phi\mu c_t}$ is the hydraulic diffusivity.

Equation (3) can be expressed in terms of dimensionless variables:

$$\frac{\partial p_D}{\partial t_D} = \frac{1}{r_D} . \frac{\partial \left(r_D \frac{\partial p_D}{\partial r_D} \right)}{\partial r_D} \tag{4}$$

with the dimensionless variables defined as:

$$r_D = \frac{r}{r_w} \tag{5}$$

$$t_D = \frac{\alpha t}{r_w^2} \tag{6}$$

$$p_D = \frac{2\pi kh}{q_s B\mu} (p_i - p) \tag{7}$$

Assuming that the well is equivalent to a line in an infinite homogenous reservoir, the line source solution, i.e. pressure at any point and time in the reservoir can be determined through:

$$p_D(r_D, t_D) = -\frac{1}{2} E_i \left(-\frac{r_D^2}{4t_D} \right) \tag{8}$$

where $E_i(x)$ is the exponential integral of x defined as:

$$E_i(x) = \int_x^\infty \frac{e^{-t}}{t} dt \tag{9}$$

Replacing the dimensionless variables with p, r and t results in the lines source solution of the form (George Stewart, 2011):

$$p(r, t) = p_i - \frac{\mathrm{q}\mu B}{4\pi kh} \left[-E_i \left(-\frac{\phi \mu c_t r^2}{4kt} \right) \right] \tag{10}$$

For

$$\frac{kt}{\phi\mu c_t r^2} > 25 \tag{11}$$

the E_i function can further be approximated using the natural log. Considering the pressure at wellbore, r=r_w (r_D=1), the analytical solution for pressure evolution over time for the line source solution becomes

$$p_w(t) = p_i - \frac{\mathrm{q}\mu B}{4\pi kh}\left[\ln\left(\frac{kt}{\phi\mu c_t r_w^2}\right) + 0.80907 + 2S\right] \tag{12}$$

Eq. (4) is the general governing equation for fluid flow in a medium, which can also be extended to mixed phase flow systems, such as CO_2 and brine. (Ehlig-Economides and Economides, 2010) has presented a complete form in terms of Buckley and Leverett (1942) displacement theory in the reservoir but here we will focus on the pressure evolution around the wellbore.

Application to a mixed CO_2 and brine system enables to use well testing and in particular the draw down test, where terminal rate is kept constant and the change of pressure over time is analyzed, for CO_2 sequestration studies.

Eq. (12) is applicable for transient periods before the pressure disturbance reaches the boundaries of the medium (George Stewart, 2011)

$$t < \frac{0.3\phi\mu c_t r_e^2}{k} \tag{13}$$

Once the pressure front has reached the boundary, the infinite acting radial flow solution is no longer valid and based on the type of fluid flow boundary conditions different governing equations have to be used (George Stewart, 2011). Current approaches for modeling fluid flow boundary conditions for CO_2 sequestration studies are limited to open or closed boundary conditions (Bachu et al., 2007a; Zhou et al., 2008).

In a closed system, the aquifer is constrained by no-flow boundaries, $\frac{dq}{dt} = 0$, and fluid flow is limited to the reservoir extent. Once the boundary is felt, the pressure evolution of a closed boundary reservoir is described by pseudo steady state behavior (Ehlig-Economides and Economides, 2010), a well described process in the oil and gas industry (George Stewart, 2011).

$$p_w(t) = p_i - \frac{\mathrm{q}\mu B}{2\pi kh}\left[\frac{2kt}{\phi\mu c_t r_e^2} + \ln\frac{r_e}{r_w} - \frac{3}{4}\right] \qquad (14)$$

The short term storage mechanisms for CO_2 are mainly limited to the solution of CO_2 in the in-situ brine and the compression of the fluids until a pressure limit, i.e. the fracture pressure or the pore pressure limit for reactivation of existing faults is reached (Amirlatifi et al., 2012). These characteristics make closed boundary estimates being the most conservative and the least storage capacities.

For "open boundary" fluid flow conditions (Baklid et al., 1996; Ehlig-Economides and Economides, 2010; Izgec et al., 2006; Kumar et al., 2005; Nghiem et al., 2004; Pruess et al., 2001; Sengul, 2006), the pore pressure at the aquifer boundaries remains at a constant level (for CO_2 sequestration studies often assumed to be hydrostatic) throughout the life of the sequestration project, i.e. $\frac{dp}{dt} = 0$. This type of boundary condition resembles the steady state or constant pressure boundary assumption in the oil and gas industry (Ehlig-Economides and Economides, 2010) and the pressure evolution is given by (George Stewart, 2011):

$$p_w = p_i - \frac{\mathrm{q}\mu B}{2\pi kh}\left[\ln\frac{r_e}{r_w}\right] \qquad (15)$$

This is an indicator of an aquifer that is connected to another aquifer or to the surface (Ehlig-Economides and Economides, 2010). Constant pressure boundary

conditions can be attained by placing brine removal wells along the boundaries with water withdrawal rates selected such that the pore pressure remains at the initial level at all times.

A third possibility for the boundary conditions is to have a gigantic aquifer such as the Sleipner field in the North Sea (Baklid et al., 1996; Holloway, 2001; Orlic et al., 2004) that resembles an infinite reservoir. Since a physical lateral boundary is not present, for this type of aquifer the transient behavior is observed continuously.

The short term storage mechanism in an open or infinite aquifer subject to CO_2 sequestration is the solution of CO_2 in the brine and the compression of the fluids in place. Unlike for the closed boundary conditions, the injected CO_2 pushes the brine further away from the injection site and thus a better chance of mixing with the brine in place occurs. This increased contact yields better solution of CO_2 in the brine, resulting in an incremental storage capacity compared to the closed system. Since the pore pressure increase is limited to the wellbore vicinity and the overall pressure increase is negligible, compared to the closed system, the geomechanical risks associated with storage under closed boundary conditions are not observed in these systems and consequently, the storage capacity is notably increased (Amirlatifi et al., 2012, 2011).

2. Model setup and results

In order to compare the influence of the previously described boundary condition scenarios and to test the case of a partially open system, a simple circular reservoir model (Fig. 1) is subjected to a draw-down test for the period of 2000 hours followed by an extended buildup for 5000 hours. Table 1 shows model setup.

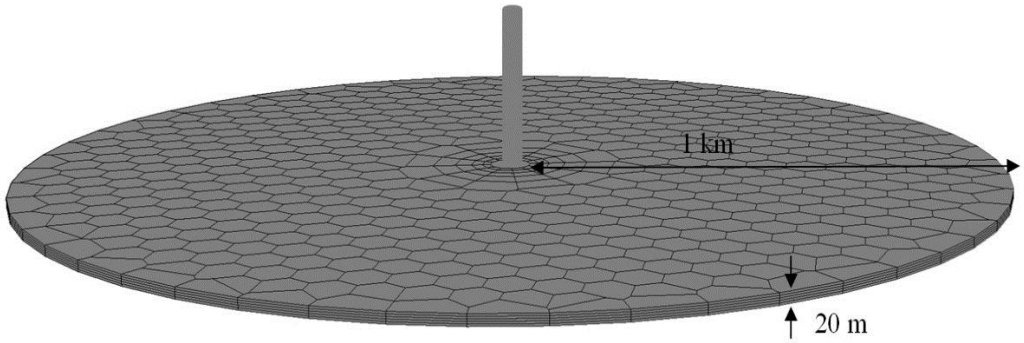

Fig.1. Schematic representation of the model (not to scale)

Fig. 2 shows the bottom-hole pressure change over time for a no-flow (closed) boundary. The initial pressure drop after onset of water withdrawal is governed by the skin effect and well bore storage (if present) followed by the transient period which ends once the pressure perturbation reaches the boundary. Once the boundaries are felt, the Cartesian plot of pressure vs. time will show a straight line portion. However, this type of representation is limited for identifying the governing fluid flow mechanism and will not be presented for the future scenarios. A better representation is obtained by the use of log-log plots of differential pressure and its derivative vs. time (George Stewart, 2011).

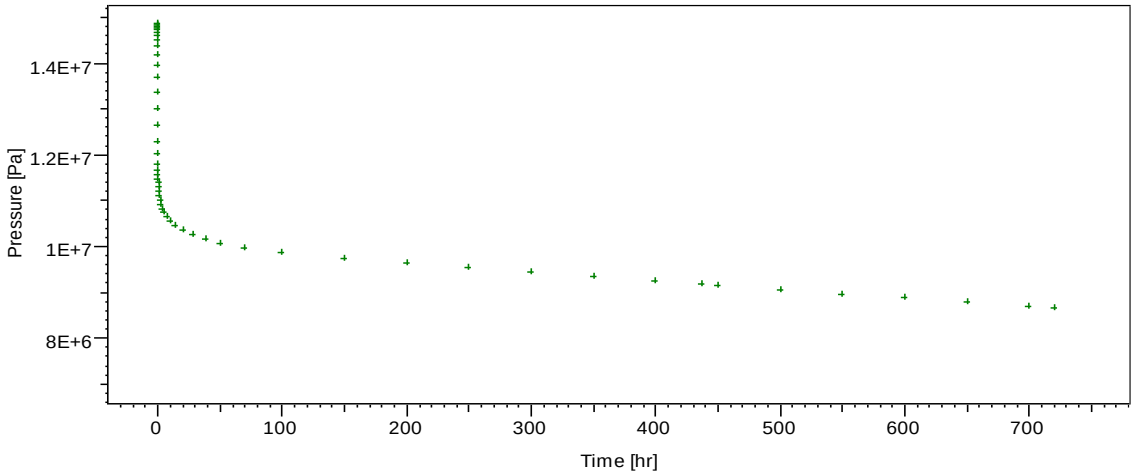

Fig. 2. Flowing bottom-hole pressure versus time for the draw-down test for the no-flow model.

Table 1 - Model Properties used for the study of draw down test behavior under different boundary conditions

Properties	Values
$r_w[m]$	0.09144
$h[m]$	20
$Reference\ Depth[m]$	1500
$\phi[]$	0.2
$B\left[\frac{m^3}{sm^3}\right]$	1.1
$\mu[Pa.Sec]$	10^{-3}
$c_t\left[\frac{1}{Pa}\right]$	$4.35113 * 10^{-10}$
$C\left[\frac{m^3}{kPa}\right]$	$2.30592 * 10^{-4}$
$S[]$	0
$k[m^2]$	$9.86923*10^{-14}$
$q\left[\frac{m^3}{Day}\right]$	500
$t_p[hr]$	2000
$t_s[hr]$	5000
$p_i[Pa]$	$1.47*10^7$
$T_i[°C]$	53

2.1 No-Flow ("closed") Boundary

Figures 3 and 4 show the pressure evolution over time for the closed system. The trend of the pressure derivative can be used to identify the time at which boundary is felt. In the drawdown test, Fig. 3, the no-flow boundary results in an elevated pressure drop that is signified by the upward tail of the derivative curve. The slope of this portion is always one.

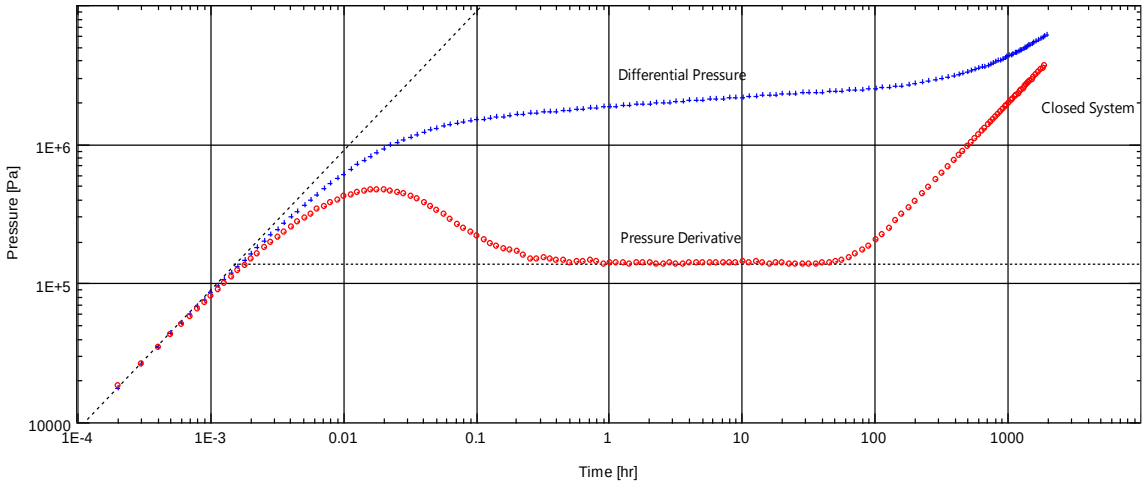

Fig. 3. Log-Log plot bottom-hole pressure difference versus flow time of the drawdown test for the no-flow model.

Fig. 4 shows the pressure change for the closed boundary in the buildup test which is identified by the pressure derivative tending towards zero.

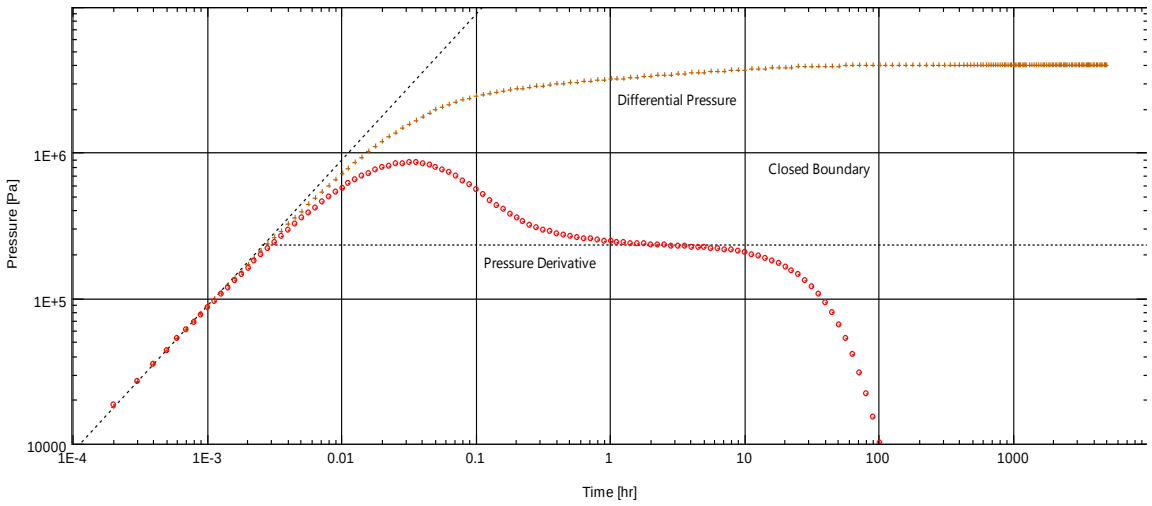

Fig. 4. Log-Log plot bottom-hole pressure difference versus flow time of the buildup test for the no-flow model.

2.2 Infinite aquifer

Figures 5 and 6 show the differential pressure evolution over time of a drawdown and buildup test for an infinite aquifer, respectively. Here, the pressure change over time is not affected by the boundary; thus no meaningful change in the pressure drop trend, differential pressure or pressure derivative is observed.

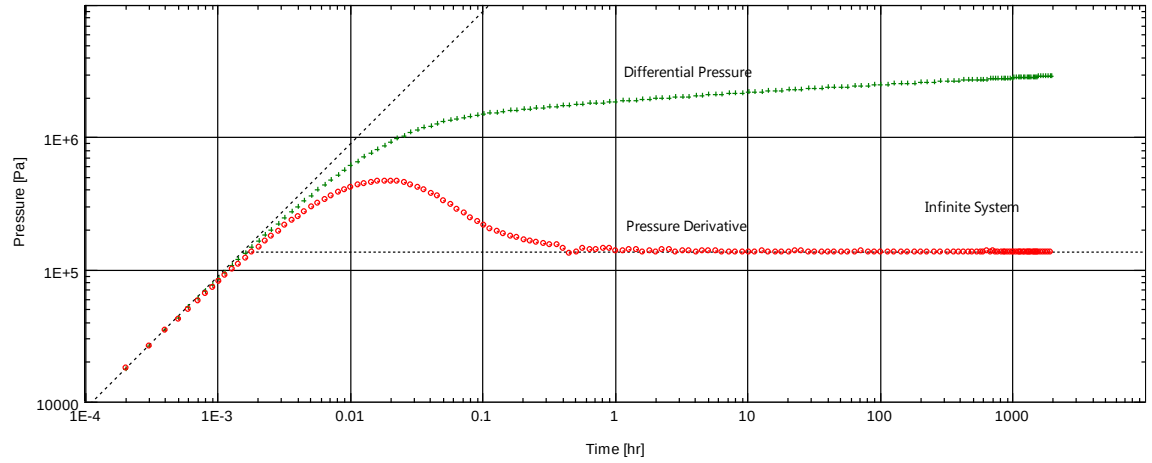

Fig. 5. Log-Log plot of bottom-hole pressure difference versus flow time for the drawdown test for the infinite aquifer model.

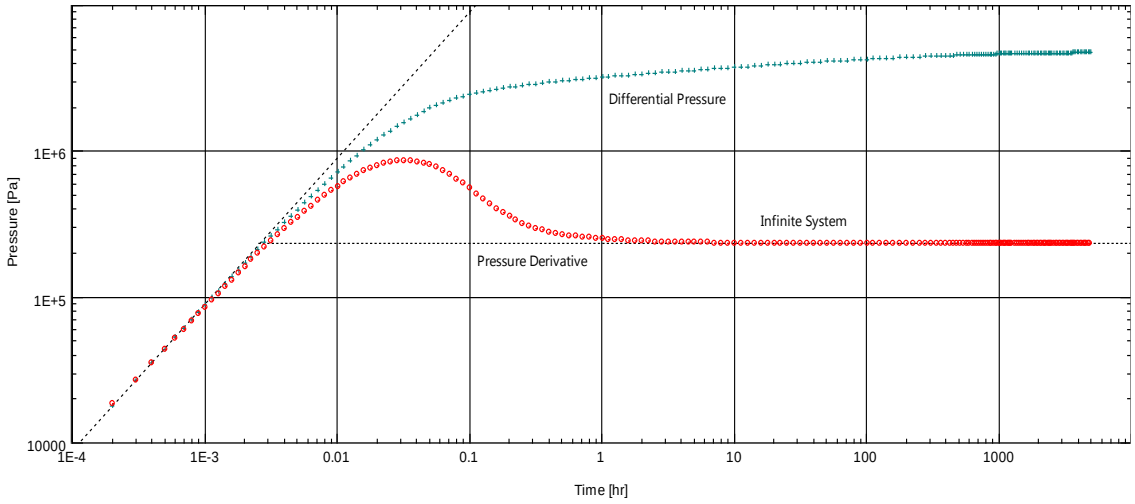

Fig. 6. Log-Log plot of bottom-hole pressure difference versus flow time for the buildup test for the infinite aquifer model.

2.3 Constant Pressure ("open") Boundary

Figures 7 and 8 show the differential pressure evolution over time of the drawdown and buildup test for the open system, respectively. The constant pressure boundary results in a constant bottom-hole pressure and as a consequence, the pressure difference between initial pressure and bottom-hole pressure will be a constant which is signified by the derivative curve values tending towards zero.

This type of boundary condition is analogous to the steady-state boundary condition in the oil and gas industry and the aquifers termed "open" in CO_2 sequestration studies.

2.4 Semi-Open Boundary

2.4.1 25% open system

Fig. 9 shows the differential pressure evolution over time for a 25% open boundary system for the drawdown test. The pressure derivative shows a slope less than 1 (which was the signature of the closed system) followed by a downward trend. This results in a

less steep decrease in the rate of pressure degradation compared to the closed boundary condition (pseudo-steady state).

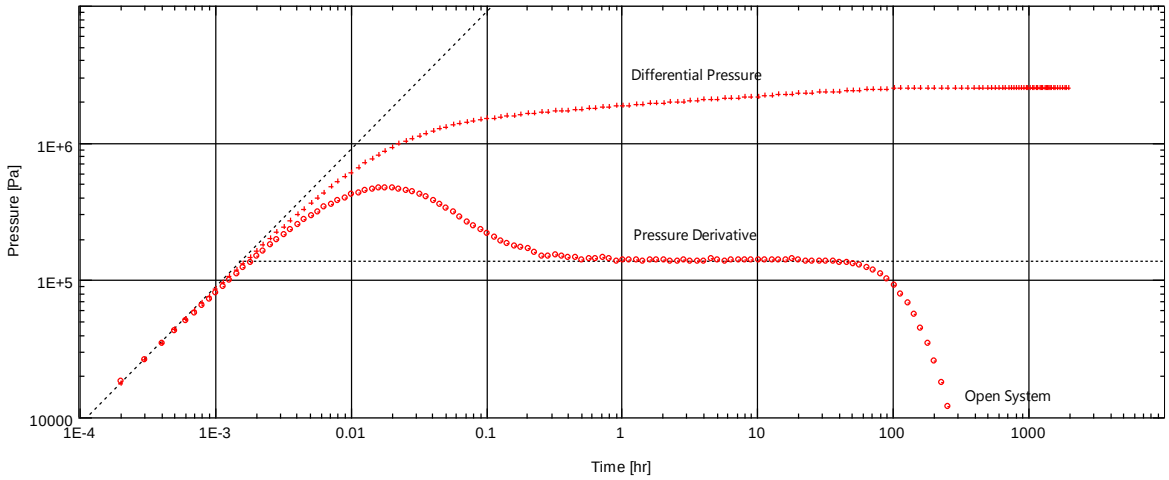

Fig. 7. Log-Log plot of bottom-hole pressure difference versus flow time of the drawdown test for the constant pressure model.

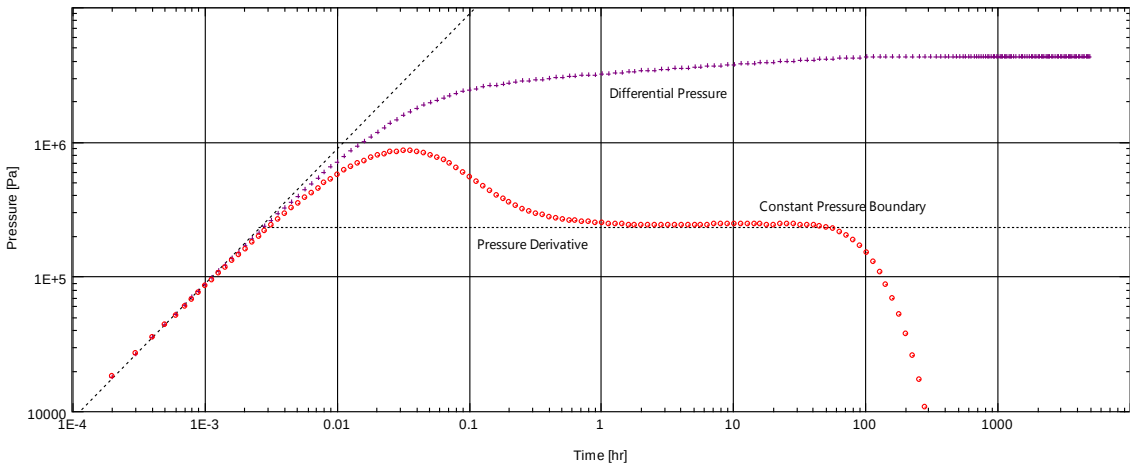

Fig. 8. Log-Log plot of bottom-hole pressure difference versus flow time of the buildup test for the constant pressure model.

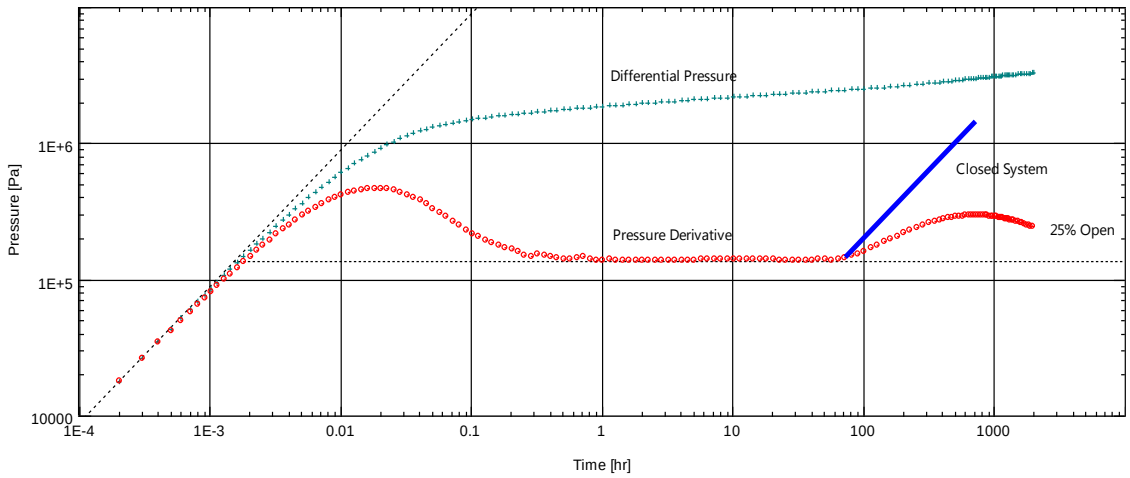

Fig. 9. Log-Log plot of bottom-hole pressure difference versus flow time for the drawdown test in a 25% open boundary model.

2.4.2 50% open system

Fig. 10 shows the pressure change over time for the drawdown test of the 50% open system. The effect of the boundary is denoted by a small hump in the pressure derivative curve followed by a continuous decrease in the pressure derivative, as it tends to zero. A conclusion may be drawn that the semi-open system is ultimately reaching a delayed steady state condition, dictated by $\frac{\partial p}{\partial t} = 0$.

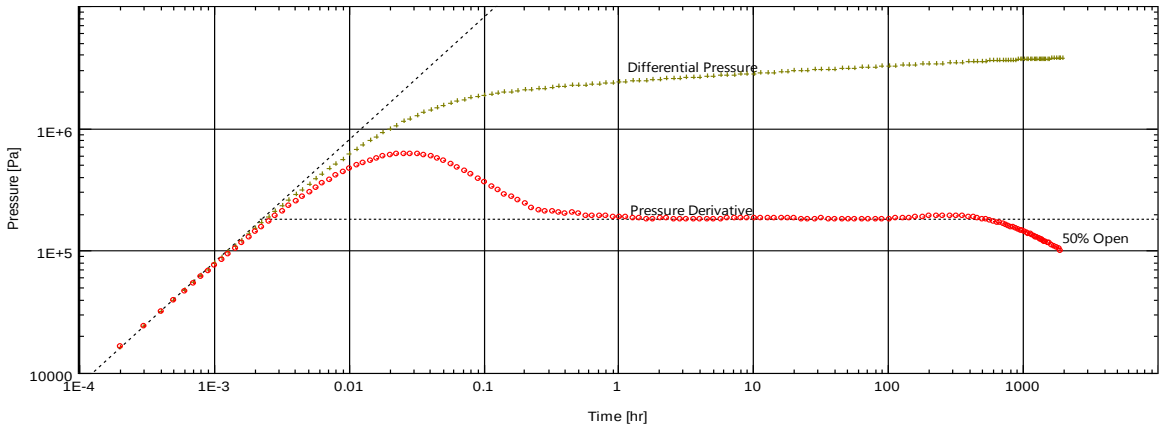

Fig. 10. Log-Log plot of bottom-hole pressure difference versus flow time for the drawdown test in a 50% open boundary model.

2.4.3 75% open system

Fig. 11 shows the differential pressure evolution over time for a 75% open boundary. As shown in this figure, the pressure derivative can be used to determine the time at which boundary is felt which is denoted by a decrease in the rate of pressure degradation as the pressure derivative tends to zero. The rate at which the pressure derivative tends to zero is the same as that of the 50% open system but the system reaches steady state conditions, as defined by $\frac{\partial p}{\partial t} = 0$, sooner than the 50% open system.

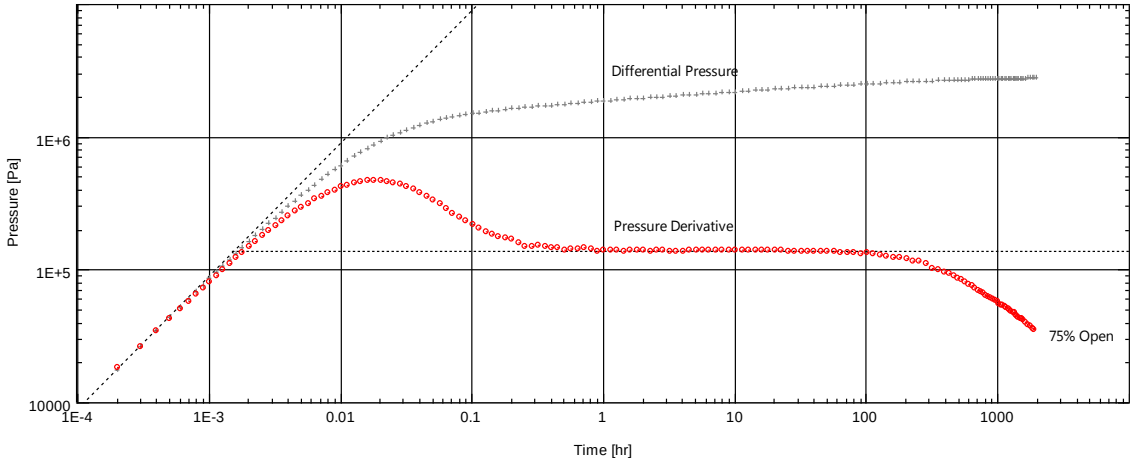

Fig. 11. Log-Log plot of bottom-hole pressure difference versus flow time for the drawdown test in a 75% open boundary model.

2.4.4 Buildup test

Fig. 12 shows the buildup test for the three semi-open systems. The three models exhibit a similar buildup trend where a slight decrease in the pressure derivatives followed by an increase in the pressure derivative is observed once the pressure perturbation reaches the boundary. It can be noted that this valley is larger in the 75% open system than for the other systems. In addition, this system has a less steep late time derivative increase, than

the 25% system or the 50% open system. The three systems behave different than the closed or constant pressure systems as the pressure derivative does not tend to zero. The late pressure response, after the valley, is mainly controlled by the fluid flow through the boundaries and the system with the most fluid throughput (i.e. the 75% open system) converges towards a similar buildup trend as the infinite system.

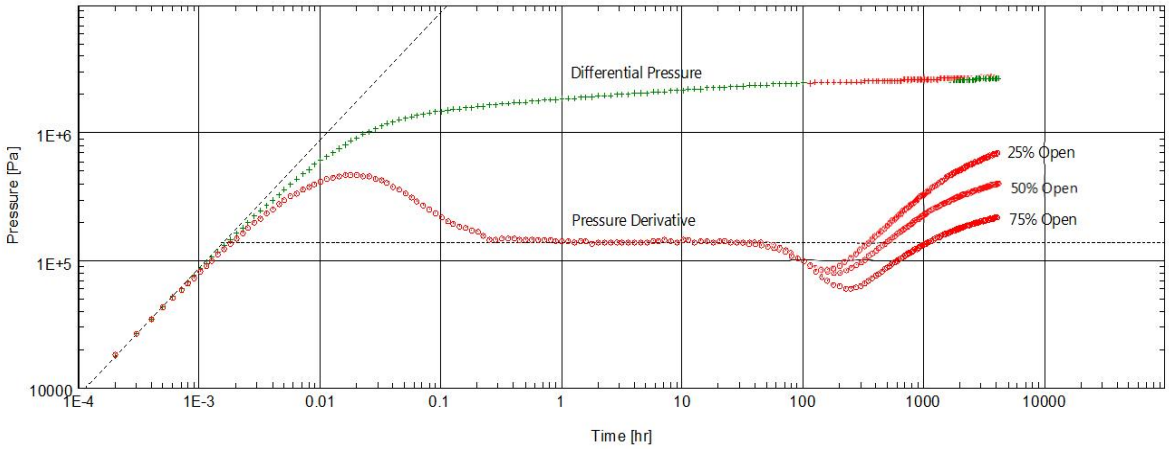

Fig. 12. Log-Log plot of bottom-hole pressure difference versus flow time for the buildup test in the 25%, 50% and 75% open boundary models.

3. Discussion

3.1 Type and Location of the Boundary

In Petroleum Engineering standard pressure transient analysis (George Stewart, 2011) utilizes the pressure derivative plot, together with some information about the reservoir (i.e. porosity, viscosity, compressibility, net pay thickness, etc.), to determine average intrinsic properties of the reservoir (e.g. average permeability), presence and value of skin in the vicinity of the well bore and the distance of the nearest boundary. In the case of dual porosity media or channel flow systems, these plots can also be used to determine

the representative parameters of the reservoir. In addition, the comparison of the different pressure derivative plots (Figure 3 through 12) show that standard pressure transient analysis is capable of identifying the aquifer drive mechanisms, i.e. the type of fluid flow boundary conditions, once the boundaries of reservoir are felt.

As a general observation, regardless of the type of boundary, the time at which the pressure derivative deviates from the straight line gives an indication of when the pressure perturbation has reached the nearest boundary. As an example, the presence of a closed system in Fig 3 is signified by the unit slope in the latter part of the pressure derivative plot. An approximation of the distance to the boundary, with the assumption of a circular reservoir, can be made by solving equation (13) for the time at which a deviation from the straight line (infinite acting radial flow regime) is observed.

$$r_e = \sqrt{\frac{4kt}{\phi \mu c_t}} \tag{16}$$

For CO_2 sequestration studies the radial extent of the reservoir together with the reservoir thickness and porosity then determines the maximum available pore space for fluids. The behavior of the tail of the pressure derivative curve enables a definite distinction between open and closed systems. Closed systems are identified by a unit slope whilst an open system is characterized by the pressure derivative values tending to zero.

3.2 Semi-Open System

The common practice in modeling of CO_2 sequestration is to either assume a closed or a completely open system. Zhou et al. (2008) introduced a semi-closed system where part of the brine and dissolved CO_2 is able to migrate vertically through a slightly permeable cap rock. Their results with respect to storage capacity signify how sensitive

fluid flow simulations of CO_2 sequestration are to the type of boundary conditions. In addition, Amirlatifi et al. (2011, 2012) study the effect of a semi-open or partially open boundary in the lateral extent. This scenario is plausible for cases with lateral varying permeability or partly sealing faults surrounding the reservoir. Such cases are equivalent to petroleum reservoirs with partial water drive mechanism (Cronquist and Alme, 1973; Kumar, 1977a; Saleh, 1990; Tippie and Abbot, 1978). For such reservoirs, (Kumar, 1977a) introduced a factor, f, into the fluid flow equation to account for the influx rate at the boundary:

$$q_e = (q_b)_{r=r_e} = f q_{wb} \tag{17}$$

Where f is the flux factor that can be determined through well testing. With the use of the f factor, different reservoir conditions can be classified as shown in Figures 9 through 12.

Table 2 - Classification of fluid flow boundary conditions based on the flux factor

$f = 0$	Semi-steady state solution (closed aquifer)
$0 < f \leq 1$	Semi-open
$f = 1$	Constant pressure (steady-state) aquifer

Following Kumar's concept the flowing well pressure change over time for radial flow will become:

$$\frac{\partial p_{wf}}{\partial t} = (f - 1)\frac{\mathrm{q}B}{\pi r_e^2 h \phi C_t} \tag{18}$$

The examples presented under Semi-Open section of the results were corresponding to f values of 0.25, 0.5 and 0.75 respectively. It should be noted that the trends shown in the results section correspond to numerical simulations.

3.3 Semi-open vs. composite system

It should be noted that many other phenomena may result in similar signatures like semi-open systems of different flux values (Figure 9 through 12) in the analysis of the pressure derivative plot. Composite systems or intersecting sealing faults are such examples. In a composite system (Carter, 1966; Olarewaju and Lee, 1987) the well is inside a homogenous zone and interacts with two homogenous zones with different intrinsic or fluid properties. Depending on the distance of the interface between the two zones and the well, diffusivity and mobility ratio, several different signatures can be observed on the pressure derivative plots that are similar to the ones presented in Figure 9 and 11 (Allain et al., 2009; Charles et al., 2001; Mattha et al., 1998). For example, intersecting sealing faults at 45^o can result in signatures similar to the 25% open boundary presented in Fig. 9. Also, an infinite reservoir with the zones interface located at 777 meters from the location of the well and a mobility ratio of

$$\mathrm{M} = \frac{\left(\frac{\mathrm{k}}{\mu}\right)_{\text{Zone 1}}}{\left(\frac{\mathrm{k}}{\mu}\right)_{\text{Zone 2}}} = 2.79 \tag{19}$$

and a diffusivity of

$$\mathrm{D} = \frac{\left(\frac{\mathrm{k}}{\mu.\phi.\mathrm{C_t}}\right)_{\text{Zone 1}}}{\left(\frac{\mathrm{k}}{\mu.\phi.\mathrm{C_t}}\right)_{\text{Zone 2}}} = 0.7583 \tag{20}$$

can give the same signatures as those presented for the 25% open system of Fig. 9.

These observations suggest that the presence of semi-open behavior signatures in the pressure derivative plot may not be used as the solitary basis to draw conclusions on the type of fluid flow boundary. In combination with other field knowledge such as seismic, these reservoir conditions can be identified or excluded, resulting in a better understanding of the storage medium and its safe storage limits.

3.4 Drawdown test vs. pressure buildup test

While in the oil and gas industry the short term drawdown test is preferred over the prolonged buildup test for economic reasons (i.e. production versus shutting the production down), for CO_2 sequestration projects initial brine production from the reservoir is not a favorable strategy and as a result, the shut-in well build up that follows a short brine removal period, is the preferable test to determine the distance of the nearest boundary and to differentiate between an infinite reservoir (Fig. 6) and a bounded (either open or closed) system (Figures 4 and 8). However, the pressure derivative analysis of a buildup test does not clearly differentiate between closed or open boundaries (Fig. 4 versus Fig. 8) because the pressure derivative in both systems tends towards zero, but a drawdown test that is run long enough for the pressure perturbation to reach the boundary can differentiate between the two systems. A combination of the drawdown followed by the buildup test, as presented in this study, is the recommended practice for CO_2 sequestration studies. The short drawdown imposes a pressure decline in the system that can be utilized for the buildup and in addition, the short period of this test means that there is less produced water to handle on the surface.

In addition to the buildup test that is achieved through shutting the well in following brine production, the buildup can also be attained through CO_2 injection and monitoring the pressure build up.

The semi open systems can be identified in the drawdown (as illustrated in Figures 9 through 11) as the pressure derivative in such systems tends to zero after the boundary is felt and the system will eventually reach an steady state condition between the fluid influx and fluid withdrawal. The time to reach the steady state depends on the f factor. The higher the f factor, the sooner the convergence to steady state. As an example, the pressure derivative in the 50% open system will tend to zero at 34209 hours, Fig. 13, but it is not economically feasible to run the drawdown test in CO_2 sequestration studies for a prolonged period of time.

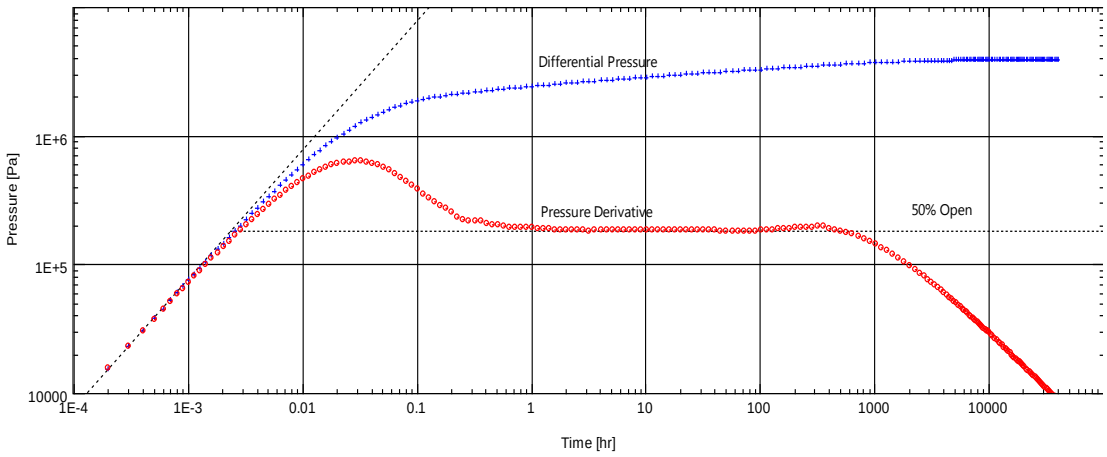

Fig. 13. Log-Log plot of bottom-hole pressure difference versus flow time for the prolonged drawdown test in a 50% open boundary model.

The valley observed in the pressure derivative of the buildup test is an indication of the "open" system that accommodates for parts of the pressure drop, once the pressure

perturbation reaches the boundary. The depth of the valley depends on the flux factor, f. The higher the f value, the deeper the valley gets, since it behaves as an open system, but the limited influx prevents the system from showing signatures of a completely open (steady state) system.

As discussed in section 3.3 (Semi-open vs. composite system) these signatures can be observed in other settings, such as composite or faulted systems, as well. A combination of signatures of these fluid flow boundary conditions during the prolonged buildup test, as depicted in Fig. 12, with the drawdown test is an exclusive sign that can be used to identify these systems.

4. Conclusion

In Petroleum Engineering pressure transient analysis represents a standard methodology to gain insight into oil and gas reservoirs and determining the location and the type of boundaries. A simple water drawdown test followed by a prolonged buildup test can identify fluid flow boundary conditions for CO_2 sequestration projects, which to the authors' knowledge is not common practice yet. The large difference in CO_2 storage capacity and the different levels of geomechanical risks associated to different fluid flow boundary conditions suggest that the presented methodology should be considered prior to fluid injection scenarios. This leverages the determination of fluid flow boundary conditions from an assumption to a quantitative analysis.

In this study the concept of flux factor was used to define a transitional boundary condition between pseudo steady state and steady state conditions to better understand the type and location of the boundaries for CO_2 sequestration studies. Several different possibilities such as composite radial flow and intersecting faults that result in similar

signatures as those of the semi-open systems were discussed. Based on the observations made in the present work, presence of semi-open behavior signatures in the pressure derivative plots may not be taken as the solitary basis of determining type of the boundary, but they should be used as an additional piece of information for better understanding of the storage medium.

Acknowledgements

The authors would like to express their gratitude for Kappa for providing the educational license of the Ecrin suite. The authors would also like to thank Dr. Runar Nygaard for his insightful recommendations and technical support

References

Allain, O., Tauzin, E., Chassignol, V., 2009. Dynamic Flow Analysis, 4.10.01 ed. KAPPA.

Amirlatifi, A., Eckert, A., Nygaard, R., Bai, B., 2011. Estimation of Reservoir Uplift , Seismicity and Failure Likelihood during CO 2 Injection through Coupled Reservoir Simulation, in: Canadian Unconventional Resources Conference. Calgary, Canada, p. CSUG/SPE SPE–148946–PP.

Amirlatifi, A., Eckert, A., Nygaard, R., Bai, B., Liu, X., Paradeis, M., 2012. Role of Geometrical Influences of CO_2 Sequestration in Anticlines, in: 46th US Rock Mechanics / Geomechanics American Rock Mechanics Assosiaction Symposium. Chicago, IL, p. ARMA 12–255.

Bachu, S., Adams, J.J., 2003. Sequestration of CO_2 in geological media in response to climate change: capacity of deep saline aquifers to sequester CO_2 in solution. Energy Conversion and Management 44, 3151–3175.

Bachu, S., Bonijoly, D., Bradshaw, J., Burruss, R., Holloway, S., Christensen, N.P., Mathiassen, O.M., 2007. CO_2 storage capacity estimation: Methodology and gaps. International Journal of Greenhouse Gas Control 1, 430–443.

Baklid, A., Korbol, R., Owren, G., 1996. SLEIPNER VEST CO_2 DISPOSAL, CO_2 INJECTION INTO A SHALLOW UNDERGROUND AQUIFER - Paper SPE

36600, in: Proceedings of SPE Annual Technical Conference and Exhibition. Society of Petroleum Engineers, pp. 1–9.

Buckley, S.E., Leverett, M.C., 1942. Mechanism of fluid displacement in sands. Transactions of the AIME 146, 107–116.

Carter, R.D., 1966. Pressure Behavior of a Limited Circular Composite Reservoir. Society of Petroleum Engineers Journal 6, 328 – 334.

Charles, D.D., Rieke, H.H., Purushothaman, R., 2001. Well-Test Characterization of Wedge-Shaped, Faulted Reservoirs. SPE Reservoir Evaluation & Engineering 4.

Comerlati, A., 2006. Fluid-Dynamic and Geomechanical Effects of CO_2 Sequestration below the Venice Lagoon. Environmental & Engineering Geoscience 12, 211–226.

Cronquist, C., 1973. Effects of Permeability Variation and Production Rate on Recovery from Partial Water Drive Gas Reservoirs, in: Proceedings of Fall Meeting of the Society of Petroleum Engineers of AIME. Society of Petroleum Engineers.

Ehlig-Economides, C., Economides, M.J., 2010. Sequestering carbon dioxide in a closed underground volume. Journal of Petroleum Science and Engineering 70, 123–130.

George Stewart, 2011. Well test design and analysis, 1st ed. PennWell, Tulsa, Oklahoma, USA.

Holloway, S., 2001. Storage of fossil fuel-derived carbon dioxide beneath the surface of the earth. Annual Review of Energy and the Environment 26, 145–166.

Holloway, S., Savage, D., 1993. The potential for aquifer disposal of carbon dioxide in the UK. Energy Conversion and Management 34, 925–932.

Ipcc, 2005. IPCC special report on carbon dioxide capture and storage, IPCC Special Report on Carbon Dioxide Capture and Storage. Cambridge University Press.

Izgec, O., Demiral, B., Bertin, H., Akin, S., 2006. Experimental and Numerical Modeling of Direct Injection of CO_2 Into Carbonate Formations - Paper SPE 100809, in: Proceedings of SPE Annual Technical Conference and Exhibition. Society of Petroleum Engineers, San Antonio, Texas.

Klara, S.M., Srivastava, R.D., McIlvried, H.G., 2003. Integrated collaborative technology development program for CO_2 sequestration in geologic formations--United States Department of Energy R&D. Energy Conversion and Management 44, 2699–2712.

Kumar, A., 1977a. Steady Flow Equations for Wells in Partial Water-Drive Reservoirs. Journal of Petroleum Technology 29, 1654–1656.

Kumar, A., 1977b. Strength of Water Drive or Fluid Injection From Transient Well Test Data. Journal of Petroleum Technology 29, 1497–1508.

Kumar, A., Noh, M., Ozah, R., Pope, G., Bryant, S., Sepehrnoori, K., Lake, L., 2005. Reservoir Simulation of CO_2 Storage in Deep Saline Aquifers. SPE Journal 10, 336–348.

Lucier, A., Zoback, M., Gupta, N., Ramakrishnan, T.S., 2006. Geomechanical aspects of CO_2 sequestration in a deep saline reservoir in the Ohio River Valley region. Environmental Geosciences 13, 85–103.

Matthäi, S., Aydin, A., Pollard, D., Stephen, G., 1998. Simulation of Transient Well-Test Signatures for Geologically Realistic Faults in Sandstone Reservoirs. SPE Journal 3.

Nghiem, L., Sammon, P., Grabenstetter, J., Ohkuma, H., 2004. Modeling CO_2 Storage in Aquifers with a Fully-Coupled Geochemical EOS Compositional Simulator. Proceedings of SPE/DOE Symposium on Improved Oil Recovery.

Olarewaju, J.S., Lee, W.J., 1987. An Analytical Model for Composite Reservoirs Produced at Either Constant Bottomhole Pressure or Constant Rate, in: Proceedings of SPE Annual Technical Conference and Exhibition. Society of Petroleum Engineers, Dallas, Texas.

Orlic, B., Schroot, B. m., Wensaas, L., 2004. Predicting ground deformation due to CO 2 injection: examples from Montmiral, France, Sleipner, Norway and Florina, Greece, in: Proceedings of 7th International Conference on Greenhouse Gas Control Technologies. Cheltenham, UK, pp. 337–339.

Pruess, K., Xu, T., Apps, J., Garcia, J., Berkeley, L., Karsten, P., Tianfu, X., John, A., Julio, G., 2001. Numerical Modeling of Aquifer Disposal of CO_2 - Paper SPE 66537, in: Proceedings of SPE/EPA/DOE Exploration and Production Environmental Conference. Society of Petroleum Engineers, San Antonio, Texas, pp. 1–16.

Rutqvist, J., Birkholzer, J.T., Cappa, F., Tsang, C.-F., 2007. Estimating maximum sustainable injection pressure during geological sequestration of CO_2 using coupled fluid flow and geomechanical fault-slip analysis. Energy Conversion and Management 48, 1798–1807.

Rutqvist, J., Birkholzer, J.T., Tsang, C.-F., 2008. Coupled reservoir–geomechanical analysis of the potential for tensile and shear failure associated with CO_2 injection in multilayered reservoir–caprock systems. International Journal of Rock Mechanics and Mining Sciences 45, 132–143.

Saleh, S., 1990. An Improved Model For The Development And Analysis Of Partial-Water Drive Oil Reservoirs, in: Proceedings of Annual Technical Meeting. Society of Petroleum Engineers.

Sengul, M., 2006. CO_2 Sequestration - A Safe Transition Technology - Paper SPE 98617, in: Proceedings of SPE International Health, Safety & Environment Conference. Society of Petroleum Engineers, Abu Dhabi, UAE.

Tippie, D.B., Abbot, W.A., 1978. Pressure Transient Analysis In Bottom Water Drive Reservoir With Partial Completion, in: Proceedings of SPE Annual Fall Technical Conference and Exhibition. Society of Petroleum Engineers.

Tran, D., Nghiem, L., Shrivastava, V., Kohse, B., 2010. Study of geomechanical effects in deep aquifer CO_2 storage, in: 44th US Rock Mechanics Symposium. ARMA, Salt Lake City, UT.

Tran, D., Shrivastava, V., Nghiem, L., Kohse, B., 2009. Geomechanical Risk Mitigation for CO_2 Sequestration in Saline Aquifers, in: Proceedings of SPE Annual Technical Conference and Exhibition. Society of Petroleum Engineers, New Orleans, Louisiana, pp. 1–18.

Zhou, Q., Birkholzer, J., 2007. Sensitivity study of CO_2 storage capacity in brine aquifers with closed boundaries: dependence on hydrogeologic properties, in: Sixth Annual Conference on Carbon Capture and Sequestration - DOE/NETL. Pittsburgh, PA.

Zhou, Q., Birkholzer, J.T., Tsang, C.-F., Rutqvist, J., 2008. A method for quick assessment of CO_2 storage capacity in closed and semi-closed saline formations. International Journal of Greenhouse Gas Control 2, 626–639.

Zoback, M., Ross, H., Lucier, A., 2006. Geomechanics and CO_2 Sequestration.

PAPER

4. GEOMECHANICAL RISK ASSESSMENT FOR CO_2 SEQUESTRATION IN A CANDIDATE STORAGE SITE IN MISSOURI

Amin Amirlatifi, Andreas Eckert, Runar Nygaard and Baojun Bai

Missouri University of Science and Technology

Abstract

CO_2 sequestration is one of the promising ways of reducing emission of greenhouse gases from coal fired power plants. Missouri is part of the plains CO_2 reduction partnership that is investigating Williston basin for CO_2 sequestration, however the state is located at the farthest point of the proposed transportation line and consequently will face the highest CO_2 compression and transportation costs. In order to mitigate this problem, several candidate CO_2 sequestration sites in the state are examined, including a pinchout formation in the Lincoln fold in North-East Missouri which was found to be the best candidate for sustainable sequestration of CO_2 emissions from nearby coal fired power plants. Results of this study show that shallow sequestration is a viable option that can help in reduction of CO_2 emissions. The results also suggest that preheated CO_2 under a three injection well scheme can lead to super critical CO_2 sequestration in the shallow aquifer.

Keywords: Coupled, Simulation, Geomechanics, CO_2, Sequestration

1. Introduction

One of the main contributors to greenhouse gas emissions in the United States is the CO_2 from coal-fired power plants that generate more than fifty percent of the electricity and have an estimated annual CO_2 emission of 2 billion metric tons (Ipcc, 2005). In spite of copious efforts for plummeting dependence on fossil fuels, they remain the prominent

source of energy for decades to come (Conti, John J.; Holtberg, Paul D.; Beamon, Joseph A.; Schaal, Michael A.; Ayoub, Joseph C.; Turnure, 2011).

Sequestering the carbon dioxide in unmineable coal seams, depleted oil and gas reservoirs and deep saline aquifers is a promising method for reducing CO_2 emissions from stationary sources, such as power plants (Bachu and Adams, 2003; Bachu et al., 1994; Koide et al., 1993; Metz et al., 2007; van der Meer, 1992). The United States Department of Energy (DOE) has created seven Regional Carbon Sequestration Partnerships (RCSPs) to examine the feasibility of CO_2 sequestration in different regions and geologic formations throughout the United States, as well as developing the technology and required infrastructures for large scale CO_2 sequestration (DOE, 2013). The Plains CO_2 Reduction (PCOR) Partnership is investigating the Williston Basin as a candidate for sequestering CO_2 emissions from power plants (Peck et al., 2012). The State of Missouri, a member of PCOR, is the 12^{th} biggest coal energy producer in the US ("Missouri and Coal - Sourcewatch," 2013) but lies at the furthest point on the proposed transportation route and consequently faces the highest CO_2 compression and transportation costs. In order to minimize the cost of CO_2 sequestration, it is desirable to find a storage site close to the power plants in the state. This study aims at identifying and characterizing a candidate geological CO_2 sequestration site in the state of Missouri that can be used to overcome the CO_2 transportation cost to the Williston Basin and to evaluate the geomechanical risks associated to various probable injection scenarios.

For the state of Missouri the Lamotte sandstone is identified as the only suitable sequestration aquifer with acceptable permeability, porosity, extension, strength and water salinity (Akpan, 2012; Miller, 2012). Despite these favorable conditions the Lamotte

Sandstone represents a relatively shallow target formation with average depths of 297m to 593m (Carr et al., 2008). While the potential, technical merit and economic feasibility of deep CO_2 sequestration into saline aquifers has been widely studied (Bachu and Adams, 2003; Bachu et al., 1994; Bergman and Winter, 1995; Gunter et al., 1996, 1993; Holt et al., 1995; Koide et al., 1993; Pruess et al., 2003, 2001; van der Meer, 1995, 1992, 1996), shallow CO_2 sequestration potential has not gained enough research interest. Inherent problems associated with shallow CO_2 sequestration are low storage capacity, the relative increase of horizontal stress at shallow depths (Jaeger et al., 2007), maximum allowable injection pressure and fracture gradient, however, the abundance of shallow aquifers makes them a prime target for short to long term storage that deserves a closer examination. Yang et al. (2013) discuss the challenges faced in shallow CO_2 sequestration and suggest brine removal as a risk reducing factor.

In this study we evaluate the CO2 sequestration feasibility for a potential pinchout structure (at a shallow depth of 396m to 457m) in the Lincoln Fold formation in the north-eastern part of Missouri. In order to assess the viability of long term CO_2 sequestration in this formation, a thorough coupled geomechanical and fluid flow simulation study is conducted on this pinchout using the Coupled Geomechanical Reservoir Simulator (CGRS) (Amirlatifi et al., 2011) that utilizes Eclipse for fluid flow simulation and Abaqus for geomechanical analysis to predict maximum sustainable pore pressure prior to the injection depending on the stress regimes. The increase in minimum horizontal stress magnitude in shallow formations and consequently the increase in the K-ratio ($k = \frac{\sigma_{h_{mean}}}{\sigma_v}$) (Hoek and Brown, 1997; Hoek et al., 2002; Turcotte and Schubert, 2002), makes the modeling of shallow sequestration in this tectonically complex setting a challenging task.

Based on the geomechanical risk assessment we investigate different injection scenarios to determine the best sustainable sequestration scheme over a period of 100 years.

2. Background

An essential component of geological CO_2 sequestration is preventing the CO_2 from escaping the storage medium. Along with the solution of CO_2 in the bine and mineralization, physical trapping plays the most pronounced short term storage. Trapping of CO_2 is achieved through a combination of one or more physical and chemical processes, as shown in Table 1 (Bachu et al., 2007b; Holtz, 2002; Koide et al., 1992). The suitability of the trap mainly depends on the geology and the depth of the trap. It should provide reasonable pore volume, permeability, structural and stratigraphic trapping mechanisms such as anticlines or faults and permissible salinity of the aquifer to be considered suitable for further analysis (Bachu et al., 1994; van der Meer, 1992). Once a suitable trap is located, its geologic storage capacity needs to be estimated (Bachu et al., 2007b). A portion of the total available pore volume can be utilized at any time due to the residual water saturation, buoyancy effects, heterogeneity (Bachu and Adams, 2003) and maximum pressure that the rock can withstand before it fails (Amirlatifi et al., 2012). The phase diagram of CO_2, Fig. 1, shows that at temperatures and pressures higher than 31.1°C and 7.38 MPa respectively, CO_2 is in its supercritical phase and this dense state will require less pore volume per stored ton of CO_2. Assuming a geothermal gradient of 20 °C/km (Turcotte and Schubert, 2002) and an atmospheric temperature of 15.5 °C, Fig. 1 can be created that converts CO_2 phase to depth. As shown in this figure, at depths deeper than 0.78 km, CO_2 will be in supercritical conditions which would make CO_2 easier to transport and results in greater storage capacity.

Table 1. Characteristics of trapping mechanisms in saline aquifers modified from Bradshaw et al. (2007).

Trapping mechanism		**Characteristics**		
		Nature of trapping	Capacity limitation/benefits	Potential size
Geological trapping Reservoir scale (km)	Structural and stratigraphic trapping	Buoyancy within anticline, fold, fault block, pinch-out. CO_2 remains below physical trap.	Without hydraulic system, limited by compression of reservoir fluid. With hydraulic system, displace formation fluid.	Significant
Geochemical trapping Well scale (cm to m)	Residual gas trapping	CO_2 fills interstices between pores of rock grains.	Can equal 15–20% of reservoir volume. Eventually dissolves into formation water	Very large
	Solubility and ionic trapping (Dissolution)	CO_2 migrates through reservoir beneath seal and eventually dissolves into formation water.	CO_2 saturated water may migrate towards the basin center. Limited by CO_2 - water contact and favor highly permeable (vertical) and thick reservoirs	Very large
	Mineral trapping	CO_2 reacts with existing rock to form new stable minerals.	Reaction rate is slow. Precipitation could reduce injectivity. Approaches 'permanent' trapping.	Significant
Hydrodynamic trapping Basin scale (100km)	Migration trapping	CO_2 migrates through reservoir beneath seal, moving with the regional flow system while other trapping mechanisms work.	No physical trap may exist; totally reliant on slow transport mechanism and chemical processes. Can include all other trapping mechanisms along the migration pathway	Very large

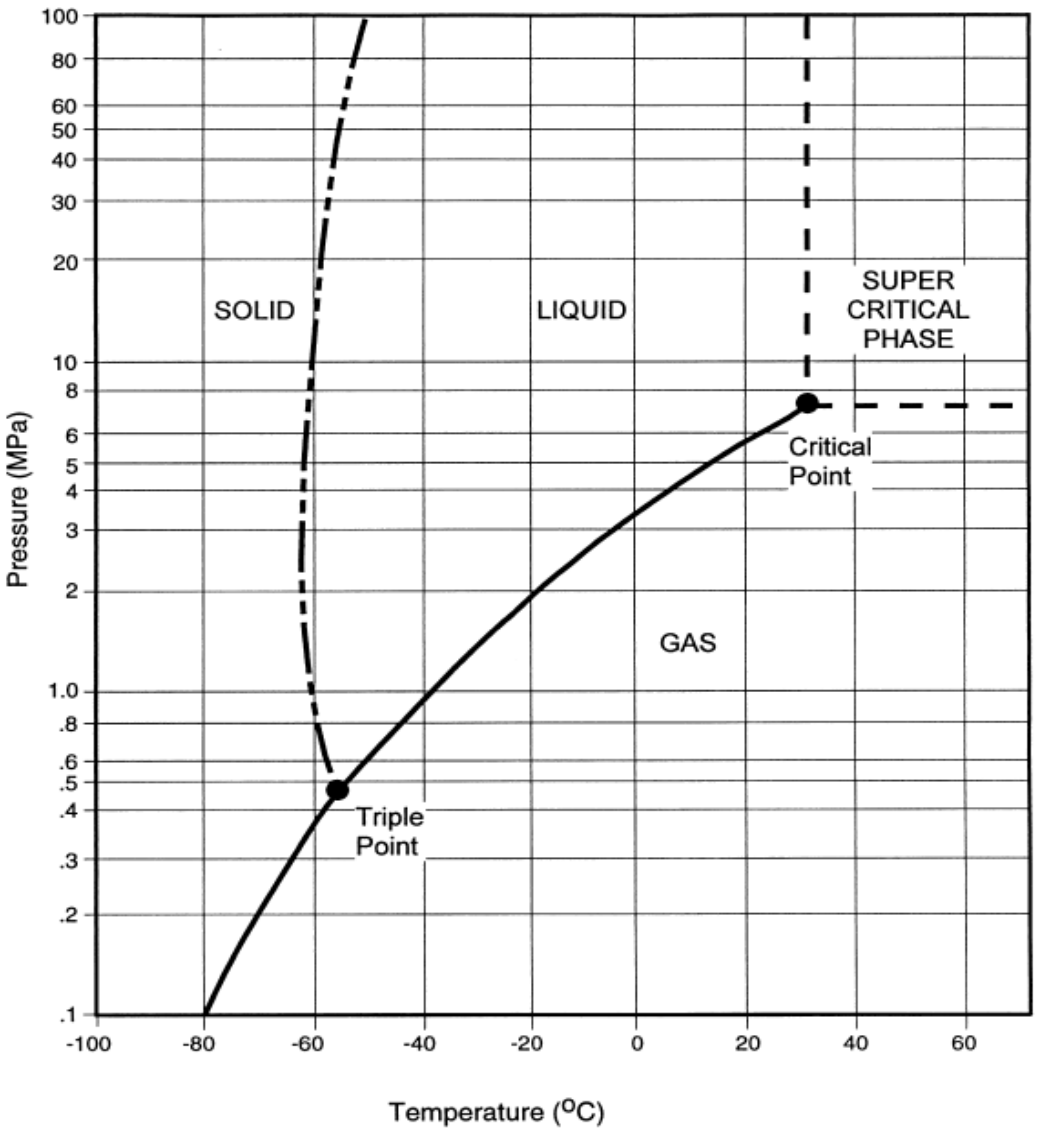

Fig. 1. Pressure Temperature Phase Diagram of CO_2 (Bachu, 2002)

The super critical CO_2 at this depth is usually 30 to 40% lighter than the brine (Ennis-King and Lincoln, 2002; Ennis-King and Paterson, 2001) and will migrate vertically, due to buoyancy, unless it is constrained by a low permeability caprock, or a geomechanical trap such as a sealing fault.

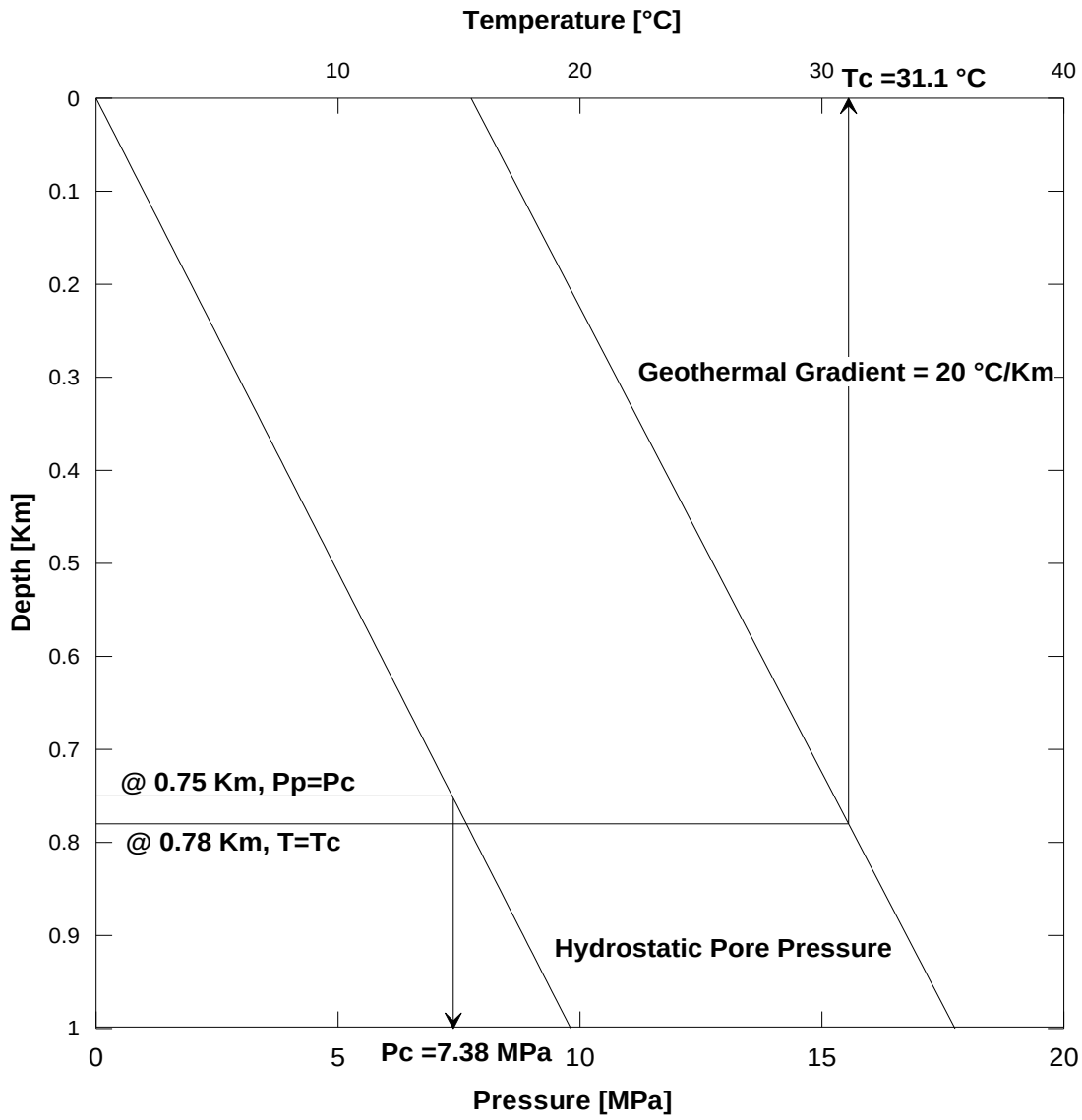

Fig. 2. Temperature and pressure for CO_2 at Different Depths (after Bachu, 2000; Holloway and Savage, 1993 and van der Meer, 1992)

For the state of Missouri the Lamotte Sandstone represents the only sequestration aquifer featuring acceptable rock properties and salinity. The Lamotte Sandstone is the first formation of the Cambrian period throughout most of Missouri that overlays the Precambrian granite. The Lamotte sandstone is capped by the Bonneterre Dolomite and higher up the shale rich Davis formation which due to its low permeability, can serve as a barrier for upward migration of fluids (Fig. 3).

Period	Lithology	Formation Name	Group	Rock Type	Maximum Thickness (m)
Lower Ordovician		Jefferson City	Ozark	Cherty/Drusy Dolomite	3050
		Roubidoux			
		Gasconade			
Upper Cambrian		Eminence			
		Potosi			
		Derby Doerun	St Francois Confining Unit	Shaly Dolomite	394
		Davis		Dolomite Shale	510
		Bonne Terre	St Francois	Dolomite/Limestone	1030
		Lamotte		Sandstone and Conglomerate	720
Precambrian Rocks			Basement Confining Unit	Granitic, Basic and Felsitic	>720

Fig. 3. Stratigraphy of the Lamotte sandstone and the overlying formations

Fig. 4 shows the structural map of the state of Missouri including depth contours of the Lamotte Sandstone. As can be seen the Lamotte Sandstone covers the whole state of Missouri at depths ranging from 320 to 2000 m but lack of suitable trapping mechanism, thin formation thickness or impermissible range of dissolved solids makes the majority of potential Lamotte sites unfit for deep CO_2 sequestration and the shallow CO_2 sequestration using CO_2 in the gas form is the prevailing option. The shallow storage scenario requires more storage volume and the storage reservoir will have less overburden to cap the CO_2 in place. The CO_2 will also be less dense and have less viscosity and therefore there is a potential risk of CO_2 leaking out of the storage reservoir.

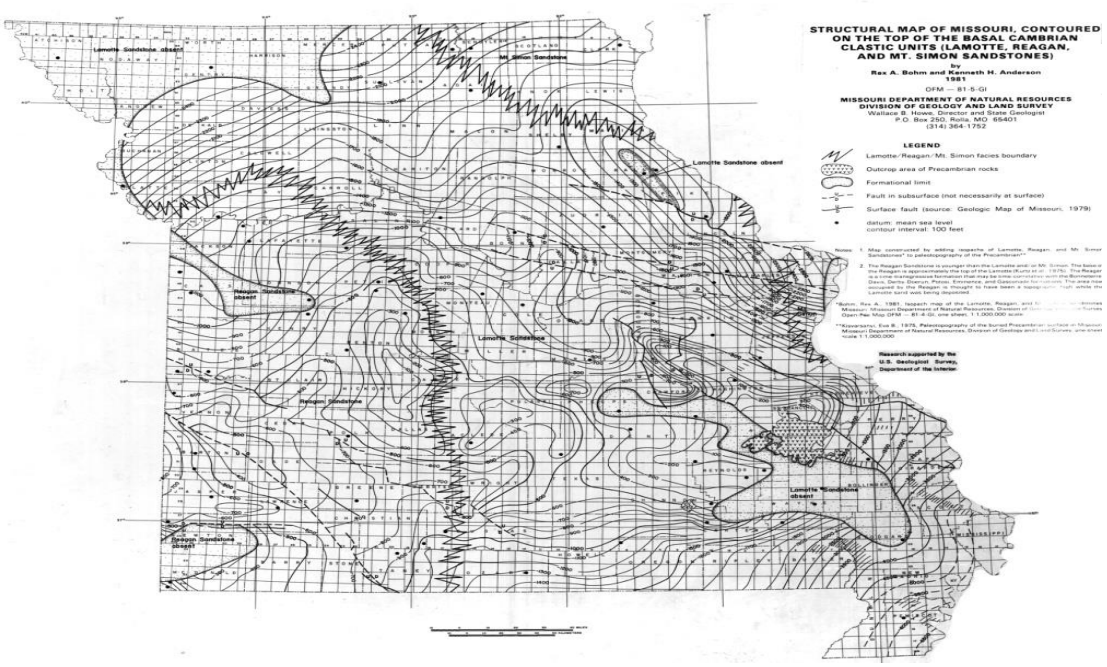

Fig. 4. Structural map of Missouri contoured on the top of the Basal Cambrian Clastic units (Lamotte, Reagan and Mount Simon sandstones) (Bohm and Anderson, 1981)

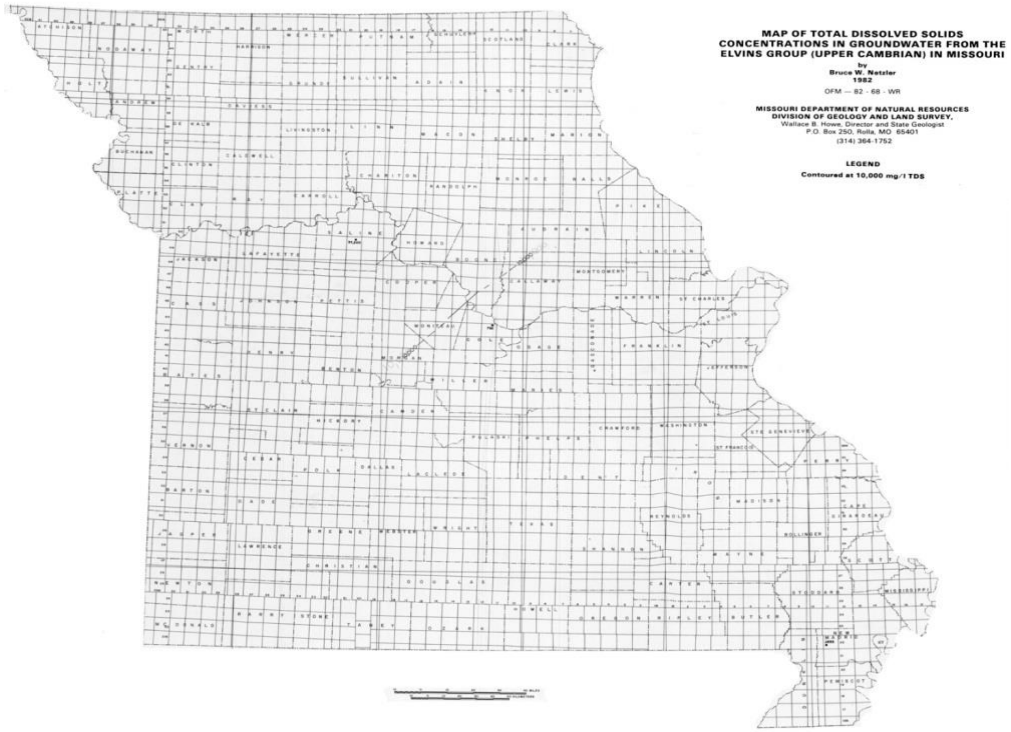

Fig. 5. Map of total dissolved solids concentrations in groundwater from the Elvins group (upper Cambrian) in Missouri (Netzler, 1982)

An initial candidate aquifer was located in Greene County, MO, near the Springfield power plant (Nygaard et al., 2012) but the water quality assessment using (Brookshire, 1997) did not comply with the minimum admissible solid content level for CO_2 sequestration and the site was abandoned. Fig. 7 shows the distribution of coal fired power plants throughout the state of Missouri. As illustrated here, the majority of coal fired power plants in the state are located in the northern parts of the state, thus it would be more desirable to find a suitable Lamotte configuration in this part of the state.

Inspection of Fig. 4 indicates a pinch-out formation at the North-Eastern part of the state which is part of the Lincoln fold, the prominent geologic feature in the eastern part of Missouri. Lincoln fold is a large anticline structure that does not have a history of recent seismic activity (Smotherman, 2010), Fig. 6, and is bounded by faults of significant lengths.

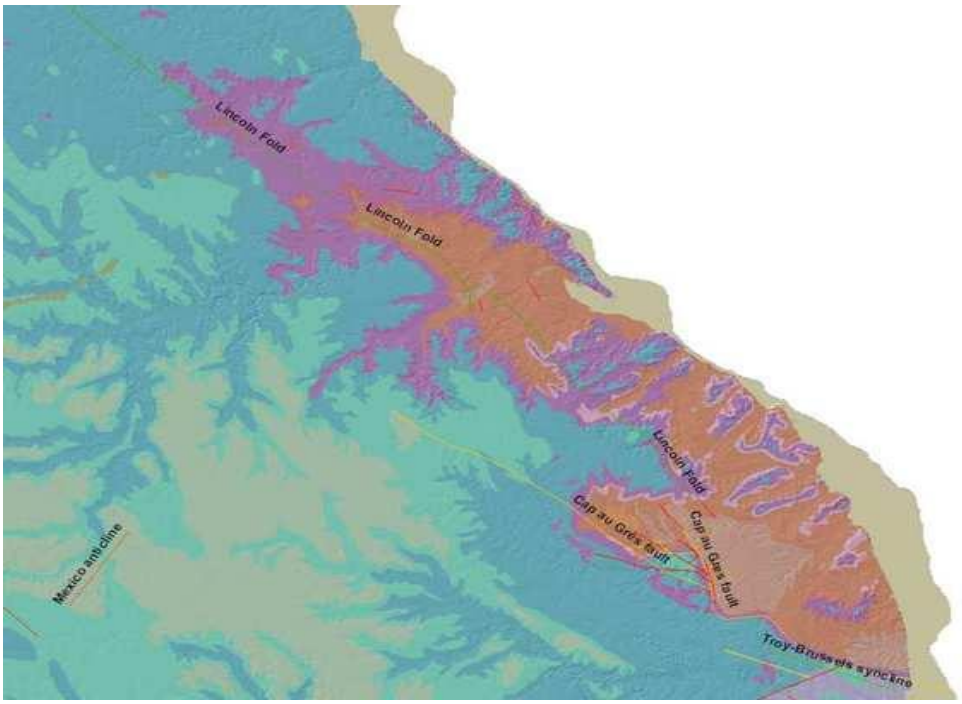

Fig. 6. Lincoln Fold in Missouri (Smotherman, 2010)

Here, the Lamotte sandstone pinches out against the Derby-Doerun formation and has a favorable thickness of 30 to 160m and lateral extent suitable for CO_2 sequestration. This formation is also close to several power plants, Fig. 7, which makes it a favorable candidate spot for long term cost effective CO_2 sequestration in the state. For example, the Hercules Power plant, which is operated by Ashland, has an estimated annual emission rate of 227,202 tons of CO_2 in Louisiana, MO ("Missouri and Coal - Sourcewatch," 2013) and is located on the limb of the candidate pinchout.

The aquifer has acceptable dissolved mineral concentration of 10,000 PPM or more, Fig. 5.

Fig. 7. Missouri Coal Fired Power Plants ("Missouri and Coal - Sourcewatch," 2013)

3. Modeling Approach

3.1. Model Setup

Assuming that the rock properties of Lamotte and Derby-Doerun formations in North-Eastern part of the state are comparable to the outcrops and the formations in the South-Eastern part of the state, the present work will use log, core and rock mechanic analysis conducted at Missouri University of Science and Technology (Akpan, 2012; Govindarajan, 2012; Kumar, 2012; Miller, 2012) to set up the rock physics models. Table 2 and Table 3 list the brine properties and mineral reactions considered in this study respectively. The initial mineral composition is taken as 60% quartz, 2% calcite and 2% dolomite and 36% other minerals. Table 4 and Table 5 show the formation properties and overall simulation properties used for the modeling respectively. The lateral extent of Lamotte formation extends past the state borders into the Illinois, but in this study the extent of the pinchout formation is limited to the state border line ($70km * 16km$).

Table 2. Water properties used for the modeling

Density, ρ_f ($\frac{kg}{m^3}$)	1021
Compressibility, Cf ($\frac{1}{\text{kPa}}$)	$3.20 * 10^{-06}$
Reference Pressure, P_{ref} (kPa)	6895
Viscosity, μ (cp)	1.25
Salinity (ppm)	10,000
Dissolved salts	NaCl, $CaCl_2$

Table 3. Mineral reactions considered in the modeling (Nygaard et al., 2012)

Mineral Reactions	**Aqueous Reactions**
$Calcite + H^+ \leftrightarrow Ca_2^+ + HCO_3^-$	$H_2O \leftrightarrow H^+ + OH^-$
$Dolomite + 2H^+ \leftrightarrow Ca_2^+ + Mg_2^+ + 2HCO_3^-$	$CO_2 + H_2O \leftrightarrow H^+ + HCO_3^-$
$Quartz \leftrightarrow SiO_2(aq)$	$CO_2 + H_2O \leftrightarrow 2H^+ + CO_3^{2-}$

In this study, brine removal, open, infinite or semi-open boundary conditions are not considered and modeling is carried out under closed boundary assumption to assess the possibility of achieving supercritical CO_2 in shallow sequestration by utilizing the pore pressure buildup. The closed boundary condition assumption and the formation extents that are limited to state boundaries should provide the most conservative estimate on the capacity of the pinchout for shallow CO_2 sequestration.

The model is meshed using the bi-logarithmic approach and grids are biased towards the outer boundaries, while using fine grid blocks around injection location(s).

Two injection scenarios are considered to determine storage capacity of the pinchout:

1. One injection well located in the middle of the pinchout model. The injection rate is 200 kTons/year (Table 5).
2. Three injection wells along the center of the model. The CO_2 injection rate of each well is equal to 200 kTons/year, resulting in a total injection rate of 600 kTons/year in the aquifer.

Table 4. Formation properties for the simulation in the pinchout model.

Property	Overburden	Derby-Doerun	Lamotte	Precambrian
Saturated rock density, $\rho_{m\ (Kg/m3)}$	2600	2500	2600	2650
Dry bulk modulus (GPa)	15	15	12	15
Matrix bulk modulus, $E\ (GPa)$	40	58.5	41.1	57.7
Poisson's ratio, ν[]	0.25	0.25	0.25	0.25
Zero stress porosity, ϕ []	0.01	0.05	0.076	0.01
Zero stress permeability, $k\ (10^{-14}m^2)$	1.0	1.25	1.58	1.0
Height, *h (m)*	200	196	161	100
Cohesion, $C_o(MPa)$	5	5	5	5
Tensile strength, $T_o(MPa)$	2.5	2.5	2.5	2.5
Angle of internal friction, θ	30	30	30	30
Compressibility, $C_m\left(\frac{10^{-9}}{kPa}\right)$	1	1	1	1
Fracture gradient, $FP\left(\frac{kPa}{m}\right)$	21	21	21	21
Average pressure gradient, $PG\left(\frac{kPa}{m}\right)$	10.154	10.154	10.154	10.154
$\frac{k_h}{k_v}$	10	10	10	10

Table 5. Overall simulation properties for the pinchout model.

CO_2 injection rate (each injection well) $\left(\frac{\boldsymbol{kTons}}{\boldsymbol{Year}}\right)$	200
CO_2 injection period $(Years)$	100
Overall model dimensions, length * width * height (m)	$70{,}000 * 16{,}000 * 600$

3.2. Model assembly

An Integrated Shared Earth Model (ISEM) for fluid flow simulation and geomechanical studies was created using available structural contour maps of different formations and Digital Elevation Maps (DEMs) in the North-Eastern part of Missouri. Use of ISEM facilitates integrated coupled geomechanical reservoir simulation from the aquifer to the surface. In the event of a caprock failure, the fluid outflow from the aquifer can be monitored and amount of fluids escaping the storage medium can be calculated.

Fig. 8 shows the steps involved in creation of ISEM.

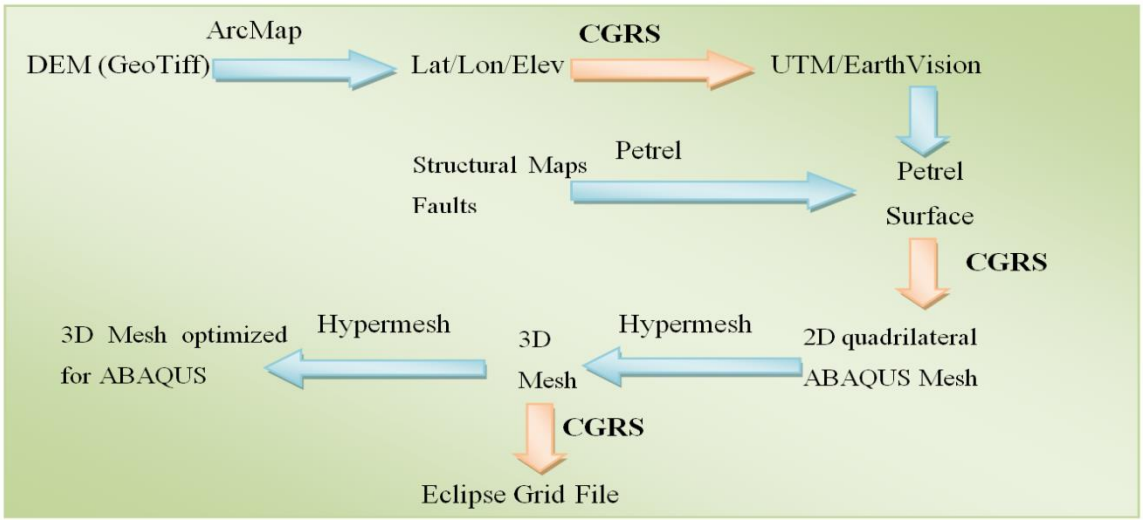

Fig. 8. Integrated Shared Earth Model (ISEM) creation workflow

Inclusion of surface topography is made possible through creation of a convertor that adapts latitude/longitude/elevation information created by ArcMAp, into UTM format, which is then imported into Petrel (Fig. 9). Formation horizons are generated in Petrel by digitizing of structural contour maps for each formation. Once the geological model is

created in Petrel (Fig. 11), it is converted into a set of 2D Abaqus surfaces by CGRS and the surfaces are assembled in Hypermesh to form the initial Finite Element mesh.

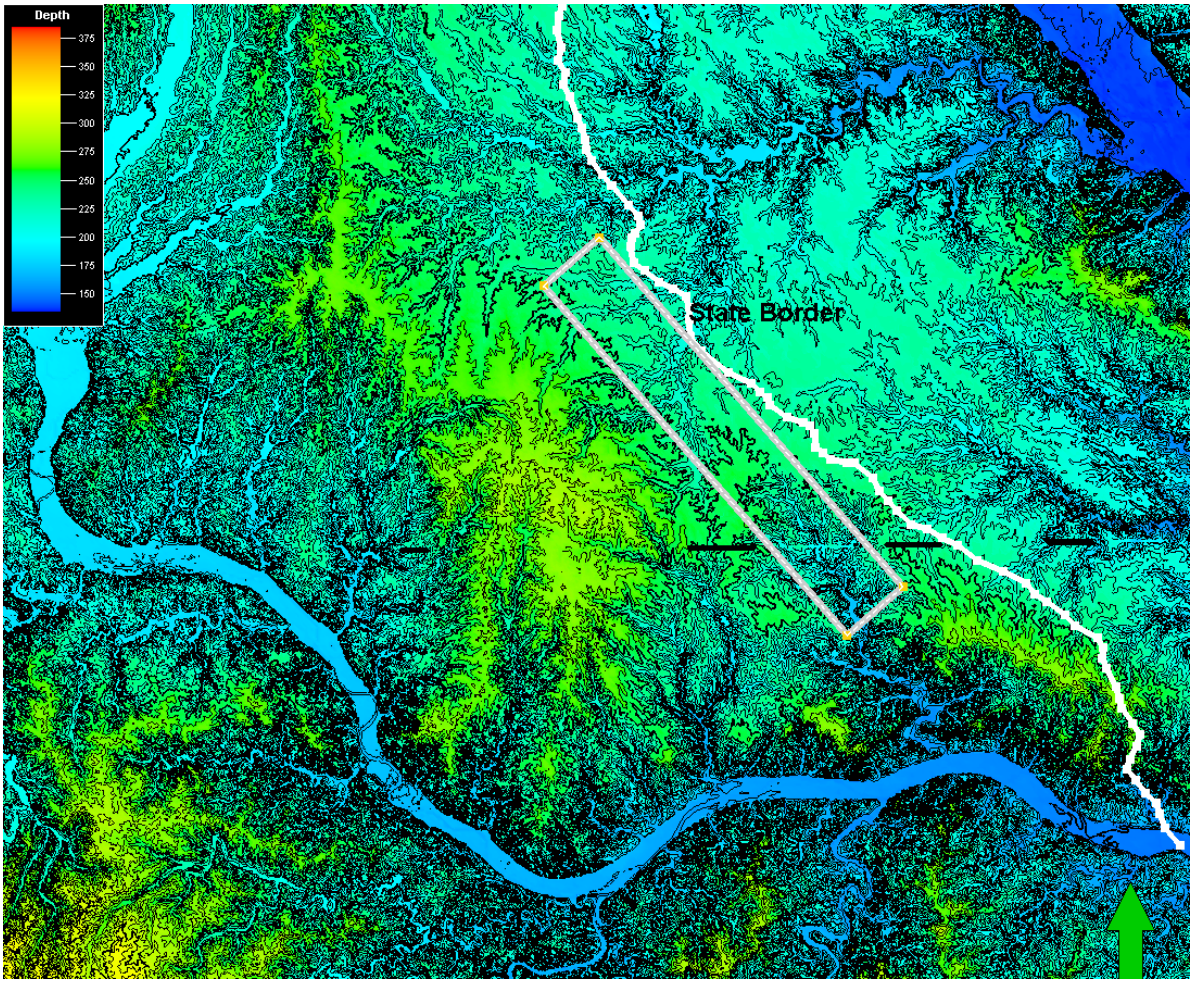

Fig. 9. Surface elevations map of N39-W92 to N40-W93 in Petrel®, showing proposed injection site extent relative to the Missouri-Illinois state border line.

This mesh is then optimized for geomechanical with the use of tetrahedral elements and higher order elements. This helps eliminate the stress concentration around the pinchout and other important geomechanical features such as faults or fracture/joint sets.

It is possible to reconstruct the geometry that is optimized for fluid flow simulations when geometrical operations such as rotation along a point or alignment on axis are performed to make the geometry consistent with geomechanical boundary conditions.

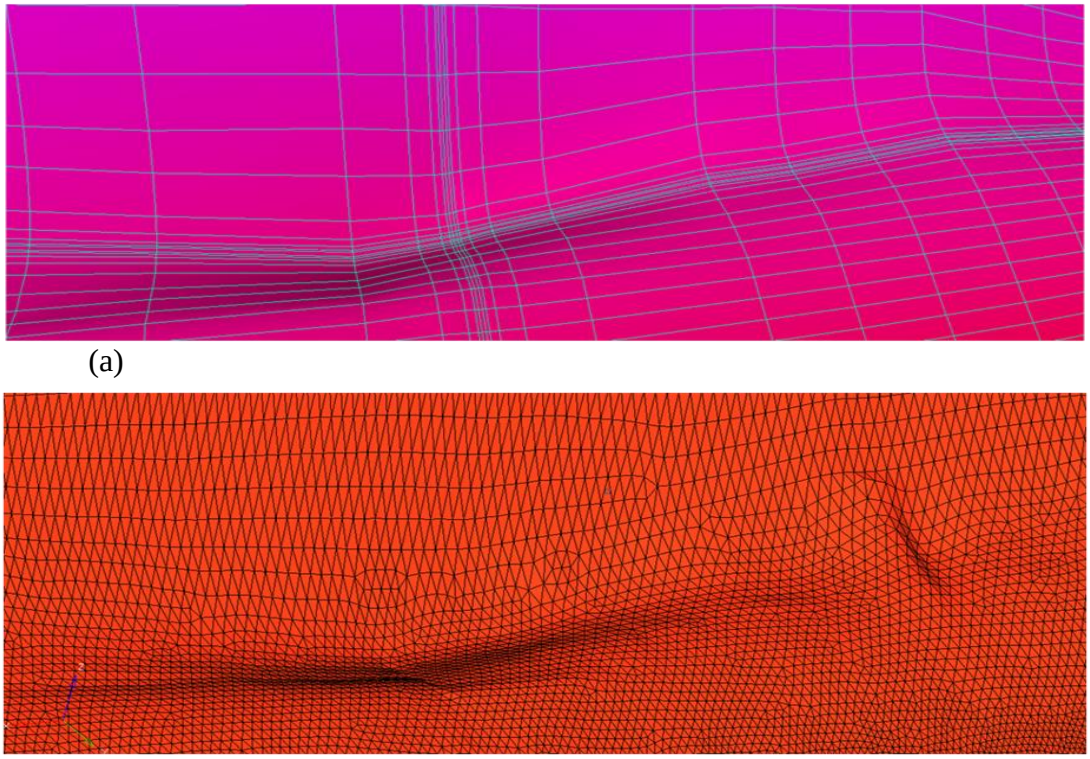

(a)

(b)

Fig. 10. Optimization of geometry for geomechanical analysis.
(a) Finite difference grid is used for fluid flow simulations.
(b) Tetrahedral finite element mesh is used for geomechanical analysis.

Fig. 11 shows the integrated shared earth model created for the Lamotte pinchout viewed from the North-West direction. As shown in this figure, the ISEM covers Precambrian and surface topography. The model is constrained inside latitude / longitude coordinates of 39°00'S / 92°20'W and 38°54'S / 91°37'W. It measures $70km * 16\ km * 600\ m$ and consists of 24 horizons and 74727 simulation grid blocks.

The geomechanical model is constrained to rollers at the sides and bottom that prevent it from expansion on the sides, allowing vertical displacements only.

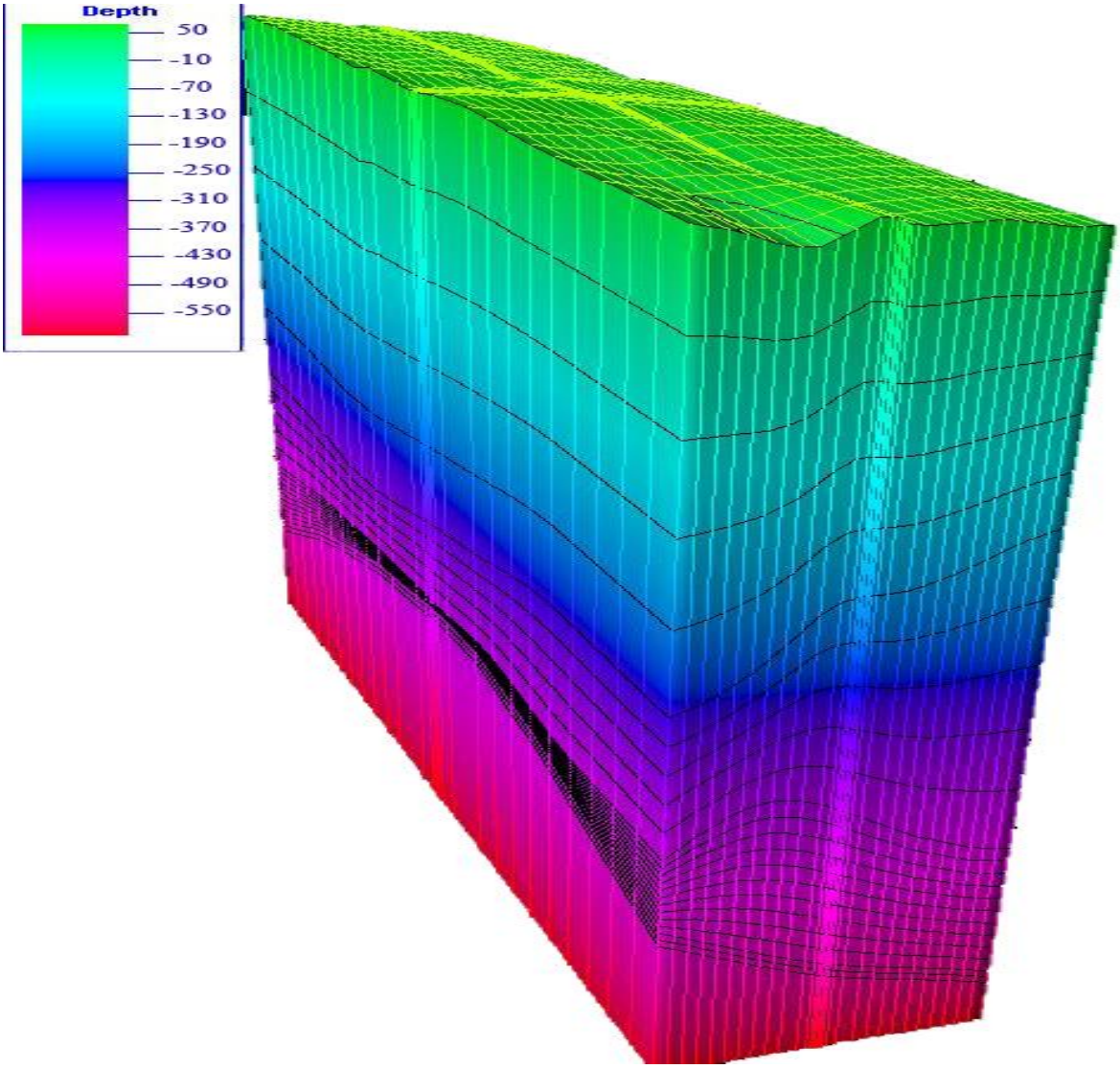

Fig. 11. Simulation grid of the Lamotte pinchout

3.3. Stress Regimes and Boundary Conditions

Surface GPS velocities ("Surface GPS Map of North-East Missouri," 2013) show an East-West trend of 1mm/year in the state of Missouri (Fig. 12) and according to the

"World Stress Map," (2013), Fig. 13, the prominent faulting regime in the North Eastern and Eastern parts of Missouri is thrust faulting and strike slip regime.

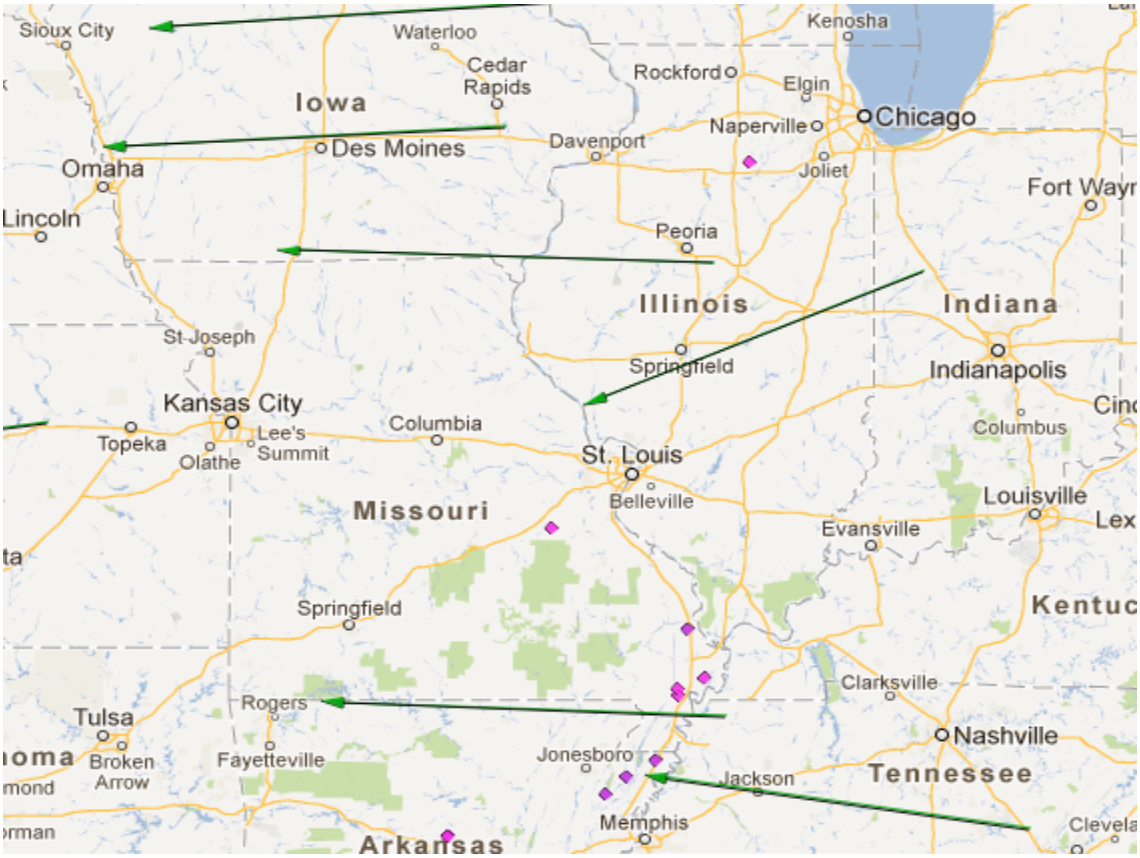

Fig. 12. Surface GPS Velocities of Missouri (magnified)("Surface GPS Map of North-East Missouri," 2013)

Due to the lack of stress measurements and based on the GPS velocities and style of faulting from the World Stress Map, the following stress regimes are considered as different scenarios for modeling of the pinchout formation:

1. Normal faulting (extensional) regime
2. Strike slip regime
3. Compressional regime

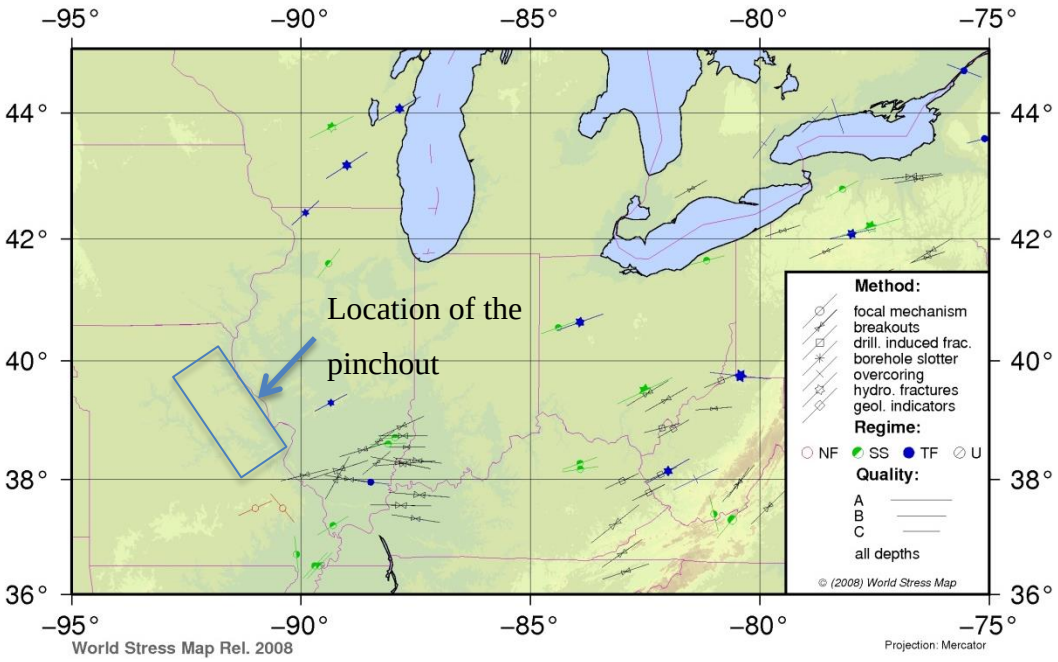

Fig. 13. Observed Stress Regimes in the State of Missouri and the Neighboring States ("World Stress Map," 2013)

In the extensional stress regime ($\sigma_1 = \sigma_v,\ \sigma_2 = \sigma_H, \sigma_3 = \sigma_h$), it is assumed that the sedimentary layers are tectonically relieved and horizontal stresses are calculated based on the uniaxial strain assumption (Byerlee, 1978). The vertical stress value at depth d is given by the integral of all vertical stresses resulting from the layers overlaying d:

$$\sigma_v = \int_0^d \rho g dz \qquad (2)$$

Thus the horizontal stress can be calculated as:

$$\sigma_h = \frac{\upsilon}{1-\upsilon}\sigma_v + \frac{(1-2\upsilon)}{(1-\upsilon)}\alpha P_o \qquad (3)$$

In strike-slip regime the vertical stress is the intermediate principal stress ($\sigma_2 = \sigma_v$) and the minimum horizontal stress is the minimum principal stress whose magnitude is given as $\sigma_3 = \sigma_h = 0.8\sigma_v$. The maximum principal stress in this regime is the maximum horizontal stress, ($\sigma_1 = \sigma_H = 1.2\sigma_v$).

The compressional regime is represented by $\sigma_H > \sigma_h > \sigma_v$ relationship. In this regime, the maximum principal stress is the maximum horizontal stress $\sigma_1 = \sigma_H = 1.25\sigma_v$ and minimum horizontal stress is the intermediate principal stress $\sigma_2 = \sigma_h = 1.1\sigma_v$.

Assuming that stress-strain relationship can be simplified to a linear elastic relationship exists between the two, Hooke's law can be used to determine the strain values that will result in different stress regimes, when applied to the base extensional regime:

$$\sigma_1 = (\lambda + 2G)\varepsilon_1 + \lambda\varepsilon_2 + \lambda\varepsilon_3 \qquad (4)$$

$$\sigma_2 = \lambda\varepsilon_1 + (\lambda + 2G)\varepsilon_2 + \lambda\varepsilon_3 \qquad (5)$$

$$\sigma_3 = \lambda\varepsilon_1 + \lambda\varepsilon_2 + (\lambda + 2G)\varepsilon_3 \qquad (6)$$

3.4. Pre-Stressing

In order to simulate realistic stress magnitudes the coupled process requires a stress initialization procedure for the finite element model (also termed pre-stressing) wherein the modeled effective stresses (we assume hydrostatic pore pressure conditions) as a result of gravitational compaction reach a state of equilibrium. A common procedure to simulate

realistic in situ stresses involves the following steps (Buchmann and Connolly, 2007; Eckert and Connolly, 2007; Hergert and Heidbach, 2011):

1) gravitational pre-stressing;

2) application of horizontal strain in order to simulate any tectonic contribution by different stress regimes in three dimensional space.

4. Results and Discussion

An initial hydrostatic pressure distribution of the Lamotte sandstone is considered for the pinch out model and is used for the geostatic equilibrium (pre-stressing) of the model. Fig. 14 shows the average pore pressure increase in the aquifer for the two CO_2 injection schemes. While one injection well imposes the minimal average pore pressure increase of 3.41 MPa, the three injection wells scenario results in a differential pore pressure increase of 6 MPa. Both injection scenarios are still within safe sequestration limits of the aquifer.

Fig. 15 and Fig. 16 show the evolution of differential stress in the one and three CO_2 injection well scenarios respectively. The incremental pore pressure increase has resulted in the decrease of the differential stress. This change in the state of stress can result in shear failure but in this study the Lamotte sandstone, as well as the caprock remain intact.

Fig. 14. Average aquifer pressure change as a function of time for one and three injection wells. The one injection well shows minimal pressure increase of 3.41 MPa over the course of 100 years while the three injection well scenario shows an overall pore pressure increase of 6 MPa over the 100 years of injection. The two injection scenarios are under the sequestration and permissible pore pressure increase limits for the aquifer of interest.

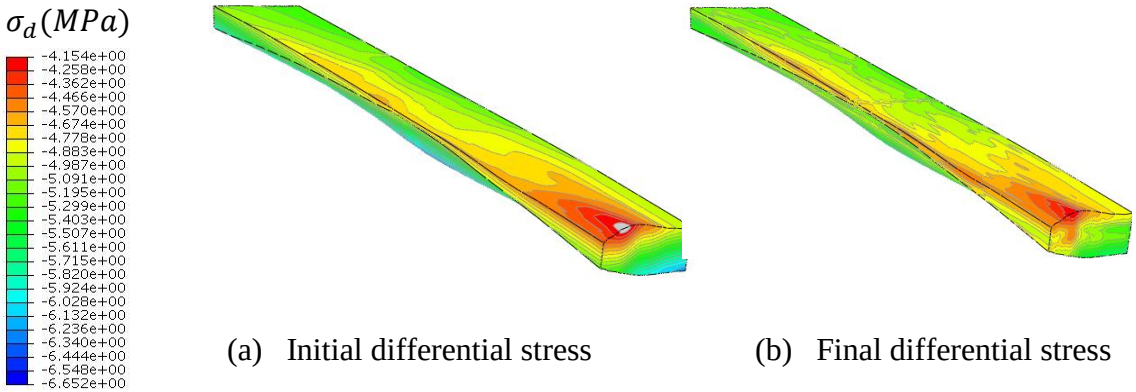

(a) Initial differential stress (b) Final differential stress

Fig. 15. Differential stress profiles at the Lamotte formation of the one CO_2 injector scenario in the pinch out model after 100 years of CO_2 injection.

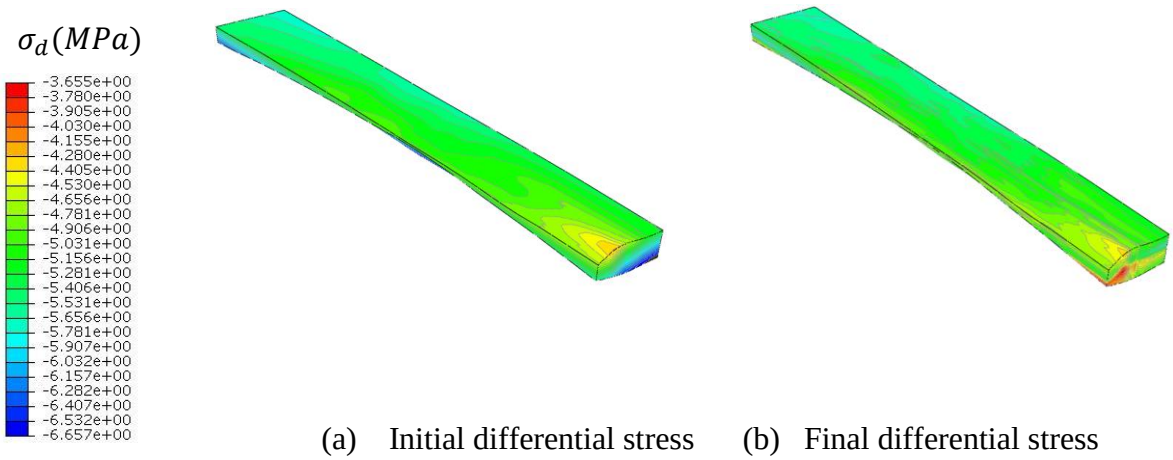

(a) Initial differential stress (b) Final differential stress

Fig. 16. Differential stress profiles at the Lamotte formation of the three CO_2 injectors scenario in the pinch out model after 100 years of CO_2 injection.

Rutqvist et al. (2007) defines the maximum sustainable pore pressure as the maximum pressure that does not lead to irreversible geomechanical changes such as rock failure or fracture/fault reactivation. Paradeis et al., (2012) have used this definition and derived the critical pore pressure difference. Writing the Mohr criterion for shear failure in terms of σ_1 to σ_3 at failure conditions one can get:

$$\sigma_1 - P_p = 2C_o \frac{\cos\phi}{1-\sin\phi} + \frac{1+\sin\phi}{1-\sin\phi}(\sigma_3 - P_p) \qquad (7)$$

This relationship applies in the cases where the differential stress is at least twice the cohesion. Applying the friction angle given in Table 4, equation (7) can be written in terms of pore pressure as:

$$P_{p,Critical-Intact} = S_o \frac{\cos\phi}{1-\sin\phi} + \frac{3\sigma_3 - \sigma_1}{2} \qquad (8)$$

This is the critical pore pressure for generation of new shear fractures in an intact rock. The pre-existing fractures are characterized by absence of the cohesion. In this case the critical pore pressure is simply

$$P_{p,Critical-Reactivation} = \frac{3\sigma_3 - \sigma_1}{2} \quad (9)$$

Similarly the pore pressure for tensile failure is given by:

$$P_{p,Critical-Tensile} = \sigma_3 + T_o \quad (10)$$

Fig. 17 shows the effective maximum and minimum principal stresses in the pinchout prior to CO_2 injection.

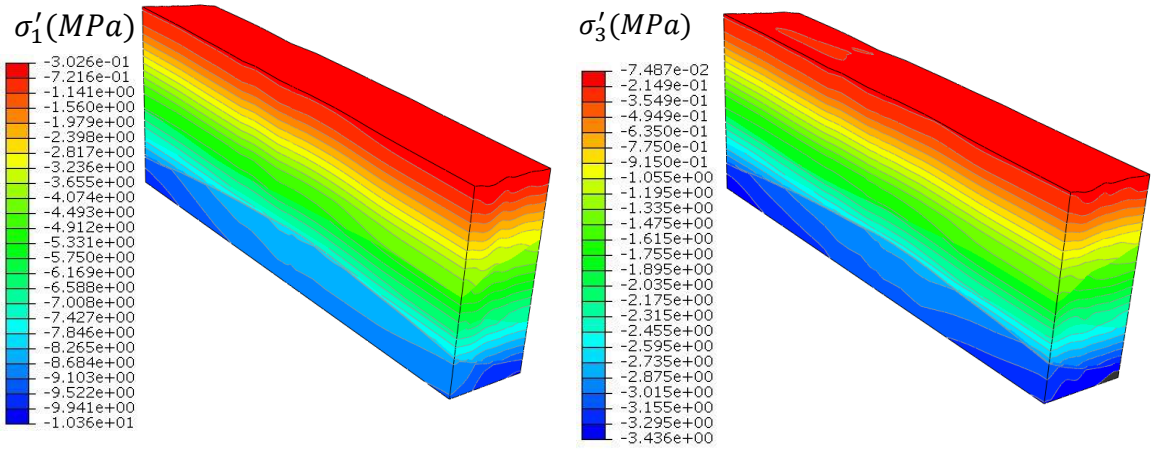

(a) Initial effective maximum stress (b) Initial effective minimum stress

Fig. 17. Effective maximum and minimum principal stresses for one injection well scenario prior to CO_2 injection

Using Fig. 17, the critical pore pressure for intact rock and the existing discontinuities can be calculated as Table 6.

Fig. 18 shows the efffect of pore pressure varition on the stability of the Lamotte formation in extensional regime. The increase in average pore pressure from an initial

hydrostatic value of 3.92 MPa to the final values of 7.3MPa for one injection well and 11.9, 11.1 and 11.3 MPa at Left, Middle and Right injection wells respectively for the three injection wells scenario is less than the incremental pore pressure required for tensile rock failure or shear failure.

Table 6. Pre-Injection critical pore pressure at the injection well for different stress regimes

Property	Extensional	Strike Slip	Compressional
$\sigma_1(MPa)$	11.72	14.06	17.58
$\sigma_3(MPa)$	6.52	9.37	11.72
$P_{p,Critical-Intact}(Mpa)$	21.24	24.35	26.11
$P_{p,Critical-Reactivation}(Mpa)$	3.92	0.70	0.879
$P_{p,Critical-Tensile}(MPa)$	9.02	11.87	14.22

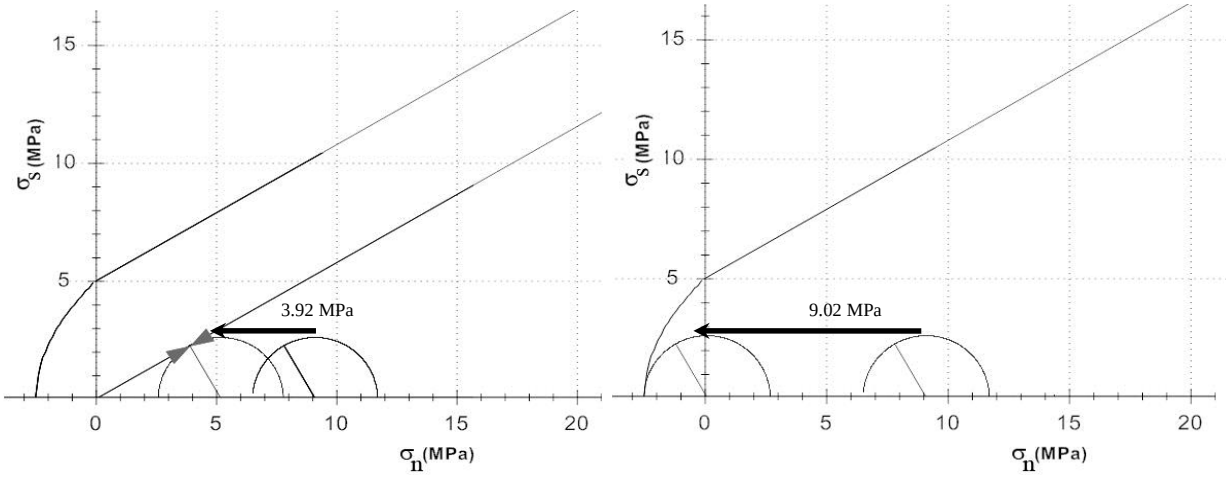

(a) (b)

Fig. 18. Effect of pore pressure variation on the stability of the pinchout formation in extensional regime.
(a) Shifting of the stable state of stress to reactivation mode due to the increase in pore pressure for 3.92 MPa. Existing discontinuities will be reactivated.
(b) Shifting of the stable state of stress to tensile failure mode due to the increase in pore pressure for 9.02 MPa which results in formation of new hydraulic fractures.

This change in pore pressure, however, results in a small uplift of about 1 mm on the surface which can be used to cross check the validity of the modeling if InSar technology is employed along with other available surface monitoring technologies.

The initial pore volume in the body of Lamotte formation enclosed in the presented boundaries is $18.385 * 10^9\ m^3$. Assuming that the density of CO_2 stays constant and equal to 1.98 Kg/m^3 throughout the course of simulation, the CO_2 injection rate of 600 kTons/Year in the three injection well scenario is equal to a CO_2 injection rate of 860,400 Sm^3/day at surface conditions. The formation volume factor of CO_2 at the initial reservoir pressure is 0.003724 Rm^3/Sm^3 which results in the injected gas volume of 3204.12 Rm^3/day. Over the period of 100 years of injection, the formation volume factor decreases to 0.002646 Rm^3/Sm^3 and the equivalent reservoir volume of the injected CO_2 will be 759.001 Rm^3/day. This means that the 31.425 x 10^9 Sm^3 of CO_2 at the surface will occupy 88.19 x 10^6 Rm^3 at reservoir conditions, an occupancy of 0.52% of the available pore volume which signifies that a very small volume of the reservoir is occupied through the use of three injection wells

In conclusion, the pinch out setting of the Lincoln fold under normal stress regime is capable of safe handling of the CO_2 injection rate of 600kTons/year through three vertical injection wells for a period of 100 years. The resulting occupancy of the formation is 0.16% for one injection well and 0.52% for three injection wells, which is much less than the expected typical maximum occupancy of closed boundary reservoirs of about 2-3% (Bachu, 2008; Bachu et al., 2007b; Kaldi and Gibson-Poole, 2008; Rutqvist et al., 2007). The average pore pressure increase in the model is not sufficient for achieving supercritical CO_2 during the injection period and CO_2 is stored in gases phase. If the CO_2

was heated up to $32°C$ before injection, then the three injection well scenario can reach the supercritical state, even though the aquifer is shallow.

5. Conclusions

In the present study a shared earth model for a candidate pinchout structure was constructed in the state of Missouri and shallow CO_2 sequestration for the emission rate of nearby coal fired power plants was studied. Numerical simulation results suggest that the pinchout is a promising sequestration site that can contain the CO_2 emissions of at least three coal fired power plants in the North-Eastern Missouri for a prolonged injection period of 100 years. Maximum occupancy of 0.52% under closed boundary conditions was achieved by using three vertical injections wells. Although CO_2 does not reach the super critical conditions in this shallow sequestration site, in-state storage that eliminates cost of transportation to Williston basin, as well as the reduced cost of drilling, completion and pumping due to the shallow sequestration make the pinchout in Lincoln fold a viable option for the state of Missouri.

Acknowledgement

The authors gratefully acknowledge financial support from US Department of Energy's National Energy Technology Laboratory under grant # DE-FE0001132. Disclaimer: "This report was prepared as an account of work sponsored by an agency of the United States Government. Neither the United States Government nor any agency thereof, nor any of their employees, makes any warranty, express or implied, or assumes any legal liability or responsibility for the accuracy, completeness, or usefulness of any information, apparatus, product, or process disclosed, or represents that its use would not

infringe privately owned rights. Reference herein to any specific commercial product, process, or service by trade name, trademark, manufacturer, or otherwise does not necessarily constitute or imply its endorsement, recommendation, or favoring by the United States Government or any agency thereof. The views and opinions of authors expressed herein do not necessarily state or reflect those of the United States Government or any agency thereof." The authors would also like to express their gratitude to Schlumberger for their generous donation of the educational license of Petrel and Eclipse.

References

Akpan, I.C., 2012. Development of a shared earth model to investigate potential for carbon dioxide sequestration in the Springfield area, MO. Missouri University of Science and Technology.

Amirlatifi, A., Eckert, A., Nygaard, R., Bai, B., 2011. Estimation of Reservoir Uplift , Seismicity and Failure Likelihood during CO 2 Injection through Coupled Reservoir Simulation, in: Canadian Unconventional Resources Conference. Calgary, Canada, p. CSUG/SPE SPE–148946–PP.

Amirlatifi, A., Eckert, A., Nygaard, R., Bai, B., Liu, X., Paradeis, M., 2012. Role of Geometrical Influences of CO_2 Sequestration in Anticlines, in: American Rock Mechanics Association. Chicago, IL, p. ARMA 12–255.

Bachu, S., 2000. Sequestration of CO_2 in geological media: criteria and approach for site selection in response to climate change. Energy Conversion and Management 41, 953–970.

Bachu, S., 2002. Sequestration of CO_2 in geological media in response to climate change: road map for site selection using the transform of the geological space into the CO_2 phase space. Energy Conversion and Management 43, 87–102.

Bachu, S., 2008. Comparison between Methodologies Recommended for Estimation of CO_2 Storage Capacity in Geological Media. the CSLF Task Force on CO_2 Storage Capacity Estimation and the US DOE Capacity and Fairways Subgroup of the Regional Carbon Sequestration Partnerships Program.

Bachu, S., Adams, J.J., 2003. Sequestration of CO_2 in geological media in response to climate change: capacity of deep saline aquifers to sequester CO_2 in solution. Energy Conversion and Management 44, 3151–3175.

Bachu, S., Bonijoly, D., Bradshaw, J., Burruss, R., Holloway, S., Christensen, N.P., Mathiassen, O.M., Bachu, S., Bonijoly, D., Burruss, R., Holloway, S., Christensen, N.P., Mathiassen, O.M., Bradshaw, J., Burruss, R., Holloway, S., Christensen, N.P., Mathiassen, O.M., 2007. CO_2 storage capacity estimation: Issues and development of standards. International Journal of Greenhouse Gas Control 1, 62–68.

Bachu, S., Gunter, W.D., Perkins, E.H., 1994. Aquifer disposal of CO_2: Hydrodynamic and mineral trapping. Energy Conversion and Management 35, 269–279.

Bergman, P.D., Winter, E.M., 1995. Disposal of carbon dioxide in aquifers in the U.S. Energy Conversion and Management 36, 523–526.

Bohm, R.A., Anderson, K.H., 1981. OFM-81-5-GI, Structural map of Missouri contoured on the top of the Basal Cambrian Clastic units (Lamotte, Reagan and Mount Simon sandstones). Rolla, MO.

Brookshire, C.N., 1997. Missouri Water Quality Assessment.

Conti, John J.; Holtberg, Paul D.; Beamon, Joseph A.; Schaal, Michael A.; Ayoub, Joseph C.; Turnure, J.T., 2011. Annual Energy Outlook 2011, Outlook. Energy Information Administration.

DOE, 2013. DOE - Fossil Energy: Partnerships Index Page [WWW Document]. URL http://www.fossil.energy.gov/programs/sequestration/partnerships (accessed 5.5.13).

Ennis-King, J., Lincoln, P., 2002. Engineering Aspects of Geological Sequestration of Carbon Dioxide. Proceedings of SPE Asia Pacific Oil and Gas Conference and Exhibition 3, 8.

Ennis-King, J., Paterson, L., 2001. Reservoir engineering issues in the geological disposal of carbon dioxide, in: Williams, D.J., Durie, R.A., McMullan, P., Paulson, C.A.J., Smith, A.Y. (Eds.), Proceedings of the Fifth International Conference on Greenhouse Gas Control Technologies. Csiro Publishing, pp. 290–295.

Govindarajan, S., 2012. Geomechanical Characterization of Reservoir & Cap Rocks for CO_2 Sequestration. Missouri University of Science and Technology.

Gunter, W.D., Bachu, S., Law, D.H.S., Marwaha, V., Drysdale, D.L., MacDonald, D.E., McCann, T.J., 1996. Technical and economic feasibility of CO_2 disposal in aquifers within the Alberta Sedimentary Basin, Canada. Energy Convers Mgmt 37, 1135–1142.

Gunter, W.D., Perkins, E.H., McCann, T.J., 1993. Aquifer disposal of CO_2-rich gases: Reaction design for added capacity. Energy Conversion and Management 34, 941–948.

Hoek, E., Brown, E.T., 1997. Practical estimates of rock mass strength. International Journal of Rock Mechanics and Mining Sciences 34, 1165–1186.

Hoek, E., Carranza-Torres, C., Corkum, B., 2002. Hoek-brown failure criterion – 2002 edition. 5th North American Rock Mechanics Symposium and 17th Tunneling Association of Canada Conference NARMSTAC 1, 267–273.

Holloway, S., Savage, D., 1993. The potential for aquifer disposal of carbon dioxide in the UK. Energy Conversion and Management 34, 925–932.

Holt, T., Jensen, J.I., Lindeberg, E., 1995. Underground storage of CO_2 in aquifers and oil reservoirs. Energy Conversion and Management 36, 535–538.

Holtz, M.H., 2002. Residual Gas Saturation to Aquifer Influx: A Calculation Method for 3-D Computer Reservoir Model Construction, in: Proceedings of SPE Gas Technology Symposium. Society of Petroleum Engineers.

Ipcc, 2005. IPCC special report on carbon dioxide capture and storage, IPCC Special Report on Carbon Dioxide Capture and Storage. Cambridge University Press.

Kaldi, J., Gibson-Poole, C., 2008. Storage capacity estimation, site selection and characterization for CO_2 storage projects. Report No: RPT08-1001, CO_2CRC, Canberra, ACT.

Koide, H., Tazaki, Y., Noguchi, Y., Iijima, M., Ito, K., Shindo, Y., 1993. Underground storage of carbon dioxide in depleted natural gas reservoirs and in useless aquifers. Engineering Geology 34, 175–179.

Koide, H., Tazaki, Y., Noguchi, Y., Nakayama, S., Iijima, M., Ito, K., Shindo, Y., 1992. Subterranean containment and long-term storage of carbon dioxide in unused aquifers and in depleted natural gas reservoirs. Energy Conversion and Management 33, 619–626.

Kumar, I., 2012. Direct Shear Testing of Fractured Rocks from Missouri Used to Evaluate Potential Fault Reactivation Induced by Carbon Dioxide Sequestration. Missouri University of Science and Technology.

Metz, B., Davidson, O., Bosch, P., Dave, R., Meyer, L., 2007. Climate Change 2007: Mitigation of Climate Change. Cambridge, United Kindgom and New York, NY, USA.

Miller, T.J., 2012. Evaluation of the Reagan and Lamotte Sandstones in Southwestern Missouri for carbon dioxide sequestration. Missouri University of Science and Technology.

Missouri and Coal - Sourcewatch [WWW Document], 2013. URL http://www.sourcewatch.org/index.php?title=Missouri_and_coal (accessed 5.5.13).

Netzler, B.W., 1982. OFM-82-68-WR, Map of total dissolved solids concentrations in groundwater from the Elvins group (upper Cambrian) in Missouri. Rolla, MO.

Nygaard, R., Bai, B., Amirlatifi, A., Yang, F., Tiamiyu, O., 2012. DOE Report DE-FE0001132: Reservoir Studies of CO_2 injection in the Lamotte sandstone formation in Southwest Missouri. Rolla, MO.

Paradeis, M., Eckert, A., Liu, X., 2012. Influences of Anticline Reservoir Geometry On Critical Pore Pressures Associated With CO_2 Sequestration, in: 46th U.S. Rock Mechanics/Geomechanics Symposium, June 24 - 27, 2012 , Chicago, Illinois. Chicago, IL, pp. 2012–319.

Peck, W., Buckley, T., Battle, E., Grove, M., 2012. Plains CO_2 Reduction (PCOR) Partnership, Practical, Environmentally Sound CO_2 Sequestration Atlas. Grand Forks, ND.

Pruess, K., Xu, T., Apps, J., Garcia, J., 2003. Numerical Modeling of Aquifer Disposal of CO_2. SPE Journal 8.

Pruess, K., Xu, T., Apps, J., Garcia, J., Berkeley, L., Karsten, P., Tianfu, X., John, A., Julio, G., 2001. Numerical Modeling of Aquifer Disposal of CO_2 - Paper SPE 66537, in: Proceedings of SPE/EPA/DOE Exploration and Production Environmental Conference. Society of Petroleum Engineers, San Antonio, Texas, pp. 1–16.

Rutqvist, J., Birkholzer, J.T., Cappa, F., Tsang, C.-F.C.-F., 2007. Estimating maximum sustainable injection pressure during geological sequestration of CO_2 using coupled fluid flow and geomechanical fault-slip analysis. Energy Conversion and Management 48, 1798–1807.

Smotherman, B., 2010. The Influence of Lineaments on the Geology of Missouri [WWW Document]. Emporia State University. URL http://academic.emporia.edu/aberjame/student/smotherman2/globaltect2.htm (accessed 8.28.12).

Turcotte, D.L., Schubert, G., 2002. Geodynamics, 2nd ed. Cambridge University Press, New York.

Van der Meer, L.G.H., 1992. Investigations regarding the storage of carbon dioxide in aquifers in the Netherlands. Energy Conversion and Management 33, 611–618.

Van der Meer, L.G.H., 1995. Storage Efficiency of Aquifers. Energy Conversion and Management 36, 513–518.

Van der Meer, L.G.H., 1996. Computer Modeling of Underground CO_2 Storage. Energy Conversion and Management 37, 1155–1160.

Yang, F., Bai, B., Dunn-Norman, S., Nygaard, R., Eckert, A., 2013. Factors affecting CO_2 storage capacity and efficiency with water withdrawal in shallow saline aquifers. Environmental Earth Sciences.

SECTION

2. CONCLUSIONS AND RECOMMENDATIONS

2.1. SYNOPSIS

The state of Missouri, a member of Plains CO_2 Reduction Partnership (PCRP), has been investigating geological CO_2 storage as a means of reducing CO_2 emissions from its coal fired power plants. Due to the high cost of compression and transportation of CO_2 from Missouri to Williston basin, the target storage formation for PCRP, the state is investigating local sequestration possibilities. Lamotte formation as an aquifer spread throughout the state that offers acceptable porosity, permeability and rock strength was selected as the prime storage target and a favorable geologic trap setting was located in North-Eastern part of the state.

Pore pressure variation due to the injection or production of fluids can result in the change in the state of stress and consequently uplift/subsidence, fracture generation/reactivation, fault reactivation and seismicity may occur. As a result, fluid flow in a porous medium under such scenarios cannot be simplified to compressibility or pressure dependent porosity/permeability changes. Modeling of such processes is achieved by incorporation of geomechanical effects resulting from fluid flow in the porous medium. CO_2 sequestration is a case that imposes high levels of pore pressure variations over a relatively short period of time and as a result fluids may not have enough time to equilibrate within the formation.

The use of fluid flow simulation, geomechanical analysis and fracture modeling represents a well understood procedure in the hydrocarbon industry, and many different software suites are coupled using a variety of approaches. However, many of these coupling modules are proprietary "in-house" applications and are not available for public access. In addition the few open source coupled simulators use finite difference approach and shared earth models based on this technique for coupled simulations and as a result have limited capabilities in modeling of complex geological settings. In order to overcome these problems and to create an open source coupling module that uses commercial fluid flow and geomechanics simulators, Coupled Geomechanical Reservoir Simulator (CGRS) was developed. The methodology and approach taken for developing this module was discussed in the first paper, "An Explicit Partial Coupling Approach for Simulating CO_2 Sequestration."

CGRS is an open source code suite of software and with modifications in input/output sections, it can be used to couple different fluid flow simulators with different geomechanical analysis packages. The geometrical flexibilities offered by CGRS suite makes it possible to create complex geometries in a finite element pre-processor, for example, and convert them to native formats for the finite difference simulators, which can be used for parametric studies on different geometries that if not impossible, are very difficult to attain in their native pre-processors. Examples of such applications were presented in the first and second papers where commingled effect of geometry and boundary conditions was studied on a pinchout setting and several different realizations of anticline structures. Knowledge from these studies prove the inevitable need for study of

fluid flow boundary conditions and realistic modeling of the geometry for determination of safe injection limits of a geologic storage medium.

Findings of second paper, "Role of Geometrical Influences of CO_2 Sequestration in Anticlines" on storage capacity of aquifers under different lateral fluid flow boundary conditions were used as the motive of the third paper, "Fluid Flow Boundary Conditions: The Need for Pressure Transient Analysis for CO_2 Sequestration Studies." In this paper pressure transient analysis is presented as a tool for eliminating the guess out of fluid flow boundary condition and making it a quantitative matter. At the time of this writing, lateral fluid flow boundary conditions are not determined quantitatively by most scholars and two extreme cases of open versus closed boundary conditions are usually studied. In the third paper, a tool set was presented that helps in identification of the lateral fluid flow boundary condition. It is also noted that in many cases the assumption of open boundary conditions and infinite aquifers are interchanged. The present work addresses this misunderstanding by presenting prominent differences in bottom-hole pressure derivative analysis of drawdown test followed by an extended build up test. In addition, to infinite lateral boundary condition, the present work suggests existence of a forth type of boundary condition, that considers a spectrum of fluid flux between the fully open boundary condition and fully closed lateral boundary. Application of drawdown test followed by the extended build up, as presented here, will be a viable tool for realization of the shared earth model for CO_2 sequestration studies.

Once the required toolset and methodologies for creating shared earth models for coupled geomechanical reservoir simulations and assessing the fluid flow boundary conditions were attained together with physical rock properties, a realistic shared earth

model was created for the candidate pinchout formation in North-Eastern Missouri and coupled analysis was conducted with emission rates of nearby coal fired power plants. Results of these studies and storage capacity of the candidate formation were presented in the fourth paper, "Geomechanical Risk Assessment for CO_2 Sequestration in a Candidate Storage Site in Missouri." Results of this study were used to evaluate the viability of the Lamotte pinchout in the Lincoln fold for sustainable CO_2 sequestration in Missouri. Mesh conversion functionalities of CGRS suite made it possible to have a shared earth model that includes topography, as well as complex geometries in the fluid flow and geomechanics simulators. Also the coupling module facilitated geomechanical analysis and risk assessments.

2.2. CONCLUSIONS

In order to mitigate the cost of pumping CO_2 emissions from coal fired power plants in the state of Missouri a candidate high salinity brine aquifer was located in the Lincoln fold in North-East Missouri and two injection schemes were studied to estimate the storage capacity of this pinchout formation.

To study effects of pore pressure variation due to the injection of CO_2 that can result in the change in the state of stress and geomechanical effects, a suite of software that include a fully automated 2-way coupled geomechanical reservoir simulator, Coupled Geomechanical Reservoir Simulator (CGRS), was developed and presented that addresses the limitations of structured FD pillar grids when complex geometries are modeled and utilize the natural and optimal meshing algorithm for each simulator. Results of this coupling module were validated by an analytical model.

In addition, importance of fluid flow boundaries on storage capacity of the aquifer was demonstrated and pressure derivative analysis of bottom-hole pressure during a water drawdown test followed by a prolonged buildup test was used to identify fluid flow boundary conditions for CO_2 sequestration projects. This approach leverages the determination of fluid flow boundary conditions from an assumption to a quantitative analysis. In this study the concept of flux factor was used to define a transitional boundary condition between pseudo steady state and steady state conditions to better understand the type and location of the boundaries for CO_2 sequestration studies.

Application of coupled geomechanical reservoir simulation through CGRS suite showed that the pinchout is a promising sequestration site that can contain the CO_2 emissions of at least three coal fired power plants in the North-Eastern Missouri for a prolonged injection period of 100 years. Maximum occupancy of 0.52% under closed boundary conditions was achieved by using three vertical injections wells. Although CO_2 does not reach the super critical conditions in this shallow sequestration site, in-state storage that eliminates cost of transportation to Williston basin, as well as the reduced cost of drilling, completion and pumping make the pinchout in Lincoln fold a viable option for the state of Missouri.

2.3. RECOMMENDATIONS AND FUTURE WORK

Although this study has provided significant insights into the suitability of the Lamotte pinchout in the Lincoln fold for in state CO_2 sequestration, the following considerations need to be addressed prior to CO_2 sequestration in the aforementioned formation:

1- Once pilot injection wells are drilled at the location, core sample analysis of the target formations need to be conducted prior to initiation of CO_2 sequestration site and the present work should be considered as an initial feasibility study.
2- Stress measurements should be conducted in the pilot wells, so that the local state of stress can be identified. Once the boundary conditions of the geomechanical model are determined, the coupled analysis should be repeated so that the actual sage storage capacity based on the local stresses is determined.
3- This study is based on certain injected gas and in situ brine compositions. Should the fluid compositions change, the simulations and mineral precipitation determinations should be repeated, so that pore throat clogging is avoided.
4- Plume monitoring can be achieved through coupling of numerical simulation results and surface monitoring technologies such as InSar. It is recommended that such surface monitoring technologies are employed for cross validation of numerical simulations and prevention of excessive uplift/land slide.

BIBLIOGRAPHY

ABAQUS 6.12 User Documentation, 2012.

Akpan, I.C., 2012. Development of a shared earth model to investigate potential for carbon dioxide sequestration in the Springfield area, MO. Missouri University of Science and Technology.

Allain, O., Tauzin, E., Chassignol, V., 2009. Dynamic Flow Analysis, 4.10.01 ed. KAPPA.

Altmann, J.B., Müller, T.M., Müller, B.I.R., Tingay, M.R.P., Heidbach, O., 2010. Poroelastic contribution to the reservoir stress path. International Journal of Rock Mechanics and Mining Sciences 47, 1104–1113.

Amirlatifi, A., Eckert, A., Nygaard, R., Bai, B., 2011. Estimation of Reservoir Uplift , Seismicity and Failure Likelihood during CO 2 Injection through Coupled Reservoir Simulation, in: Canadian Unconventional Resources Conference. Calgary, Canada, p. CSUG/SPE SPE–148946–PP.

Amirlatifi, A., Eckert, A., Nygaard, R., Bai, B., Liu, X., Paradeis, M., 2012. Role of Geometrical Influences of CO_2 Sequestration in Anticlines, in: American Rock Mechanics Association. Chicago, IL, p. ARMA 12–255.

Aziz, K., Settari, A., 1979. Petroleum Reservoir Simulation. Applied Science Publishers Limited, London.

Bachu, S., 2000. Sequestration of CO_2 in geological media: criteria and approach for site selection in response to climate change. Energy Conversion and Management 41, 953–970.

Bachu, S., 2002. Sequestration of CO_2 in geological media in response to climate change: road map for site selection using the transform of the geological space into the CO_2 phase space. Energy Conversion and Management 43, 87–102.

Bachu, S., 2008. Comparison between Methodologies Recommended for Estimation of CO_2 Storage Capacity in Geological Media. the CSLF Task Force on CO_2 Storage Capacity Estimation and the US DOE Capacity and Fairways Subgroup of the Regional Carbon Sequestration Partnerships Program.

Bachu, S., Adams, J.J., 2003. Sequestration of CO_2 in geological media in response to climate change: capacity of deep saline aquifers to sequester CO_2 in solution. Energy Conversion and Management 44, 3151–3175.

Bachu, S., Bonijoly, D., Bradshaw, J., Burruss, R., Holloway, S., Christensen, N.P., Mathiassen, O.M., 2007a. CO_2 storage capacity estimation: Methodology and gaps. International Journal of Greenhouse Gas Control 1, 430–443.

Bachu, S., Bonijoly, D., Bradshaw, J., Burruss, R., Holloway, S., Christensen, N.P., Mathiassen, O.M., 2007b. CO_2 storage capacity estimation: Issues and development of standards. International Journal of Greenhouse Gas Control 1, 62–68.

Bachu, S., Gunter, W.D., Perkins, E.H., 1994. Aquifer disposal of CO_2: Hydrodynamic and mineral trapping. Energy Conversion and Management 35, 269–279.

Baklid, A., Korbol, R., Owren, G., 1996. Sleipner Vest CO_2 Disposal, CO_2 Injection Into A Shallow Underground Aquifer - Paper SPE 36600, in: Proceedings of SPE Annual Technical Conference and Exhibition. Society of Petroleum Engineers, pp. 1–9.

Bergman, P.D., Winter, E.M., 1995. Disposal of carbon dioxide in aquifers in the U.S. Energy Conversion and Management 36, 523–526.

Bohm, R.A., Anderson, K.H., 1981. OFM-81-5-GI, Structural map of Missouri contoured on the top of the Basal Cambrian Clastic units (Lamotte, Reagan and Mount Simon sandstones). Rolla, MO.

Bostrom, B., 2009. Development of a Geomechanical Reservoir Modelling Workflow and Simulations, in: Proceedings of SPE Annual Technical Conference and Exhibition. Society of Petroleum Engineers, New Orleans, Louisiana.

Brookshire, C.N., 1997. Missouri Water Quality Assessment.

Buchmann, T., Connolly, P., 2007. Contemporary kinematics of the Upper Rhine Graben: A 3D finite element approach. Global and Planetary Change 58, 287–309.

Buckley, S.E., Leverett, M.C., 1942. Mechanism of fluid displacement in sands. Transactions of the AIME 146, 107–116.

Byerlee, J., 1978. Friction of rocks. Pure and Applied Geophysics PAGEOPH 116, 615–626.

Capasso, G., Mantica, S., 2006. Numerical Simulation of Compaction and Subsidence Using ABAQUS, in: ABAQUS Users' Conference. Cambridge, MA USA, pp. 125–144.

Cappa, F., Rutqvist, J., 2011. Modeling of coupled deformation and permeability evolution during fault reactivation induced by deep underground injection of CO_2. International Journal of Greenhouse Gas Control 5, 336–346.

Carr, T., Frailey, S., Reeves, S., Rupp, J., Smith, S., 2008. Methodology for Development of Geologic Storage Estimates for Carbon Dioxide. Capacity and Fairways Subgroup, Geologic Working Group, DOE Regional Carbon Sequestration Partnerships, US Department of Energy, NETL Carbon Sequestration Program.

Carter, R.D., 1966. Pressure Behavior of a Limited Circular Composite Reservoir. Society of Petroleum Engineers Journal 6, 328 – 334.

Charles, D.D., Rieke, H.H., Purushothaman, R., 2001. Well-Test Characterization of Wedge-Shaped, Faulted Reservoirs. SPE Reservoir Evaluation & Engineering 4.

Chen, Z., Huan, G., Ma, Y., 2006. Computational methods for multiphase flows in porous media. Society for Industrial and Applied Mathematics, Dallas, Texas.

Collins, G.S., Melosh, H.J., Ivanov, B. a., 2004. Modeling damage and deformation in impact simulations. Meteoritics & Planetary Science 39, 217–231.

Comerlati, A., 2006. Fluid-Dynamic and Geomechanical Effects of CO_2 Sequestration below the Venice Lagoon. Environmental & Engineering Geoscience 12, 211–226.

Conti, John J.; Holtberg, Paul D.; Beamon, Joseph A.; Schaal, Michael A.; Ayoub, Joseph C.; Turnure, J.T., 2011. Annual Energy Outlook 2011, Outlook. Energy Information Administration.

Coulomb, C.A., 1776. Essai sur une application des regles des maximis et minimis a quelquels problemesde statique relatifs. a la architecture. Mem. Acad. Roy. Div. Sav. 7, 343–387.

Cronquist, C., Alme, M., 1973. Effects of Permeability Variation and Production Rate on Recovery from Partial Water Drive Gas Reservoirs, in: Proceedings of Fall Meeting of the Society of Petroleum Engineers of AIME. Society of Petroleum Engineers.

Darcy, H., 1856. Les fontaines publiques de la ville de Dijon, 1856. Dalmont, Paris.

Davies, J., Davies, D., 1999. Stress-Dependent Permeability: Characterization and Modeling. Proceedings of SPE Annual Technical Conference and Exhibition.

Dean, R., Gai, X., Stone, C., Minkoff, S., 2006. A Comparison of Techniques for Coupling Porous Flow and Geomechanics. SPE Journal 11, 132–140.

DOE, 2013. DOE - Fossil Energy: Partnerships Index Page [WWW Document]. URL http://www.fossil.energy.gov/programs/sequestration/partnerships (accessed 5.5.13).

Drucker, D.C., Prager, W., 1952. Soil mechanics and plastic analysis or limit design. Quarterly of applied mathematics 10, 157–165.

Eckert, A., Connolly, P., 2007. Stress and fluid-flow interaction for the Coso Geothermal Field derived from 3D numerical models. GRC Transactions 385–390.

Ehlig-Economides, C., Economides, M.J., 2010. Sequestering carbon dioxide in a closed underground volume. Journal of Petroleum Science and Engineering 70, 123–130.

Engelder, T., Fischer, M.P., 1994. Influence of poroelastic behavior on the magnitude of minimum horizontal stress, Sh, in overpressured parts of sedimentary basins. Geology 22, 949–952.

Ennis-King, J., Lincoln, P., 2002. Engineering Aspects of Geological Sequestration of Carbon Dioxide. Proceedings of SPE Asia Pacific Oil and Gas Conference and Exhibition 3, 8.

Ennis-King, J., Paterson, L., 2001. Reservoir engineering issues in the geological disposal of carbon dioxide, in: Williams, D.J., Durie, R.A., McMullan, P., Paulson, C.A.J., Smith, A.Y. (Eds.), Proceedings of the Fifth International Conference on Greenhouse Gas Control Technologies. Csiro Publishing, pp. 290–295.

George Stewart, 2011. Well test design and analysis, 1st ed. PennWell, Tulsa, Oklahoma, USA.

Goodman, H., Connolly, P., 2007. Reconciling subsurface uncertainty with the appropriate well design using the geomechanical model (MEM) approach. The Leading Edge 26, 585–588.

Govindarajan, S., 2012. Geomechanical Characterization of Reservoir & Cap Rocks for CO_2 Sequestration. Missouri University of Science and Technology.

Gunter, W.D., Bachu, S., Law, D.H.S., Marwaha, V., Drysdale, D.L., MacDonald, D.E., McCann, T.J., 1996. Technical and economic feasibility of CO_2 disposal in aquifers within the Alberta Sedimentary Basin, Canada. Energy Convers Mgmt 37, 1135–1142.

Gunter, W.D., Perkins, E.H., McCann, T.J., 1993. Aquifer disposal of CO_2-rich gases: Reaction design for added capacity. Energy Conversion and Management 34, 941–948.

Gutierrez, M., Lewis, R.W., 1998. The Role of Geomechanics in Reservoir Simulation, in: Proceedings of SPE/ISRM Rock Mechanics in Petroleum Engineering. Society of Petroleum Engineers, Trondheim, Norway.

Gutierrez, M., Øino, L., Nygård, R., 2000. Stress-dependent permeability of a de-mineralised fracture in shale. Marine and Petroleum Geology 17, 895–907.

Helmig, R., Class, H., Huber, R., Sheta, H., Ewing, R., Hinkelmann, R., Jakobs, H., Bastian, P., 1998. Architecture of the Modular Program System MUFTE-UG for Simulating Multiphase Flow and Transport Processes in Heterogeneous Porous Media. Mathematische Geologie 2, 123–131.

Hergert, T., Heidbach, O., 2011. Geomechanical model of the Marmara Sea region-II. 3-D contemporary background stress field. Geophysical Journal International 3, 1090–1120.

Hillis, R.R., 2001. Coupled changes in pore pressure and stress in oil fields and sedimentary basins. Petroleum Geoscience 7, 419–425.

Hillis, R.R., 2003. Pore pressure/stress coupling and its implications for rock failure. Geological Society, London, Special Publications 216, 359–368.

Hoek, E., Brown, E.T., 1997. Practical estimates of rock mass strength. International Journal of Rock Mechanics and Mining Sciences 34, 1165–1186.

Hoek, E., Carranza-Torres, C., Corkum, B., 2002. Hoek-brown failure criterion – 2002 edition. 5th North American Rock Mechanics Symposium and 17th Tunneling Association of Canada Conference NARMSTAC 1, 267–273.

Holloway, S., 2001. Storage of fossil fuel-derived carbon dioxide beneath the surface of the earth. Annual Review of Energy and the Environment 26, 145–166.

Holloway, S., Savage, D., 1993. The potential for aquifer disposal of carbon dioxide in the UK. Energy Conversion and Management 34, 925–932.

Holt, T., Jensen, J.I., Lindeberg, E., 1995. Underground storage of CO_2 in aquifers and oil reservoirs. Energy Conversion and Management 36, 535–538.

Holtz, M.H., 2002. Residual Gas Saturation to Aquifer Influx: A Calculation Method for 3-D Computer Reservoir Model Construction, in: Proceedings of SPE Gas Technology Symposium. Society of Petroleum Engineers.

Inoue, N., Fontoura, S., 2009. Answers to Some Questions About the Coupling Between Fluid Flow and Rock Deformation in Oil Reservoirs, in: Proceedings of SPE/EAGE Reservoir Characterization and Simulation Conference. Society of Petroleum Engineers, Abu Dhabi, UAE, pp. 1–13.

Ipcc, 2005. IPCC special report on carbon dioxide capture and storage, IPCC Special Report on Carbon Dioxide Capture and Storage. Cambridge University Press.

Izgec, O., Demiral, B., Bertin, H., Akin, S., 2006. Experimental and Numerical Modeling of Direct Injection of CO_2 Into Carbonate Formations - Paper SPE 100809, in: Proceedings of SPE Annual Technical Conference and Exhibition. Society of Petroleum Engineers, San Antonio, Texas.

Jaeger, J.C., Cook, N.G.W., Zimmerman, R.W., 2007. Fundamentals of Rock Mechanics, 4th Editio. ed. John Wiley & Sons.

Kaldi, J., Gibson-Poole, C., 2008. Storage capacity estimation, site selection and characterization for CO_2 storage projects. Report No: RPT08-1001, CO_2CRC, Canberra, ACT.

Klara, S.M., Srivastava, R.D., McIlvried, H.G., 2003. Integrated collaborative technology development program for CO_2 sequestration in geologic formations--United States Department of Energy R&D. Energy Conversion and Management 44, 2699–2712.

Koide, H., Tazaki, Y., Noguchi, Y., Iijima, M., Ito, K., Shindo, Y., 1993. Underground storage of carbon dioxide in depleted natural gas reservoirs and in useless aquifers. Engineering Geology 34, 175–179.

Koide, H., Tazaki, Y., Noguchi, Y., Nakayama, S., Iijima, M., Ito, K., Shindo, Y., 1992. Subterranean containment and long-term storage of carbon dioxide in unused aquifers and in depleted natural gas reservoirs. Energy Conversion and Management 33, 619–626.

Kumar, A., 1977a. Steady Flow Equations for Wells in Partial Water-Drive Reservoirs. Journal of Petroleum Technology 29, 1654–1656.

Kumar, A., 1977b. Strength of Water Drive or Fluid Injection From Transient Well Test Data. Journal of Petroleum Technology 29, 1497–1508.

Kumar, A., Noh, M., Ozah, R., Pope, G., Bryant, S., Sepehrnoori, K., Lake, L., 2005. Reservoir Simulation of CO_2 Storage in Deep Saline Aquifers. SPE Journal 10, 336–348.

Kumar, I., 2012. Direct Shear Testing of Fractured Rocks from Missouri Used to Evaluate Potential Fault Reactivation Induced by Carbon Dioxide Sequestration. Missouri University of Science and Technology.

Lewis, R.W., Sukirman, Y., 1993. Finite element modelling of three-phase flow in deforming saturated oil reservoirs. International Journal for Numerical and Analytical Methods in Geomechanics 17, 577–598.

Longuemare, P., Mainguy, M., Lemonnier, P., Onaisi, A., Gérard, C., Koutsabeloulis, N., 2002. Geomechanics in Reservoir Simulation: Overview of Coupling Methods and Field Case Study. Oil & Gas Science and Technology 57, 471–483.

Lucier, A., Zoback, M., Gupta, N., Ramakrishnan, T.S., 2006. Geomechanical aspects of CO_2 sequestration in a deep saline reservoir in the Ohio River Valley region. Environmental Geosciences 13, 85–103.

Mainguy, M., Koutsabeloulis, N., Longuemare, P., 2001. COUPLING GEOMECHANICS AND RESERVOIR MODELS : APPLICATION TO THE ROLE OF FRACTURES AND FAULTS, in: Evaluation of Hydrocarbon Reservoirs and Technologies to Enhance Production. Rueil-Malmaison - France.

Mattha, S.K., Federal, S., Aydin, A., Pollard, D.D., Stanford, U., Roberts, S.G., U, A.N., 1998. Simulation of Transient Well-Test Signatures for Geologically Realistic Faults in Sandstone Reservoirs.

Metz, B., Davidson, O., Bosch, P., Dave, R., Meyer, L., 2007. Climate Change 2007: Mitigation of Climate Change. Cambridge, United Kindgom and New York, NY, USA.

Miller, T.J., 2012. Evaluation of the Reagan and Lamotte Sandstones in Southwestern Missouri for carbon dioxide sequestration. Missouri University of Science and Technology.

Minkoff, S.E., Stone, C.M., Arguello, J.G., Bryant, S., Eaton, J., Peszynska, M., Wheeler, M.F., 1999. Staggered In Time Coupling of Reservoir Flow Simulation and Geomechanical Deformation: Step 1 — One-Way Coupling, in: Proceedings of SPE Reservoir Simulation Symposium. Society of Petroleum Engineers, Houston, Texas, p. 2.

Minkoff, S.E., Stone, C.M., Bryant, S., Peszynska, M., Wheeler, M.F., 2003. Coupled fluid flow and geomechanical deformation modeling. Journal of Petroleum Science and Engineering 38, 37–56.

Missouri and Coal - Sourcewatch [WWW Document], 2013. URL http://www.sourcewatch.org/index.php?title=Missouri_and_coal (accessed 5.5.13).

Netzler, B.W., 1982. OFM-82-68-WR, Map of total dissolved solids concentrations in groundwater from the Elvins group (upper Cambrian) in Missouri. Rolla, MO.

Nghiem, L., Sammon, P., Grabenstetter, J., Ohkuma, H., 2004. Modeling CO_2 Storage in Aquifers with a Fully-Coupled Geochemical EOS Compositional Simulator. Proceedings of SPE/DOE Symposium on Improved Oil Recovery.

Nygaard, R., Bai, B., Amirlatifi, A., Yang, F., Tiamiyu, O., 2012. DOE Report DE-FE0001132: Reservoir Studies of CO_2 injection in the Lamotte sandstone formation in Southwest Missouri. Rolla, MO.

Olarewaju, J.S., Lee, W.J., 1987. An Analytical Model for Composite Reservoirs Produced at Either Constant Bottomhole Pressure or Constant Rate, in: Proceedings of SPE Annual Technical Conference and Exhibition. Society of Petroleum Engineers, Dallas, Texas.

Orlic, B., Schroot, B. m., Wensaas, L., 2004. Predicting ground deformation due to CO_2 injection: examples from Montmiral, France, Sleipner, Norway and Florina, Greece, in: Proceedings of 7th International Conference on Greenhouse Gas Control Technologies. Cheltenham, UK, pp. 337–339.

Paradeis, M., Eckert, A., Liu, X., 2012. Influences of Anticline Reservoir Geometry On Critical Pore Pressures Associated With CO_2 Sequestration, in: 46th U.S. Rock Mechanics/Geomechanics Symposium, June 24 - 27, 2012 , Chicago, Illinois. Chicago, IL, pp. 2012–319.

Peaceman, D.W., 1977. Fundamentals of Numerical Reservoir Simulation. Elsevier Scientific Publishing Company, Amsterdam, The Netherlands.

Peck, W., Buckley, T., Battle, E., Grove, M., 2012. Plains CO_2 Reduction (PCOR) Partnership, Practical, Environmentally Sound CO_2 Sequestration Atlas. Grand Forks, ND.

Philip, Z., Jennings, J., Olson, J., Laubach, S., Holder, J., 2005. Modeling Coupled Fracture-Matrix Fluid Flow in Geomechanically Simulated Fracture Networks. SPE Reservoir Evaluation & Engineering 8, 300–309.

Pruess, K., Xu, T., Apps, J., Garcia, J., 2003. Numerical Modeling of Aquifer Disposal of CO_2. SPE Journal 8.

Pruess, K., Xu, T., Apps, J., Garcia, J., Berkeley, L., Karsten, P., Tianfu, X., John, A., Julio, G., 2001. Numerical Modeling of Aquifer Disposal of CO_2 - Paper SPE 66537, in: Proceedings of SPE/EPA/DOE Exploration and Production Environmental Conference. Society of Petroleum Engineers, San Antonio, Texas, pp. 1–16.

Rudnicki, J.W.J., 1986. Fluid Mass Sources and Point Forces in Linear Elastic Diffusive Solids. Mechanics of Materials 5, 383–393.

Rutqvist, J., Birkholzer, J.T., Cappa, F., Tsang, C.-F.C.-F., 2007. Estimating maximum sustainable injection pressure during geological sequestration of CO_2 using coupled fluid flow and geomechanical fault-slip analysis. Energy Conversion and Management 48, 1798–1807.

Rutqvist, J., Birkholzer, J.T., Tsang, C.-F., 2008. Coupled reservoir–geomechanical analysis of the potential for tensile and shear failure associated with CO_2 injection in multilayered reservoir–caprock systems. International Journal of Rock Mechanics and Mining Sciences 45, 132–143.

Rutqvist, J., Birkholzer, J.T., Tsang, C.-F.C.-F., 2006. Modeling of geomechanical proceses during injection in amultilayered reservoir-caprock system and implications on site characterization, in: Conference: CO_2SC Symposium, 20-22 March2006. Berkeley, California.

Rutqvist, J., Wu, Y.S., Tsang, C.-F., Bodvarsson, G., 2002. A modeling approach for analysis of coupled multiphase fluid flow, heat transfer, and deformation in fractured porous rock. International Journal of Rock Mechanics and Mining Sciences 39, 429–442.

Saleh, S., 1990. An Improved Model For The Development And Analysis Of Partial-Water Drive Oil Reservoirs, in: Proceedings of Annual Technical Meeting. Society of Petroleum Engineers.

Sengul, M., 2006. CO_2 Sequestration - A Safe Transition Technology - Paper SPE 98617, in: Proceedings of SPE International Health, Safety & Environment Conference. Society of Petroleum Engineers, Abu Dhabi, UAE.

Settari, A., Mourits, F.M., 1994. Coupling of geomechanics and reservoir simulation models, in: Siriwardane, H.J., Zaman., M.M. (Eds.), Computer Methods and Advances in Geomechanics. (Edited by H. J. Siriwardane and M. M. Zaman.). Morgantown, W. Va, USA, pp. 2151–2158.

Settari, A., Mourits, F.M., 1998. A Coupled Reservoir and Geomechanical Simulation System. SPE Journal 3, 219–226.

Settari, A., Walters, D., 1999. Advances in Coupled Geomechanical and Reservoir Modeling With Applications to Reservoir Compaction, in: Proceedings of SPE Reservoir Simulation Symposium. Society of Petroleum Engineers, Houston, Texas.

Sheldon, J.W., Zondek, B., Cardwell, W.T., 1959. One-dimensional, incompressible, non-capillary, two-phase fluid flow in a porous medium. Petroleum Transactions SPE AIME 216, 290–296.

Smotherman, B., 2010. The Influence of Lineaments on the Geology of Missouri [WWW Document]. Emporia State University. URL http://academic.emporia.edu/aberjame/student/smotherman2/globaltect2.htm (accessed 8.28.12).

Snow, D.T., 1968. Rock fracture spacings, openings, and porosities. Journal of Soil Mechanics & Foundations Div 94, 73–91.

Stone, H.L., Garder Jr., A.O., 1961. Analysis of Gas-Cap or Dissolved-Gas Drive Reservoirs. Society of Petroleum Engineers Journal 1, 92–104.

Streit, J.E., Hillis, R.R., 2004. Estimating fault stability and sustainable fluid pressures for underground storage of CO_2 in porous rock. Energy 29, 1445–1456.

Surface GPS Map of North-East Missouri [WWW Document], 2013. URL http://facility.unavco.org/data/dai2/app/dai2.html (accessed 1.5.13).

Thomas, G.W., Thurnau, D.H., 1983. Reservoir Simulation Using an Adaptive Implicit Method. Society of Petroleum Engineers Journal 23, 759–768.

Thomas, L.K., Chin, L.Y., Pierson, R.G., Sylte, J.E., 2003. Coupled Geomechanics and Reservoir Simulation. SPE Journal 8, 350–358.

Tingay, M.R.P., Hillis, R.R., Morley, C.K., Swarbrick, R.E., Okpere, E.C., 2003. Pore pressure/stress coupling in Brunei Darussalam—implications for shale injection. In: Van Rensbergen, P., Hillis, R.R., Maltman, A.J. and Morley, C.K. (eds.) Subsurface Sediment Mobilization. Geological Society of London Special Publication 216, 369–379.

Tippie, D.B., Abbot, W.A., 1978. Pressure Transient Analysis In Bottom Water Drive Reservoir With Partial Completion, in: Proceedings of SPE Annual Fall Technical Conference and Exhibition. Society of Petroleum Engineers.

Tortike, W.S., S.M., F.A., 1987. A Framework for Multiphase Nonisothermal Fluid Flow in a Deforming Heavy Oil Reservoir, in: Proceedings of SPE Symposium on Reservoir Simulation. Society of Petroleum Engineers, San Antonio, Texas, pp. 385–391.

Tran, D., Nghiem, L., Shrivastava, V., Kohse, B., 2010. Study of geomechanical effects in deep aquifer CO_2 storage, in: 44th US Rock Mechanics Symposium. ARMA, Salt Lake City, UT.

Tran, D., Shrivastava, V., Nghiem, L., Kohse, B., 2009. Geomechanical Risk Mitigation for CO_2 Sequestration in Saline Aquifers, in: Proceedings of SPE Annual Technical Conference and Exhibition. Society of Petroleum Engineers, New Orleans, Louisiana, pp. 1–18.

Tsang, C.-F., 1999. Linking Thermal, Hydrological, and Mechanical Processes in Fractured Rocks. Annual Review of Earth and Planetary Sciences 27, 359–384.

Turcotte, D.L., Schubert, G., 2002. Geodynamics, 2nd ed. Cambridge University Press, New York.

Van der Meer, L.G.H., 1992. Investigations regarding the storage of carbon dioxide in aquifers in the Netherlands. Energy Conversion and Management 33, 611–618.

Van der Meer, L.G.H., 1995. Storage Efficiency of Aquifers. Energy Conversion and Management 36, 513–518.

Van der Meer, L.G.H., 1996. Computer Modeling of Underground CO_2 Storage. Energy Conversion and Management 37, 1155–1160.

Verdon, J.J.P., Kendall, J.-M.J.-M.J.-M., White, D.J., Angus, D.A., 2011. Linking microseismic event observations with geomechanical models to minimise the risks of storing CO_2 in geological formations. Earth and Planetary Science Letters 305, 143–152.

Vidal-Gilbert, S., Nauroy, J.-F., Brosse, E., 2009. 3D geomechanical modelling for CO_2 geologic storage in the Dogger carbonates of the Paris Basin. International Journal of Greenhouse Gas Control 3, 288–299.

World Stress Map [WWW Document], 2013.

Xikui, L., Zienkiewicz, O.C., 1992. Multiphase flow in deforming porous media and finite element solutions. Computers & Structures 45, 211–227.

Yang, F., Bai, B., Dunn-Norman, S., Nygaard, R., Eckert, A., 2013. Factors affecting CO_2 storage capacity and efficiency with water withdrawal in shallow saline aquifers. Environmental Earth Sciences.

Zhou, Q., Birkholzer, J., 2007. Sensitivity study of CO_2 storage capacity in brine aquifers with closed boundaries: dependence on hydrogeologic properties, in: Sixth Annual Conference on Carbon Capture and Sequestration - DOE/NETL. Pittsburgh, PA.

Zhou, Q., Birkholzer, J.T., Tsang, C.-F., Rutqvist, J., 2008. A method for quick assessment of CO_2 storage capacity in closed and semi-closed saline formations. International Journal of Greenhouse Gas Control 2, 626–639.

Zienkiewicz, O., Taylor, R., Zhu, J., 2005. The finite element method: its basis and fundamentals, 6th ed. Elsevier Butterworth-Heinemann, Oxford.

Zoback, M., Ross, H., Lucier, A., 2006. Geomechanics and CO_2 Sequestration.

VITA

Amin Amirlatifi was born in 1981, in Gorgan, Iran. He received a BSc. Degree in Petroleum engineering-Reservoir engineering with honor from the Petroleum University of Technology, Ahwaz, Iran, in 2004. He also received a MSc. in Chemical and Petroleum engineering-Reservoir engineering from Petroleum University of Technology, Tehran, Iran, in 2005, a MSc. degree in Chemical and Petroleum engineering-Reservoir engineering from University of Calgary, Canada, in 2005 and a PhD in Petroleum Engineering from Missouri University of Science and Technology (MST) in December 2013. He has published several papers regarding coupled geomechanical analysis. Amirlatifi is a member of Society of Petroleum Engineers (SPE), American Association of Professional Geologists (AAPG) and American Rock Mechanic Association (ARMA).